

Doctoral thesis

Doctoral theses at NTNU, 2022:326

Baiheng Wu

# Synthesis of Human-in-the-Loop Navigational Operations towards Maritime Autonomous Surface Ships

**NTNU**  
Norwegian University of Science and Technology  
Thesis for the Degree of  
Philosophiae Doctor  
Faculty of Engineering  
Department of Ocean Operations and Civil  
Engineering



Norwegian University of  
Science and Technology



Baiheng Wu

# **Synthesis of Human-in-the-Loop Navigational Operation towards Maritime Autonomous Surface Ships**

Thesis for the Degree of Philosophiae Doctor

Ålesund, October 2022

Norwegian University of Science and Technology  
Faculty of Engineering  
Department of Ocean Operations and Civil Engineering



Norwegian University of  
Science and Technology

**NTNU**

Norwegian University of Science and Technology

Thesis for the Degree of Philosophiae Doctor

Faculty of Engineering

Department of Ocean Operations and Civil Engineering

© Baiheng Wu

ISBN 978-82-326-5455-0 (printed ver.)

ISBN 978-82-326-5796-4 (electronic ver.)

ISSN 1503-8181 (printed ver.)

ISSN 2703-8084 (online ver.)

Doctoral theses at NTNU, 2022:326

Printed by NTNU Grafisk senter



## Abstract

Maritime transportation is indispensable to the world economy as it dominates over 95 % of the trade volume, so stakeholders have been striving to promote maritime transportation efficiency and sailing security. Benefitted from the technical progress of advanced guidance, navigation, and control techniques, industrial digitalization, and artificial intelligence, the concept of maritime autonomous surface ships (MASS) has emerged. However, according to the regulatory scoping exercise by the International Maritime Organization, several critical phases with different degrees of autonomy are prerequisites to achieving full ship autonomy. In these phases, human practitioners participate the navigation operations loop at various levels in terms of intervention and operating venues, which means human navigators will stay in the loop until the final phase - fully autonomous ships - comes. Though, as professionals, human navigators have recorded numerous safe sailings and accumulated rich experience on the ship bridge, the major cause of most marine accidents is still attributed to human factors. In this regard, the research on human-in-the-loop (HITL) navigational operations will have impact on not only the enhancement of marine traffic safety, especially in the period when human navigators still play the dominant roles on the ship bridge; but also on the development of MASS, as humans contribute both expert knowledge and faulty cases onboard and in complex marine traffic systems as the input of the ship intelligence.

The study of synthesis of HITL navigational operations is thus motivated and proposed to address the human-related issues towards the development of MASS by integration of maximizing expertise knowledge, monitoring on-bridge operations, summarizing human navigational logics and modeling the mechanism, and providing practical decision support tools. In establishing such a synthesis study framework, experimental facilities are based on different maritime ship-bridge simulators, while techniques involved in the route map can be categorized into three groups in terms of the aim of utilization: on-bridge monitoring & data collection (e.g., sensor fusion, computer vision, and motion/gesture/eye-movement tracking), analysis and learning of operational behaviors (e.g., statistics, pattern recognition, and expert system), and online surveillance & decision support (e.g., situation awareness, risk management, and collision avoidance algorithms). The experimental platforms incorporate the techniques in the route map and then become the rudiment of intelligent ship bridges on MASS.

This dissertation explores the synthesis of HITL navigational operations towards MASS, especially in the experimental design & implementation and HITL applications. The techniques in the route map are adapted and applied in different scenarios based on various platforms. Three case studies are conducted to demonstrate how the synthesis study framework can be carried out to comprehend HITL navigational operations. The first relates to expertise-knowledge-aided path routing to increase sailing safety; the second conceptualizes navigating patterns analysis and illustrates a built-on decision

---

support system for collision avoidance; the third discusses the navigational visual attention and improves the measurement solution. The case studies validate the applicability of the synthesis study framework.

**Keywords:** maritime autonomous surface ships (MASS), human-in-the-loop (HITL), behavioral analysis, decision support, navigating patterns, and visual attention.

## Acknowledgment

The research presented in this dissertation was conducted at the Norwegian University of Science and Technology in Ålesund within the Department of Ocean Operations and Civil Engineering (IHB). Financial support was provided by the Knowledge-Building Project for Industry “Digital Twins for Vessel Life Cycle Service” from the Research Council of Norway under Project 280703.

First of all, I would like to thank my supervisors, Profs. Guoyuan Li, Houxiang Zhang, and Hans Petter Hildre, for shaping my academic thinking capability, motivating me to be an independent researcher, and granting me plenty of freedom in exploring the terra incognita.

I would like specially thank Dr. Tongtong and Dr. Peihua Han, who had been pursuing the Ph.D. degree with me.

I appreciate the help and support offered by all my colleagues at the Intelligent Systems Lab (formerly Mechatronics Lab) and all my friends that I met at NTNU in Ålesund and Trondheim.

Thank all my friends nearby and far away for your companionship and witness of my growth.

I express great appreciation and admiration to Shaohui for being with me on those good and bad days.

At last, special gratitudes are expressed to my parents, Yan Tang and Haixiang Wu, and I wish we may reunite soon.



# Contents

<b>Abstract</b>	<b>i</b>
<b>Acknowledgment</b>	<b>iii</b>
<b>List of Publications</b>	<b>ix</b>
<b>List of Abbreviations</b>	<b>xi</b>
<b>Nomenclature</b>	<b>xiii</b>
<b>List of Figures</b>	<b>xv</b>
<b>List of Tables</b>	<b>xvii</b>
<b>1 Introduction</b>	<b>1</b>
1.1 Background and motivation . . . . .	1
1.2 Research questions . . . . .	3
1.3 Scope of work . . . . .	5
1.3.1 Research objectives . . . . .	5
1.3.2 Interconnection between the research objectives . . . . .	6
1.4 Contributions of the dissertation . . . . .	7
1.5 Structure of the dissertation . . . . .	7
<b>2 Methodology</b>	<b>9</b>
2.1 Platforms . . . . .	10
2.1.1 Preliminary Study . . . . .	10
2.1.2 Quantitative Study . . . . .	12
2.1.3 Testbed for Verification and Demonstration . . . . .	13
2.2 Design & Implementation . . . . .	13
2.3 Utilization . . . . .	15
2.3.1 Monitoring & Data Collection . . . . .	15
2.3.2 Operations Analysis and Learning . . . . .	17
2.3.3 Online Surveillance & Decision Support . . . . .	17
2.4 Chapter summary . . . . .	18

---

<b>3</b>	<b>Case study: Expertise-knowledge aided path routing</b>	<b>19</b>
3.1	Methodology . . . . .	20
3.1.1	Data collection and pre-processing . . . . .	20
3.1.2	Definition for scenarios by human expertise . . . . .	20
3.1.3	Empirical criteria based on human expertise . . . . .	21
3.1.4	Separability precheck . . . . .	21
3.1.5	Support vector machine . . . . .	23
3.1.6	Likelihood map and safety level calculation . . . . .	23
3.1.7	Verification how the safety level benefits in MPC . . . . .	24
3.1.8	Assessing the safety level by the contour map . . . . .	25
3.2	Results . . . . .	25
3.2.1	Classification result . . . . .	25
3.2.2	Likelihood heat maps and derived contours . . . . .	26
3.2.3	Verification in MPC loop . . . . .	28
3.2.4	Safety level assessment . . . . .	29
3.3	Chapter summary . . . . .	30
<b>4</b>	<b>Case study: Navigating patterns analysis and application</b>	<b>31</b>
4.1	Methodology . . . . .	31
4.1.1	Experimental environment . . . . .	31
4.1.2	Related metrics . . . . .	31
4.2	Experiment I: Navigating patterns analysis . . . . .	34
4.2.1	Experiment setup and implementation . . . . .	34
4.2.2	Pattern analysis . . . . .	35
4.2.3	Summary . . . . .	39
4.3	Experiment II: guidance support system testing . . . . .	40
4.3.1	Description of the guidance support system . . . . .	40
4.3.2	Summary . . . . .	41
4.4	Chapter summary . . . . .	41
<b>5</b>	<b>Case Study: Visual-attention analysis and measurement</b>	<b>43</b>
5.1	Eye-tracker-based visual attention analysis . . . . .	43
5.1.1	Metrics . . . . .	43
5.1.2	Experimental Design . . . . .	44
5.1.3	Visual attention in critical operations . . . . .	45
5.1.4	Usability evaluation of electronic chart system . . . . .	47
5.2	Camera-based deep learning model for visual attention measurement . . . . .	49
5.2.1	Methodology & Setup . . . . .	49
5.2.2	Results & Discussion . . . . .	51
<b>6</b>	<b>Conclusion and Further Work</b>	<b>57</b>

---

6.1	Summary of contributions . . . . .	57
6.2	Summary of publications . . . . .	58
6.3	Future work . . . . .	59
<b>References</b>		<b>61</b>
<b>Appendix</b>		<b>69</b>
<b>A Paper I</b>		<b>71</b>
<b>B Paper II</b>		<b>79</b>
<b>C Paper III</b>		<b>93</b>
<b>D Paper IV</b>		<b>111</b>
<b>E Paper V</b>		<b>119</b>
<b>F Paper VI</b>		<b>129</b>
<b>G Paper VII</b>		<b>137</b>





## List of Publications

This dissertation is based on research resulting in five journal papers and one conference paper. They are all enclosed in the appendix section. In the following list of publications, the papers are listed chronologically, but in the main body of the text a more thematic presentation order is prioritized over the chronological one.

- I **Wu, B.**, Li, G., Zhao, L., Hildre, H. P., & Zhang, H. A human-expertise based statistical method for analysis of log data from a commuter ferry. *In 2020 15th IEEE Conference on Industrial Electronics and Applications (ICIEA)* (pp. 1471-1477). IEEE. 2020. [C1]
- II **Wu, B.**, Li, G., Wang, T., Hildre, H. P., & Zhang, H. (2021). Sailing status recognition to enhance safety awareness and path routing for a commuter ferry. *Ships and Offshore Structures*, vol. 16(sup1), pp. 1–12, 2021. [J1]
- III **Wu, B.**, Li, G., Zhao, L., Aandahl, H. I. J., Hildre, H. P., & Zhang, H. (2021). Navigating Patterns Analysis for Onboard Guidance Support in Crossing Collision-Avoidance Operations. *IEEE Intelligent Transportation Systems Magazine*. vol. 14, no. 3, pp. 62-77, May-June 2022. [J2]
- IV **Wu, B.**, Zhao, L., Thattavelil Sunilkumar, S. R., Hildre, H. P., Zhang, H., & Li, G.: Eye-tracker-based Visual Attention Investigation in Maritime Collision-Avoidance Operations. *In 2022 IEEE 17th International Conference on Control & Automation (ICCA)*, pp. 285-2920. IEEE, 2022. [C2]
- V **Wu, B.**, Han, P., Hildre, H. P., Zhao, L., Zhang, H., & Li, G.: A Camera-based Deep-Learning Solution for Visual Attention Zone Recognition in Maritime Navigational Operations. *In 2022 IEEE/RSJ International Conference on Intelligent Robots and Systems (IROS 2022)*, 2022. Accepted. [C3]
- VI **Wu, B.**, Zhao, L., Hildre, H. P., Zhang, H., & Li, G.: Evaluation on Effectiveness of Electronic Chart System for Maritime Navigators Based on Visual Attention and Risk Assessment. *Submitted to IEEE Access*. [J3]
- VII **Wu, B.**, Sæter, M.L., Hildre, H. P., Zhang, H., & Li, G.: Experiment Design and Implementation for Human-in-the-Loop Study Towards Maritime Autonomous Surface Ships. *IEEE SMC 2022 International Conference on Systems, Man, and Cybernetics*. Accepted. [C4]

---

The following papers will not be discussed in this dissertation. They may, however, be considered relevant due to co-authorship and similar topics:

- i Zhao, L., Li, G., Remøy, K., **Wu, B.** and Zhang, H., 2020, November. Development of Onboard Decision Supporting System for Ship Docking Operations. *In 2020 15th IEEE Conference on Industrial Electronics and Applications (ICIEA)* (pp. 1456-1462). IEEE.
- ii Wang, T., Li, G., **Wu, B.**, Æsøy, V. and Zhang, H., 2021. Parameter identification of ship manoeuvring model under disturbance using support vector machine method. *Ships and Offshore Structures*, 16(sup1), pp.13-21.
- iii Han, P., Li, G., Skjong, S., **Wu, B.** and Zhang, H., 2021, May. Data-driven sea state estimation for vessels using multi-domain features from motion responses. *In 2021 IEEE International Conference on Robotics and Automation (ICRA)* (pp. 2120-2126). IEEE.
- iv Zhao, L., Thattavelil Sunilkumar, S. R., **Wu, B.**, Li, G., & Zhang, H.: Towards an Online Decision Support System to Improve Collision Risk Assessment at Sea, *IEEE Intelligent Transportation Systems Magazine*. Accepted.
- v **Wu, B.**, Aandahl, H. I., Bosneagu, R., Sæter, M., Cosofret, D., Avram, E.R., Zhang, H., and Li, G.: Survey for Interdisciplinary Co-supervision on Bachelor Thesis in Nautical Science, *Ready for submission to EDUCON2023 – IEEE Global Engineering Education Conference*.

## List of Abbreviations

AIS	Automatic Identification System
AOI	Area of Interest
ARPA	Automatic Radar Plotting Aid
CA	Collision Avoidance
CaBDeeL	Camera-based Deep Learning model
CLF	Classifier
CNN	Convolutional Neural Network
CO	Critical operation
COLREGs	Convention on the International Regulations for Preventing Collisions at Sea
CPA	the Closest Point of Approach
CRA	Collision Risk Assessment
CRI	Collision Risk Index
CRS	Cruising (scenario in a commuter route)
CVG	Converging (scenario in a commuter route)
DCPA	Distance at the Closest Point of Approach
DCK	Docking (scenario in a commuter route)
DPT	Departing (scenario in a commuter route)
ECDIS	Electronic Chart Display and Information System
ECS	Electronic Chart System
EEG	Electroencephalography
GPS	Global Positioning System
GNSS	Global Navigation Satellite Systems
GUI	Graphic User Interface
HITL	Human-in-the-Loop

---

ICT	Information & communication technologies
IMO	International Maritime Organization
IMU	Inertia measurement unit
ISO	International Maritime Organization
KDE	Kernel density estimation
MASS	Maritime Autonomous Surface Ships
MPC	Model predictive control
MSL	Mean safety level
NP	Navigating Pattern
NPA	Navigating Patterns Analysis
NTNU	the Norwegian University of Science and Technology
OH	Optimal hyperplane or maximum margin hyperplane
OS	Own Ship
RO	Research objective
RPM	Revolutions per minute
RQ	Research question
RSL	Receding safety level
R/V	Research vessel (Gunnerus)
SL	Safety Level
SVM	Support vector machine
TCPA	Time to the Closest Point of Approach
TRN	Turning (scenario in a commuter route)
TS	Target Ship
t-SNE	t-distributed stochastic neighbor embedding
TW	Time window
VAZ	Visual Attention Zone

## Nomenclature

$C_A$	Coriolis-centripetal matrix (of added mass)
$C_{RB}$	Coriolis-centripetal matrix (of rigid body)
$D$	Damping matrix (in Chapter 3); distance (in Chapter 4)
DIF	Domain intersection factor
$d_{\text{passing}}$	Passing distance
$d_{OS}^{\text{arrival}}$	Distance to the destination
$h$	Smoothing parameter
$K$	Kernel for scaling
$L$	Label set
$L'$	Label set in each binary classifier
$M_A$	Mass matrix (of added mass)
$M_{RB}$	Mass matrix (of rigid body)
$\hat{p}$	Estimated density
$\hat{p}_N$	Normalized estimated density
$R(\psi)$	Rotate matrix
$W$	Weight coefficient
$t_{\text{passing}}$	Time when one vessel first pass the other
$T_{AOI-j}$	Total duration time on the area of interest $j$ .
$\eta$	NED position and heading vector
$\nu$	Linear and rotational velocity vector
$\tau$	Force vector
$\psi$	Heading angle
$\theta_R$	Course of the relative velocity between two encountering vessels
$\alpha_{TS}$	Azimuth angle of target ship to the center of own ship



## List of Figures

1.1	Interconnection of published paper in the dissertation. . . . .	6
2.1	Illustration of synthesis research of HITL navigational operations towards MASS. . . . .	10
2.2	Experimental platforms. (Terminology: Electronic Chart Display and Information System (ECDIS); Electronic Chart Systems (ECS)); Automatic Radar Plotting Aids(ARPA).) . . . . .	11
2.3	Participation in experiment design process. . . . .	14
2.4	Intelligent ship-bridge system for research on HITL navigational operations. . . . .	15
2.5	Applied multi-sensor monitoring scenes. . . . .	16
2.6	Analysis procedures. . . . .	17
2.7	Interconnection of experimental platforms and analysis methods in this dissertation. . . . .	18
3.1	Collection of 21 commuter sailings. . . . .	19
3.2	Framework of the proposed decision support system for sailing status recognition and safety evaluation (map resource: the Norwegian Mapping Authority). . . . .	20
3.3	Visualization of dimension reduction result by t-SNE. . . . .	22
3.4	Confusion matrix reflecting precision by scenarios (left: CLF No.4; middle: CLF No. 9; right: CLF No. 14). . . . .	26
3.5	Heat maps of different scenarios. . . . .	27
3.6	Heat maps of different scenarios. . . . .	27
3.7	Path following simulation by MPC . . . . .	28
3.8	Online testing of the sailing status recognition. . . . .	29
3.9	Calculated MSL and RSL (Diluted lines are the real time safe level). . . . .	29
4.1	Workflow of this case study. . . . .	32
4.2	Illustration of DCPA. . . . .	32
4.3	Illustration the calculation of the passing distance at $t_{\text{passing}}$ . . . . .	34
4.4	Scenario layout of the experimental CA sailing. . . . .	35
4.5	Distribution of DCPA in terms of different navigating patterns. . . . .	36
4.6	Plot of $d_{\text{passing}}$ /DCPA values. 5 intervals on $x$ -axe are S-B-B, S-S-S, S-S-B, B-S-S, and B-B-B. They are painted with distinguishable background colors. . . . .	38

4.7	Distance to the destination at T=550 s. The dash lines in red and blue are trendlines of datasets S-S-S and S-B-B. . . . .	39
4.8	Illustration of the GUI of the developed system. . . . .	40
5.1	Area of interest (AOI) on the simulator. . . . .	44
5.2	Designed scenario on the map. . . . .	45
5.3	Illustration of the workflow to this research. . . . .	45
5.4	Transition times of each AOI and the total count. . . . .	46
5.5	Features to the duration of fixation for each AOI. . . . .	47
5.6	Total fixation time for each AOI. . . . .	47
5.7	Workflow of this work (Picture of Tobii Pro glasses 2 is credited to the official website to Tobii Pro®). . . . .	48
5.8	Workflow of the CaBDeeL solution (images containing facial identity have been blurred for demonstration in the figure according to the General Data Protection Regulation (GDPR)). . . . .	50
5.9	Structure of CNN-based deep-learning algorithm. . . . .	51
5.10	Two scenarios: (a) heavy traffic with collision avoidance demand; (b) cruise in light traffic. . . . .	52
5.11	Confusion matrices in the two scenarios of CaBDeeL (500 epochs). . . . .	53
5.12	Matts plot of (1) top-left: back-view (only used for demonstration, not relevant to CaBDeeL); (2) top-right: front-view (input image to CaBDeeL; the facial image shown here is blurred according to GDPR); (3) bottom-left: eye-tracker glasses marked video; (4) bottom-right: CaBDeeL recognized VAZ is highlighted. . . . .	53
5.13	Transition frequency between every two VAZs in the two scenarios (transitions per minute). The blue lines depicts for Scenario (a) and the yellow lines depicts for Scenario (b). . . . .	54
5.14	Total duration proportion of each VAZ in the two scenarios. . . . .	55



## List of Tables

1.1	Specification of MASS I-IV . . . . .	2
2.1	Usage of different platforms in Fig. 2.2 . . . . .	13
3.1	Classification of log data . . . . .	21
3.2	empirical criteria for the commuting route decomposition . . . . .	22
3.3	Illustration of the classifier evolution process. . . . .	26
3.4	Verification of safety level in loop. . . . .	28
4.1	Ship information and experimental conditions setup . . . . .	35
4.2	Expert evaluation on each CA and its info . . . . .	37
4.3	Mean DCPA for CA with different TSs . . . . .	38
4.4	DCPA scales of different navigating patterns . . . . .	40
4.5	Test results with the developed system . . . . .	41
5.1	Statistics scales on duration of fixation features for complete sailings . . .	48
5.2	Statistics on transition frequencies in complete sailings . . . . .	49
5.3	Comparison on sampling rate/accuracy . . . . .	52
5.4	Sampling rate/accuracy comparison in the two scenarios . . . . .	53
5.5	Duration of fixation features . . . . .	54



The maritime industry has been experiencing technological revolutions from the time of birth. Recently, conforming to the progress of informatics and communication technologies, the maritime industrial conventions are being reshaped from human-centered navigation to a unmanned transportation network. As staying in the transition period, there are many challenges to be solved to achieve the full ship autonomy, while before the fully autonomous ships are deployed, human navigators will continue to perform dominantly in the maritime traffic and contribute to the development of the maritime autonomous surface ships (MASS). This dissertation mainly focuses on how to establish a synthesis study framework for human-in-the-loop (HITL) navigational operations towards MASS to address the questions about the interaction between human and semi-intelligent ships.

### 1.1 Background and motivation

Maritime traffic has been playing one of the most essential roles in many aspects of the human society over the past hundreds of years, while the demand on seaborne-transport trades has been increasing drastically over the decades. According to United Nations' figures, the total seaborne trade volume booms 1 283% from 800 million metric tons in 1955 to 11 071 million metric tons in 2019, and contributes 86% to 2020's year-round world trade [1][2]. By contrast to the thriving market of the maritime transport, a 3% shortage gap of seafarers exists and continues expanding which is predicted to reach an extremum until 2026 [3]. In another survey by the Norwegian Shipowners' Association, nearly 80% interviewees agree ICT (information & communication technologies) and dataprocessing to be the most important competency in next ten years, while 40% think this competency is difficult to obtain; seafaring experience is the second important competency with 66% supporters, while 64% regard it as the most difficult competency to obtain [4]. The above figures indicate that a solution is imperative to accommodate the heavy expenditure and shortage of human labour in the increasing maritime transport market. As the development of technologies in the scope of the marine cybernetics and artificial intelligence, the promotion of the ship-autonomy level is deemed to be a promising option. At the same time, when the development of MASS undergoes, human navigators keep their dominant roles in the navigation loop on the ship bridge. In this regard, it is essential to conduct research on HITL navigational operations to relentlessly improve sailing performance in terms of safety and efficiency.

Switching the perspective to the onboard sailing practice, human-factor-induced errors are dominant in marine accidents and perils. According to different statistics, about 60% to 96% marine accidents are attributed to human-factor-induced errors [5][6]. However, this attribution trends to decline in recent years [7]. This trend is evident in the

European Union that human erroneous actions result in 67% of the accidents between 2011 to 2014; while this figure decreases to 54% in statistics between 2014 to 2019. While as the proportion of human erroneous attributed accidents decreases, it is interesting to notice that the human erroneous type of shore management (by contrast to shipboard operations) gradually increases from 17.6% to 24.2%. It implies that the duties and roles of coastal management group (shore-based control center) and onboard crew are in transition [8][9]. These data provide further support that research on HITL navigational operations is in urgent need of implementation to confront the predicaments caused by human factors.

On the other hand, as climate change and environment degradation become global issues, prompt solutions are demanded on how to effectively increase the traffic efficiency and reduce the emission [10]. The implementation of maritime autonomous ships is an option by means of planning the fuel-optimal sailing route [11], actuating with the fuel-efficient control commands [12][13], reducing the demand on human labors [14], and so on.

In this context, the concept of the maritime autonomous surface ships (MASS) gradually raises. The terminology (MASS) is registered with the International Standard Organization (ISO) by the International Maritime Organization (IMO) in 2019. Before the registration, there are several names for the type of ships which can function full or partial autonomy, such as autonomous surface vehicles (ASV) and unmanned surface vehicles (USV), and related research works have been conducted extensively for decades in scopes of ship modelling, path planning, motion control, and etc [15][16][17][18][19]. Though the terminology of MASS appears late, it does not mean that the MASS will be launched soon, as remotely controlled ships are expected to enter the water in 2020s, and in different forecastings, the full MASS will come into being between 2035-2060 [20][21].

According to IMO, MASS are classified at four levels (I-IV) in terms of human crew presence and ship intelligence degrees [22]. While except for the level MASS-IV where ships are fully automated, the human crew are considered to be in the loop either onboard or remotely, either as the decision-maker or monitor [23]. Autonomous ships and intelligent maritime transportation are promising and desired, but not until issues in technology, ethics, and sociology, are addressed [24][25].

Table 1.1: Specification of MASS I-IV

Level	Crew	Human Control	Autonomy
I	Onboard	Onboard	Decision support
II	Onboard	Remote	Crew ready to takeover
III	Off board	Remote	No onboard intervention
IV	Off board	No intervention	Full

Table 1.1 illustrates the details of human presence, intervention, and ship autonomy of MASS I-IV. It plans how MASS gradually gains independence from human crews level by level, from onboard operation to remote control, from human-centered maneuvering to human as monitor, etc. It can be summarized that, only MASS at final degree (IV) of autonomy are without HITL; in other three precedent degrees, human navigators are

always in the loop, more or less. There are essential factors to consider in each step of progress to secure safety and add redundancy. When approaching to the development of MASS, the traffic system is also a concern. Learning human navigators' operational and navigational logic and mechanisms and feeding the ship intelligence with the expertise and knowledge may improve the coexistence of traffic when there are different types of ship governance.

## 1.2 Research questions

The focus of this dissertation is concerned with HITL navigational operations for MASS. This prompts the first question of this dissertation:

- **RQ1: How is HITL issue accommodated in the development of MASS)?**

In order to answer this question, it is necessary to clarify the definitions of HITL and MASS by investigating the existed classification standard, practice recommendations, and industrial practice from different stakeholders (including international/local organizations [22], classification societies [26][27], research institutes [28], and related companies). Reviewing and summarizing the related documents and works will lead to the next research question:

- **RQ2: What are the challenges to the development of MASS?**

Though there are different classification standards by different entities, generally issues in discussion are human attendance (in terms of venues) and intervention levels. Current research works and applications usually focus more on the development of ship intelligence and autonomy instead of paying attention to human interactions. But if directly stepping in the last phase, it is not rare to see a lot of designed algorithm and methods overriding current navigational regulations and conventions. However, as there are necessary phases before achieving the full autonomy, it is imperative to gradually increase system autonomy and redundancy to cooperate with human navigators and other manned target ships in traffic. This requirement leads to the next research question:

- **RQ3: Why is the research on HITL navigation important to the development of MASS?**

As three out of four MASS levels keep the human crew in the loop to different extents, this suggests that HITL maritime research should still be a core issue for the development of MASS [29][30]. In another respect, though human-factor-related failures are dominant in statistics, human navigators are still the most eligible players. They are well-educated and trained professionals, and they have recorded countless safe-sailing hours. Therefore, taking advantage of their occupational and expertise knowledge is also beneficial to the development of MASS [31]. From the whole maritime transportation environment, a transition period is to be expected where manned, semi-autonomous, fully-automated ships may encounter each other in the traffic, and the unpredictability and difficulty of intercommunication between human and ship intelligence, and in this time being, human navigators shall continue perform their competence and provide their expertise onboard. This leads to the following research question:

- **RQ4: How can human navigators' operational data be collected and represented?**

The development of the artificial intelligence and sensor technology enable us to access to human data through multiple channels such as brain waves (electroencephalogram) [32], eye movement [33], gestures [34], body movement [35], and so on [36]. With the help of the sensors, we have the chance to know how human navigators respond to the situations, especially in critical scenes such as collision risks and avoidance which is one of the most concerning tasks in maritime operations [37]. Furthermore, benefitted from the progress in machine learning techniques, novel intelligent sensing approaches can be developed such as camera-based visual attention tracking and head orientation estimation.

In addition to the human physical and psychological data, sailing data (e.g. onboard log data) are also capable to reflect navigational performance as log data often contain the key information (such as human commands, the ship motion and response, and the environmental conditions) that can be utilized to build a model that can demonstrate the whole sailing procedure explicitly [38]. As the modern ships and simulators are made digitalized nowadays, access to ship data is made easier.

For representing data, expertise interpretation with is a way as professionals may category and label data according to conventions and their practical experience in the domain. This leads to the following research question:

- **RQ5: How can above expertise knowledge and experience benefit the development of MASS?**

There have been researchers utilizing the automatic identification system (AIS) data for autonomous navigation [39][40], using the on-board data to monitor the status of the ship health [41][42], and trying to find the human expertise's navigation mechanism from their behavior [43]. Interpreted and modeled data can reflect the mechanism of how humans operate their vessels systematically. In return, the established mechanism can help develop ship intelligence in terms of path planning and routing, intelligent on-board surveillance, on-board decisions support, and etc. This leads to the final research question:

- **RQ6: How does existed experimental platforms support above issues?**

There are substantial experimental resources and platforms at NTNU such as research vessel R/V Gunnerus and different types of maritime simulators, they are illustrated in the following chapter. Both real ships and simulators can be used to collect massive experimental data, while taking the research resource efficiency into consideration, real ship data are usually used for qualitative study and question identification at the beginning of a project and verification and demonstration at the end. Simulators, benefitted from its low cost and feasibility, are preferred to be used to gather data for quantitative study. In practice, using realistic simulator cabins to collect human-centered maneuvering data for training and research purposes has been popular [44][43]. Simulator-based data have been used to analyze risk level and human performance in various scenarios [45].

### 1.3 Scope of work

#### 1.3.1 Research objectives

In seeking to answer the above research questions, this dissertation seeks to obtain the following research objectives (ROs):

- ✓ **RO1: Constructing the experimental design and implementation scheme based on different ship-bridge facilities for a synthesis study framework of HITL navigational operations for MASS.**

Human operators will continue to perform dominant roles onboard for the next decades. A cyber-physical human framework should be conceived for the experiment design and implementation in the maritime domain: based on multiple experimental platforms with data exchange ports, apply monitoring on and learning from navigators' behaviors, and adapt the ship-bridge system to provide decision support in terms of guidance, navigation, and control. These platforms are utilized for data collection, scenario design, testbeds to demonstrate and verify new techniques and algorithm. Paper VII explores this issue in details, while all papers collected in this dissertation are within the interest of RO1. RO1 is then decomposed into the following research objectives:

- ✓ **RO2: Exploring the method for monitoring and collecting human navigators operational behaviors' data onboard.**

As mentioned in RQ4, as the development of sensor technology and algorithm progress, there are multiple ways collecting onboard navigators' data. Nevertheless, some of them have reached the state-of-the-art, while in some domains, the methods are yet to be optimized, such as visual attention monitoring. As the conventional method is using eye-tracker glasses which may bring infeasibility to the navigators and be sensitive to the environment conditions, other non-intrusive and economic solutions are to be expected. This issue is discussed in paper V.

- ✓ **RO3: Establishing a set of approaches to interpret and analyze the navigational behaviors, strategies, and logic.**

Collected ship motion and navigational operation data are plain, necessary pre-processing and interpretation are needed to make them practical to the guidance and navigation. Data from different domains, including ship motion and machinery data which reflect navigators' orders and human visual attention during navigation on the ship bridge, are interpreted to make them comprehensible. This issue is discussed in papers I, III, IV, VI,

- ✓ **RO4: Proposing on-board decision support tools to promote HITL navigational performance and sailing safety.**

The efforts made in collecting and interpreting onboard navigational data are towards the aim of development of MASS at HITL levels. There are different ways of providing

onboard decision support and derived systems. In terms of the mechanisms, the decision support may be either rule-based and algorithm-based. Besides the development of novel decision support systems, it is of more importance to accommodate the developed system effectively cooperated with the navigators, which means in addition to the algorithm development, there are more concerning problems such as human-machine interactions ethics. This issue is discussed in papers II and III.

### 1.3.2 Interconnection between the research objectives

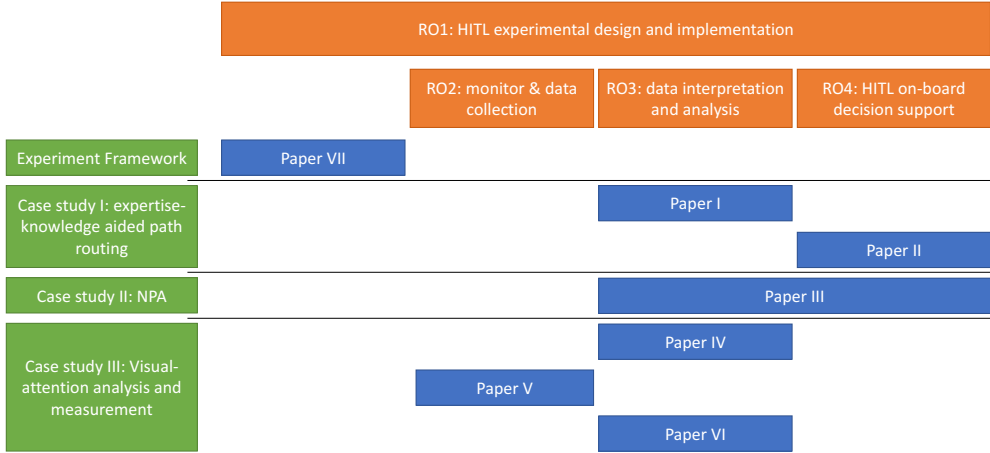


Figure 1.1: Interconnection of published paper in the dissertation.

The interconnection between the research objectives and the papers published are shown in Fig. 1.1. All three case studies are presented in the scope of RO1, as each of them provides an approach to adapt data collected from different experimental platforms and are processed to facilitate different utilizations. Paper VII, which systematically introduces the experimental design and implementation on different platforms and forms the basic methodology of this dissertation, is associated with RO1. Paper I collected R/V Gunnerus ship motion and onboard machinery data from a commuter route in Trondheim and interpret them with human expertise so it locates in RO3; paper II is a continuation of paper I in terms of path routing optimization to enhance sailing safety and it is sorted into solving RO3 as it provides onboard support.

Case study II contains paper III, which collects data from maritime simulators and analyze them with conceptualized definitions of navigating patterns (NP). The concluded NPs are used to build a collision avoidance (CA) system. This complete work is concerned with both RO3 and RO4.

Papers IV and VI use eye-tracker glasses to record navigators eye movement data and provide approaches to evaluate navigators attention in navigational critical operations and verify the effectiveness of additional supporting functions on a screen, and are deemed to be concerning with RO3. Paper V comes up with a camera-based deep learning method to estimate navigators' visual attention on the ship bridge, and lies in the scope of RO2.



## 1.4 Contributions of the dissertation

The major contributions of this dissertation are as follows, which is related the research objective above:

- Present the fundamental framework to use different maritime experimental facilities to conduct HITL navigational operation study. It is related to all four ROs.
- Propose a method to interpret log data by expertise knowledge and use the derived conclusion to optimize path routing in terms of sailing safety. It is related to RO3 and RO4.
- Conceptualize the framework of navigating patterns analysis and use the summarized NPs to provide onboard support for navigators. It is related to RO3 and RO4.
- Implement visual attention analysis to assess navigators visual activity in critical operations and verify the usability of displayed decision support functions. A non-intrusive and economic visual attention tracking and estimation solution is also developed to promote the experimental feasibility. It is related RO2 and RO3.

## 1.5 Structure of the dissertation

This introductory chapter presented the background for the dissertation research, establishing its main goals and defining the scope of work. The rest of this dissertation unfolds as follows. Chapter 2 introduces the experimental and methodological foundation of the synthesis study framework of HITL navigational operations towards MASS. Chapter 3 presents the first case study, which focuses on the expertise-knowledge aided path routing. This chapter is based on paper I and II. Chapter 4 relates to papers III, and discuss navigating patterns analysis and its application for onboard decision support. Chapter 5 presents visual-attention analysis and how the measurement is improved instrumentally. This chapter is based on papers IV, V, and VI. Chapter 6 concludes the dissertation, summarizes the contributions, and indicates the directions for future works.



Learning and accumulating knowledge from the practice is a tradition in this industry; the precedent practitioners have recorded and concreted their experience as routines, regulations, practice recommendations, etc. Their efforts have significantly improved marine traffic safety and efficiency [46]. While keeping this conventional way, the emerging technologies, including machine learning, data mining, and sensor fusion, enable us to objectively model human navigators' behavior with data-based methods. Moreover, simulators designed in accordance with the onboard ship-bridge environment and facilitated with actual navigational operations' functionalities expand the flexibility and accessibility of experiment design and implementation process [47] [48].

With the substantial experiment facilities, research in the scope of HITL onboard operations is designed and implemented. The wearable electroencephalography (EEG) equipment is used to record the navigators' brain active level to detect the signals of fatigue and assess the fatigue levels [49] [50] [51]. The navigators wear the wearable eye tracker to trace their eye movement to reflect their visual interests and transition between different areas of interest (AOIs), and it has been used in operational analysis, including crane lifting [43][33], high-speed cruising [52], and ship maneuvering for collision avoidance [53]. Both massive simulator-generated and real-ship data help to conclude and summarize the navigators' generality and similarity in navigational operations wu [54] [55]. In addition to the traditional analytical method and expert interpretation, algorithms, for example, support vector machine (SVM), are also utilized to realize classification and recognition tasks in HITL maritime domain [56].

In this chapter, the following contents are covered:

- the details of the laboratory environment of maritime simulators and research vessels owned by NTNU (as shown in Fig. 2.2);
- how they facilitate experimental design and implementation for HITL navigational operations modeling;
- how they are used to support the onboard decision and contribute to the development of MASS.

Fig. 2.1 illustrates the framework of synthesis research of HITL navigational operations. Based on a variety of experimental platforms, the research can be categorized in two ways: human-centered intelligent ship bridge system, which focuses on the navigators' physical and psychological activities while on assignment; and onboard expertise data study, which leverages maneuvering and operational data to learn and summarize

occupational expertise and experience. Both ways lead to similar goals: promoting on-board navigational performance and providing decision support tools. All components in the loop illustrated in Fig. 2.1 contextualize the idea of synthesis study of HITL in maritime navigation. The framework of methodology introduced in this chapter presents the work in paper VII.

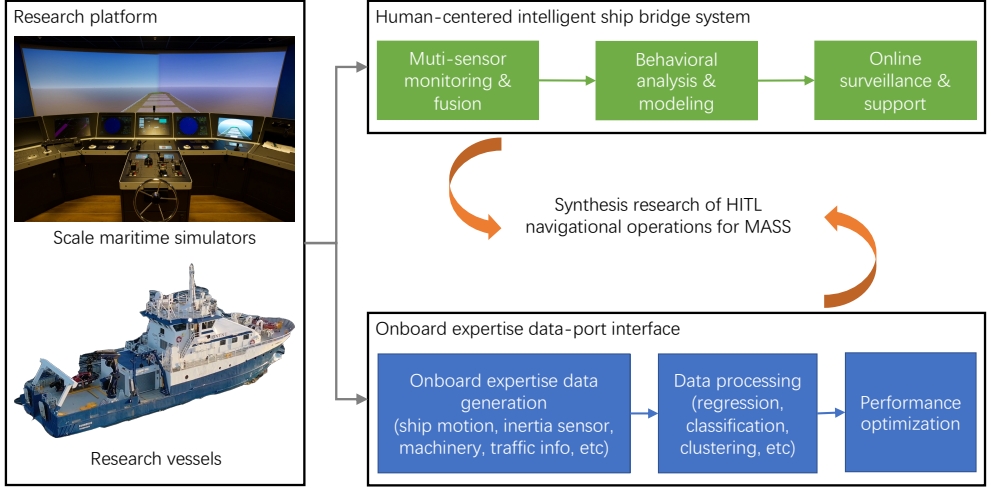


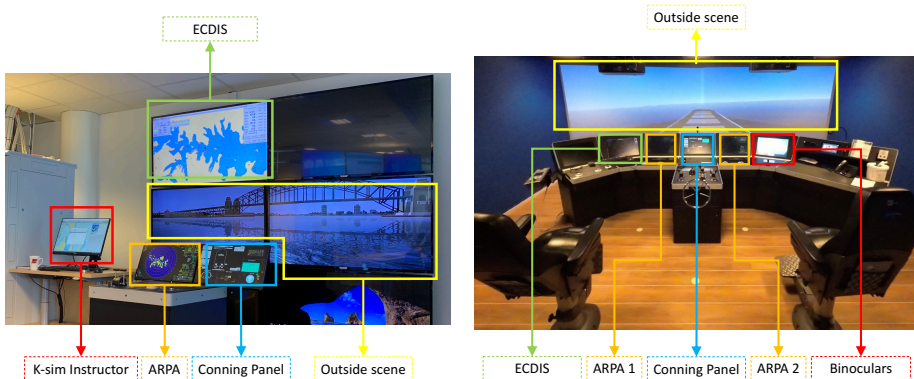
Figure 2.1: Illustration of synthesis research of HITL navigational operations towards MASS.

## 2.1 Platforms

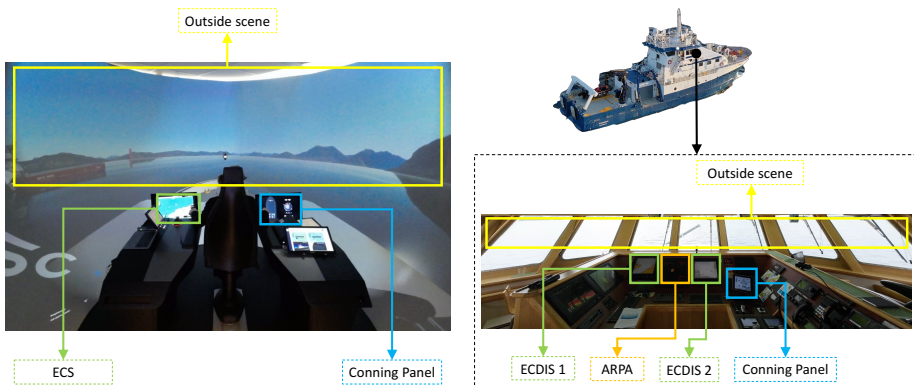
The simulators in Fig. 2.2a and 2.2b are from Kongsberg®, and the former is for research aim while the latter is for navigator training; The ship-bridge system with fixed seat shown in Fig. 2.2c is often seen on compact vessels and catamarans, and this simulator projects the outside scene on a dome screen which provides an immersive navigational experience; Fig. 2.2d is the research vessel R/V Gunnerus (equipped with a bow thruster for the positioning operation at 200 kW and two main azimuth thrusters, each with the propulsion at 500 kW [57]) which can perform most maneuvering operations and tasks (for example, dynamic positioning, zig-zag path following).

### 2.1.1 Preliminary Study

The preliminary study applies to the problems which are never being focused on and concerned by existing research and to questions that have been well studied to some extent. However, some hypotheses are made to dig deeper. Such a study exists whenever a new research project is launched. To verify that the problem is concerned does exist and is worth a look into, a preliminary study should be carried out on a small scale in both experimental design and the number of participants. This procedure may increase the experimental efficiency and avoid unnecessary failures. The platforms in Fig. 2.2a and 2.2c are often used for preliminary study.



(a) Compact simulator from Kongsberg® for preliminary research design. (b) Kongsberg® maritime training simulator.



(c) Immersive ship-bridge simulator powered by OSC. (d) NTNU's research vessel R/V Gunnerus and its ship bridge.

Figure 2.2: Experimental platforms. (Terminology: Electronic Chart Display and Information System (ECDIS); Electronic Chart Systems (ECS)); Automatic Radar Plotting Aids(ARPA).)

Main differences between simulators in Fig. 2.2a and 2.2b are:

- K-sim Instructor which coordinates the experiment implementation, is in the control (briefing) room for the standard maritime training simulator in Fig. 2.2b. At the same time, the K-sim Instructor computer is put just aside from the ship-bridge system in Fig. 2.2a. This configuration makes the tune-test process much easier and more efficient for researchers to design and modify the scenario;
- as the name suggests, the simulator in Fig. 2.2a is compact. It is only facilitated with basic functions (no binoculars screen, back view, and only one ARPA system).

Thus the compact simulator is not capable of being used as a training platform but is eligible for research aim.

The simulator in Fig. 2.2c is flexible for research because, different from Kongsberg® products, it is not yet commercialized. NTNU, as the stakeholder sharing its intelligence property to the hardware, has the opportunity to shape the simulator and its capability in accordance with exact demands in NTNU's scope.

Sometimes the research vessel is also used for preliminary study. Though the simulator platforms are made verisimilar to reality, two issues made preliminary studies on real vessels non-substitutable:

- the experimental scenarios on the simulators are set up by known physical laws and based on accepted deduced principles/inference. However, there are unknown natural mechanisms that result in the difference between the simulator setup and what it simulates; this applies especially to new problems;
- as simulator setup can be made arbitrarily sometimes the experimental designer might deviate too far from the actual situations, and it makes the efforts meaningless and costs in time and money in vain.

In this regard, a research vessel is the best platform to discover any uncharted problems and phenomena. It also applies to humans in a laboratory simulator environment, and actual open-sea conditions are still different after all.

### 2.1.2 Quantitative Study

A quantitative study takes place when the problem is preliminarily verified as worth a comprehensive study. Simulators in Fig. 2.2b are used for quantitative study the most. There are five standard maritime training simulators at NTNU i Ålesund, four of them are the same as in Fig. 2.2b and another one is equipped with a dome screen wall and made on an even larger scale (equal to a regular ferry). The experimental setup and scenario are designed and defined in the central control room by K-sim Instructor, and all participants are operating in the same environments. These facilities are initially for maritime navigators' training, but this process can be deemed as a typical way of massive data collection. In this group of simulators, two types of experiments are carried out:

- individual scenario: all participants are operating individually, and their own ships are invisible to each other, which means they are carrying the same task out in

Table 2.1: Usage of different platforms in Fig. 2.2

Platform	Preliminary	Quantitative	Testbed
Fig. 2.2a	✓	-	-
Fig. 2.2b	-	✓	✓
Fig. 2.2c	✓	✓	✓
Fig. 2.2d	✓	✓	✓

different copies. Using this group of simulators to implement such an experiment drastically saves time and expense as five sets of data can be collected simultaneously from five simulators, and simulator-based experiments do not burn even a drop of diesel.

- cooperative scenario: since there are five simulators, their own ships can be configured as visible to each other to become target ships to other navigators. Taking advantage of this, experimental scenarios which need cooperation and intercommunication (in a traffic system) can also be implemented.

Simulator in Fig. 2.2c is also used for the quantitative study. Since the standard maritime training simulators' schedules are tightly occupied almost every day for teaching, training, and research tasks, and this non-standard self-developed platform cannot be used for teaching and training aims, it has plenty of time intervals for research tasks.

### 2.1.3 Testbed for Verification and Demonstration

As new decision support systems and other automatic functions are developed, they need to be tested, verified, and demonstrated. Platforms in Fig. 2.2b, 2.2c have been used as testbeds for these aims. These two platforms have different data exchange interfaces:

- data output: both platforms are capable of exporting real-time data, including ship maneuvering figures, geographical information, and environmental loads. These data export enables us to develop a decision support system for navigational performance enhancement;
- data input: only platform in Fig. 2.2c has the potential to integrate algorithms in the loop. This feature outperforms K-sim platforms, making the test of automated ship guidance, navigation, and control possible.

The research vessel is definitely also a good testbed, and there have been relevant research items carried out based on data onboard Gunnerus [58] [59]. Moreover, it may have a similar problem as the K-sim platform in Fig. 2.2b, where besides the technical problem of data input, onboard safety and ethical issues might be concerned.

The usage of each platform is summarized as in Table 2.1.

## 2.2 Design & Implementation

As shown in Fig. 2.3, there are mainly three groups of experimenters:

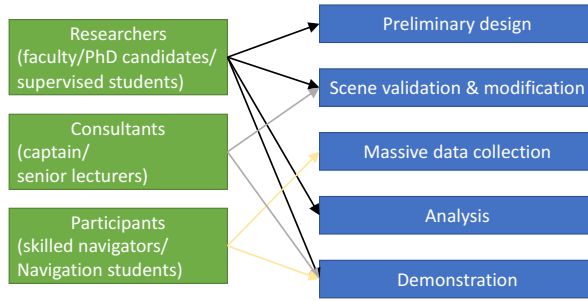


Figure 2.3: Participation in experiment design process.

- researchers: who are in charge of and responsible for the whole experiment throughout all procedures, including design, execution, analysis, and demonstration;
- consultants: who provide expertise and occupational suggestions to improve the experiment process;
- participants: who carry out the specific experiment tasks on experimental platforms.

Besides, there are five steps in general when designing and implementing an experiment:

- preliminary design: the researchers come up with novel research ideas and problems to explore. They should do a preliminary literature review to concrete the problem based on the current state-of-the-art and propose a preliminary route map to improve the method or explore the problem;
- validation & modification: as the problem to be explored might deviate from the researchers' exact interests and professions, consultants are invited to provide expertise. In HITL maritime domain, captains and university lecturers often play these roles by discussion and workshop to improve the experimental design to trim the irrational parts and make it more practical;
- massive implementation: researchers are responsible for organizing massive data collection and supervising the experiment implementation (to secure the process according to the plan), but the participants who carry out the tasks are usually skilled navigators and navigation students (in the bachelor's program);
- analysis: researchers are in charge of the data interpretation and analysis and developing new decision support/automatic functions and algorithms; the supervisor in this step can also perform supervision over students;
- verification & demonstration: as researchers develop the new functions and algorithms, they are obligated to organize new experimental sessions to verify the results and performance of refined products; as the main difference between consultants and participants is their experience, in the demonstration phase, practitioners



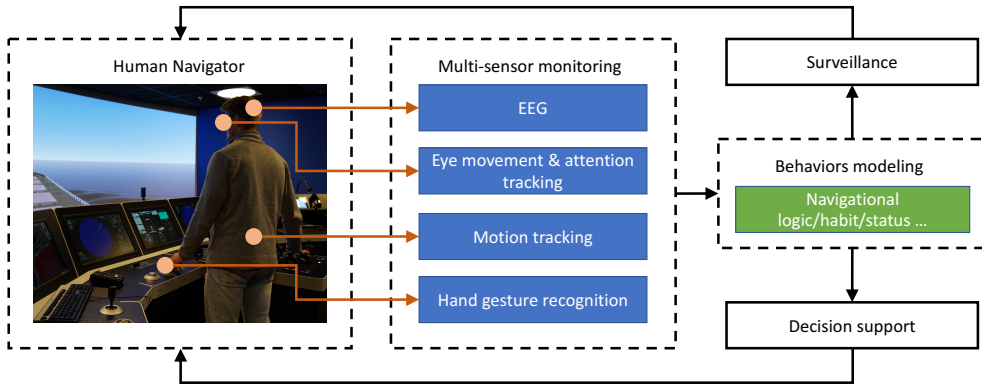


Figure 2.4: Intelligent ship-bridge system for research on HITL navigational operations.

with different levels of experience are invited to provide their opinions for any further improvement.

### 2.3 Utilization

Fig. 2.4 depicts the workflow of an intelligent ship-bridge system in general. The following parts are included in this framework:

- executives: the human navigators are also the bearers to be monitored and recorded by the multi-sensor system;
- multi-sensor monitoring: more channels of sensors are expected in the monitoring systems to provide cross-explain to the navigators' behaviors; However, the more sensors equipped, the more influence might be caused on the navigators' performance. In this context, non-intrusive solutions are preferable. If not available, the number of sensor channels should be controlled; the applied examples are shown in Fig. 2.5;
- behavior modeling: data interpretation and data mining by machine learning algorithms to explore the potential navigational mechanisms;
- derived functions: some passive functions without intervention to the control loop are developed based on the modeled navigational behaviors.

The workflow of behavior modeling and derived functions parts are shown in Fig. 2.6.

#### 2.3.1 Monitoring & Data Collection

Tools for monitoring can be sorted as intrusive and non-intrusive. The solutions to visual attention tracking are various: wearable eye trackers are still popular and versatile in conducting various research items (as in Fig. 2.5c, wearable eye tracker is capable of presenting precise visually transitting path with glance durations), and has been widely

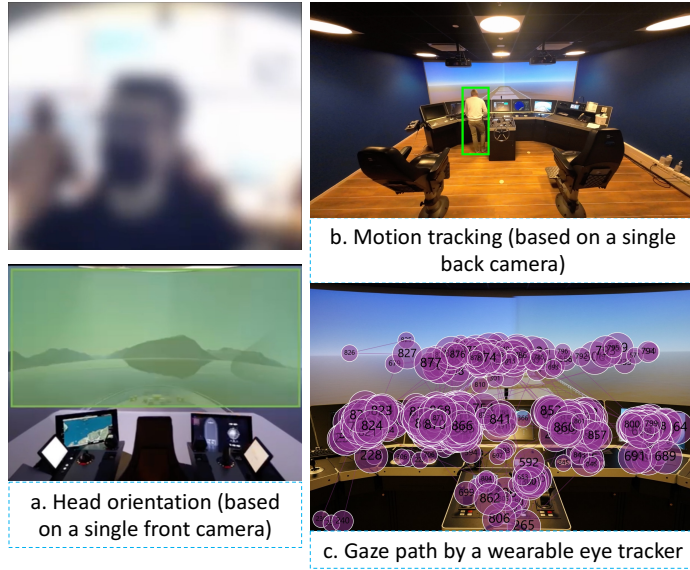


Figure 2.5: Applied multi-sensor monitoring scenes.

used in research in maritime domain: to monitor the fatigue status and mental workload [60][61], test the usability of virtual reality equipment and simulators [62], improve the nautical training [63]. As for specific maritime operations, studies have been conducted on high-speed cruising [64] and heavy crane lifting [43].

Non-intrusive camera-based (RGB/RGBD) algorithms are developed based on collected videos, as shown in Fig. 2.5 and in this dissertation. In this application, by feeding a deep learning neural network with images with facial and head orientational information, the trained algorithm can tell the navigator's visual attention zones (the navigator is looking at the green zone in Fig. 2.5a). Related works in the computer vision field are beneficial to the development of such solution in the maritime domain as many attempts and efforts have been put on using cameras to realize visual attention recognition. The approaches to achieve it can be sorted into mainly two classes: eye-gaze tracking [65] and head orientation detection [66], and the two ways are often combined in recent mainstream. Lee *et al.* carried out an interesting study by using eye gaze as a remote controller to a TV, and 2D geometric transform was used to achieve eye gaze mapping in the process [67]; Cheung *et al.* developed a low-cost solution by applying a simulated 3D head model based on a web camera to achieve eye gaze tracking [68]; Chi *et al.* designed a global calibration method on a multi-camera structure, which solved the problem when calibration reference was not within camera's range [69]; Gudi *et al.* applied the convolutional neural network (CNN) algorithm to evaluate different types of inputs, including the whole face, two eyes, and single eye based on a webcam as well [70]; Dai *et al.* integrated binocular features and spatial attention mechanism into the CNN algorithm [71]. The fore-mentioned algorithms and applications indicate that current

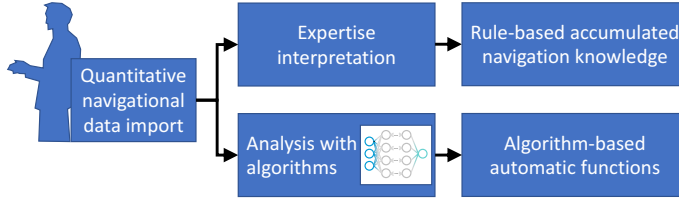


Figure 2.6: Analysis procedures.

computer vision techniques can perform precise and robust visual attention recognition with low-cost solutions.

In the implementation in this dissertation, the configuration of cameras for tracking and tracing varies. Both single- and dual-camera systems are configured in the experiment environments. The head orientation detection is dealt with a single camera system, and visual attention and motion of unseating navigators are studied with a dual-camera system. The more data in this stage, the easier the analysis process can be in the following step.

### 2.3.2 Operations Analysis and Learning

To deal with collected data, there are two different ways. One is data interpretation based on expertise, and another is the algorithm-based data-driven method (as illustrated in Fig. 2.6). The two methods have their virtues:

- Expertise interpretation: first, expertise may bring a qualitative assessment of the data and rationalize the logic of navigational operations; it is not handful for them to discover existed problems; a step further, by using analytical methods to calculate correlations between different variables, and conducting interviews with experimenters, expertise interpretation may give an intuitionistic and comprehensible result. This may prove a boon to navigational training and teaching.
- Data-driven algorithms: mature machine learning algorithms such as SVM and neural network/deep learning have a satisfying performance in classification and pattern recognition tasks. They are qualified to track navigators' visual attention, body motion, and gestures. It is a good choice for developing automatic functions and automated products, but as the calculation is done within a black box, the processing is difficult to clarify and explain. However, this also triggers the research interest in explainable artificial intelligence.

### 2.3.3 Online Surveillance & Decision Support

Fig. 2.5a shows how the deep learning algorithm classifies visual attention zones, and Fig. 2.5b illustrates how the trained convolutional-neural-network algorithm traces the navigator's motion (body movement). These algorithms are developed for passive surveillance, but it has the potential to detect anomalies that may occur and give warnings and signals to avoid failures.

Based on the established surveillance network, analysis of navigational operations and behaviors, different types of decision support tools and systems can be developed for specific navigational tasks.

2.4 Chapter summary

This chapter introduces the fundamentals of HITL experiments. Different experimental platforms and their capability in different experimental scenarios in this dissertation are also briefly introduced. Two ways of data analysis, including expertise interpretation and algorithm-based analysis, are briefly discussed.

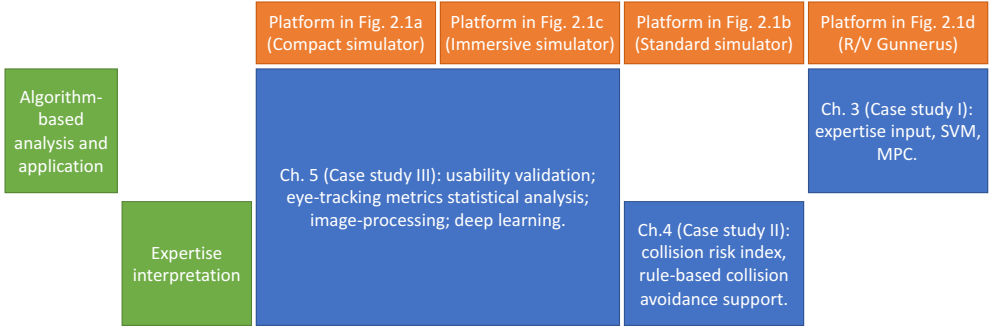


Figure 2.7: Interconnection of experimental platforms and analysis methods in this dissertation.

Fig. 2.7 shows how experimental platforms and corresponding data analysis methods are contained in different chapters. Chapter 3 presents expertise-knowledge-aided path routing, which uses R/V Gunnerus as the platform for the data source. Chapter 4 illustrates navigating patterns analysis, which uses standard maritime simulators; Chapter 5 demonstrates the visual attention analysis, which mainly uses the immersive simulator dome as the platform but also uses the compact simulator for preliminary scenario design (which is not discussed in detail). The three case studies form the main part of this dissertation, with the main goal to implement the synthesis study of HITL navigational operations.

## Case study: Expertise-knowledge aided path routing

One of the major concerns that may hamper the development of autonomous ships is its uncertainty when facing unexpected situations. The capacity to handle cases of complicated conditions of current autonomous ships, especially in the case of danger and emergency, is highly contentious. In this respect, human expertise is believed to outperform ship intelligence as humans are able to address unexpected situations synthetically based on their knowledge and experience [72] [73] [74]. On the other hand, it is suggested that ship intelligence should be applied in some simple cases first [75]. A commuter ferry that executes a regular route between two unaltered ports can be seen as a pragmatic example as it simplifies the autonomous navigation process to a large extent.

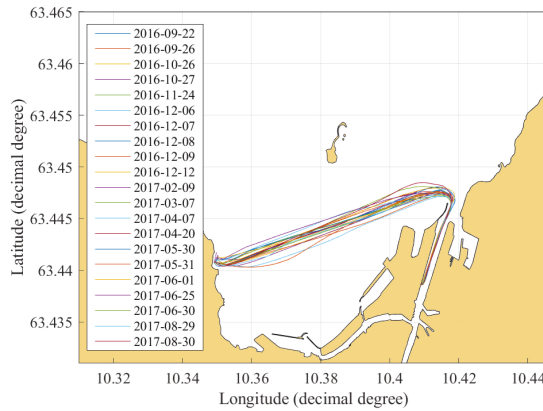


Figure 3.1: Collection of 21 commuter sailings.

This chapter presents research results from papers I and II. The data used in this paper are collected from a commuting route located in Trondheim, Norway. The commuting route connects the Trondhjem Biological Station and the berthing point at the estuary of the Nidelva river. The commuting route is executed by NTNU's research vessel R/V Gunnerus (as the source of onboard log data input). The log data record the information of 21 sailings from September 2016 to August 2017 as shown in Fig. 3.1. The presented works are expected to answer following questions:

- how onboard log data can be interpreted in guidance of expertise?
- how the expertise knowledge may support the navigation in loop?

### 3.1 Methodology

The general framework is shown as Fig. 3.2 and the commuting route is conceptually marked as the white curve in the map. The workflow includes several key steps: data collection and preprocessing, the design of SVM and its implementation on log data, interpretation of the classification result and its visualization, and at last, a quantitative evaluation function is proposed to assess the level of sailing safety of the ferry based on the classification result of the accumulated historical log data.

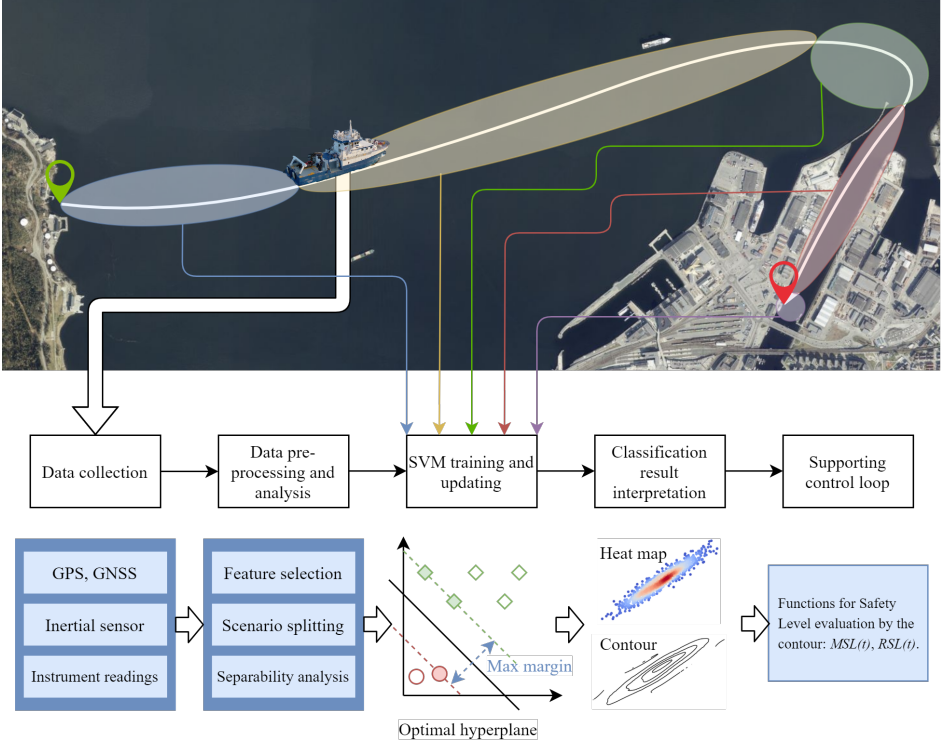


Figure 3.2: Framework of the proposed decision support system for sailing status recognition and safety evaluation (map resource: the Norwegian Mapping Authority).

#### 3.1.1 Data collection and pre-processing

According to the navigation and maneuvering habits of captains, featured items are selected from collected data. They are listed and sorted as in Table 3.1. All eight featured items in Table 3.1 are designated as variables for training the scenario recognition algorithm.

#### 3.1.2 Definition for scenarios by human expertise

According to human expertise, a commuting sailing route can be divided into different scenarios in terms of maneuvering commands and the vessel response which can be

Table 3.1: Classification of log data

Ship behaviors	Machinery actuators
heading ( $^{\circ}$ )	bow thruster feedback (%)
speed (knots)	portboard-rpm feedback (%)
pitch ( $^{\circ}$ )	starboard-rpm feedback (%)
	portboard-Azi feedback ( $^{\circ}$ )
	starboard-Azi feedback ( $^{\circ}$ )

reflected by collected log data. In this customized commuting route, five scenarios are separated from the whole sailing, which are described in detail as following:

- Departing (DPT): the ferry sets off from the port and keeps accelerating;
- Cruising (CRS): the ferry usually reaches the rated RPM and travels on the route smoothly;
- Turning (TRN): the ferry adjusts its course towards another direction. Deceleration and angular speed increase in this phase;
- Converging (CVG): the ferry moves in the narrow channel at a speed lower than the rated, and it finally gets parallel to the coastline with a short distance;
- Docking (DCK): the ferry is with no surge speed but only sway, by using the bow thruster to push itself into the berthing point.

The rough illustration of the separation is shown in the map in Fig. 3.2, as five scenarios are marked with ovals in different colors.

### 3.1.3 Empirical criteria based on human expertise

Based on the collected data and according to human expertise, empirical criteria are given as listed in Table 3.2. Basically, since there are several items describing one scenario simultaneously, by which the accuracy has been guaranteed to determine the ferry's status at the moment, the value range of the data is constrained softly to avoid misjudging caused by the common fluctuation of the ship status during a sailing (even in a steady state).

Hereupon, the original database is constructed as Eq. 3.1, where  $X$  represents for a database consisted by  $n$  items described by 8 variables mentioned in Table 3.1.

$$\begin{aligned}
 \log \text{ data} &= \{X; L\}, X \in \mathbb{R}^{n \times 8}, L \in \mathbb{R}^{n \times 1} \\
 L &= \{l_1, l_2, \dots, l_n\} \\
 \forall l_i \in L, l_i &\in \{\text{departing, cruising, turning, converging, docking}\}
 \end{aligned} \tag{3.1}$$

### 3.1.4 Separability precheck

Before designing the algorithm for the classifier, it is proper to have a preview of the data to check whether the database is separable. The database can be examined by

Table 3.2: empirical criteria for the commuting route decomposition

	DPT	CRS	TRN	CVG	CK
<b>Ship behaviors</b>					
heading ( $\psi$ , °)	$\frac{\Delta\psi}{\Delta t} < -0.3$	$ \frac{\Delta\psi}{\Delta t}  < 0.1$	$\frac{\Delta\psi}{\Delta t} > 0.5$	$ \frac{\Delta\psi}{\Delta t}  < 0.1$	–
grounding speed ( $v$ , knot)	$\leq 6$	$\geq 10$	$\frac{\Delta v}{\Delta t} < -0.02$	$[4, 6]$	$\leq 2$
pitch (°)	–	$abs^* > 0.5$	–	$abs > 0$	–
<b>Machinery actuators</b>					
bow thruster (%)	$abs > 0.1$	–	–	–	$abs > 10$
port-rpm (%)	$abs < 60$	$abs > 75$	$abs \in [40, 60]$	$abs \in [40, 60]$	$abs \in [0, 30]$
stbd-rpm (%)	$abs < 60$	$abs > 75$	$abs \in [40, 60]$	$abs \in [40, 60]$	$abs \in [0, 30]$
port-azi (°)	$abs > 0.5$	$abs < 1$	$abs > 0.5$	$abs < 2$	$> 50$
stbd-azi (°)	$abs > 0.5$	$abs < 1$	$abs > 0.5$	$abs < 2$	$abs < 1$

\*  $abs$  is the abbreviation of *absolute value*.

t-distributed stochastic neighbor embedding (t-SNE) algorithm [76]. By the algorithm, the high-dimensional database is converted into a visualizable low-dimensional database:

$$X = \{x_1, x_2, \dots, x_n\} \in \mathbb{R}^{n \times 8} \xrightarrow{\text{t-SNE}} Y = \{y_1, y_2, \dots, y_n\} \in \mathbb{R}^{n \times 2} \quad (3.2)$$

The t-SNE result is shown as in Fig. 3.3. From the visualized result, it can be clearly found that there is a trend for each scenario to get clustered, hence it can be inferred that the sailing route can be separated into different scenarios based on the selected data.

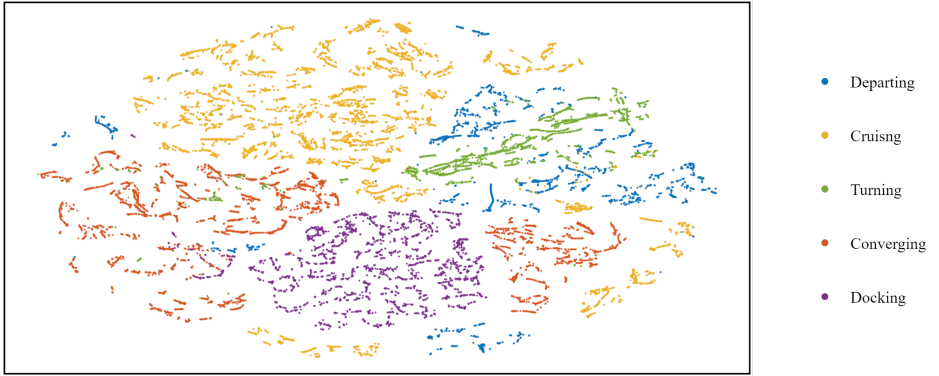


Figure 3.3: Visualization of dimension reduction result by t-SNE.

Since the database is with a dimensionality at 8, which can be considered as a high dimensional database. From the precheck of t-SNE dimension reduction and the pair



plots, It is putatively assumed scenarios in the sailing route described by log data are approximate linear separable.

### 3.1.5 Support vector machine

SVM algorithm is chosen to build a classifier to solve the classification problem. The SVM algorithm is trained with collected log data according to eight features in Table 3.1. In practice, the multiclass classification problem is converted into several binary classification problems [77]. Then, there will be a specific classifier  $CLF_k$  for scenario  $k$ , and 5 in total for all scenarios. Taking scenario  $k$  as an example, for the data points whose original labels are the same as scenario  $k$ , they will be given new labels 1; otherwise, they will be given new labels -1. Then a new vector  $L'$  will be created by updated labels, and the vector will substitute the original label  $L$ . This process can be expressed as:

$$CLF_k : \begin{cases} l'_i = 1, \text{ if } l_i = j; \\ l'_i = -1, \text{ otherwise.} \end{cases} \quad (3.3)$$

For each binary classifier, there is a specific optimal hyperplane:

$$OH_k : W_k X + b_k = 0, \quad (3.4)$$

where  $W_k$  is the normal vector to the hyperplane. The optimal hyperplane lies between two parallel hyperplanes:

$$\begin{aligned} OH_k^+ : W_k X + b_k &= 1; \\ OH_k^- : W_k X + b_k &= -1; \end{aligned} \quad (3.5)$$

Points on and above hyperplane  $OH_k^+$  will be assigned label 1, and finally turns into label  $k$ . And points on and below hyperplane  $OH_k^-$  will be assigned label -1, and finally will not be classified into the dataset of scenario  $k$ .

### 3.1.6 Likelihood map and safety level calculation

As log data accumulated along the sailings run times by times, the database for training the SVM classifier is getting larger. Besides the 8 featured data items, the geographical information is also recorded. Therefore, another database can be constructed based on the geographical information of those data points which are correctly classified by the classifier. And data points can be drawn on a geographical map reflecting the site of each scenario in the sailing route. Then the map can be converted into a heat map in terms of the density of the geographical distribution of data points. At this step, kernel density estimation method helps to calculate the estimated density at each datum point  $x_j$ :

$$\hat{p}(x_j) = \frac{1}{mh} \sum_{i=1}^m K\left(\frac{x_j - x_i}{h}\right), \quad (3.6)$$

in the expression,  $h(h > 0)$  is a smoothing parameter;  $K$  is the kernel for scaling, and Gaussian kernel is chosen in this paper to estimate the density. Then a 2D heat

map illustrating the density distribution can be drawn accordingly. Since the database is updated after new sailing data is appended, the numerical value of the density will become larger and larger, which implies that raw density value itself does not contain standard useful information to help the human to make decision. Therefore, to avoid it from being nothing but fancy, the density scale is normalized into  $[0, 1]$ :

$$\hat{p}_N(x_j) = \frac{\hat{p}(x_j) - \min(\hat{p})}{\max(\hat{p}) - \min(\hat{p})}, \quad (3.7)$$

The normalized density 1 refers to the densest site on the sailing route, while 0 refers to the sparsest site. The ferry is believed to be safer when travelling on a site where the normalized density is higher, while the captain should be vigilant when the ferry goes into the low normalized density site. Meanwhile, heatmaps can be converted to contours by an interpolation operation based on the normalized density distribution. Cubic spline interpolation method can be applied to realize this conversion. Then the map is gridded, and the density is calculated by the interpolation. By connecting grid points with the same density value, the contour map is obtained to demonstrate a continuously approximation of the density distribution at the vicinity area of the scenario. The distribution function  $SL(y)$  can be obtained by ploy-fitting the statistics of the safety level, where  $y$  represents the position.

### 3.1.7 Verification how the safety level benefits in MPC

The concept of safety level is integrated into the cost function to implement the MPC (model predictive control). The vessel kinematics can be represented as Eq. 3.8. The right-hand side of the kinetics equation  $\tau$  is the input force which equals  $[f_u f_v t_r]'$ , where  $H$  equals  $[1 \ 0 \ 0; 0 \ 1 \ 0]$ , and  $y$  equals  $[NE]'$ .

$$\begin{aligned} \dot{\eta} &= R(\psi)\nu, \\ M_{RB}\dot{\nu} + M_A\dot{\nu}_r + C_{RB}(\nu)\nu + C_A(\nu_r)\nu_r + D(\nu_r)\nu_r &= \tau, \\ y &= H\eta. \end{aligned} \quad (3.8)$$

The original cost function is defined as:

$$J(t) = (y(t+1) - y_{ref})^\top Q(y(t+1) - y_{ref}) + \Delta u(t+1)^\top R \Delta u(t+1). \quad (3.9)$$

The optimization goal is to minimize the cost function  $J$ , the positive term  $(1 - SL(y))$  is used to conform the implication of safety level and the optimization target. The cost function is thus augmented as:

$$J^*(t) = (y(t+1) - y_{ref})^\top Q(y(t+1) - y_{ref}) + \Delta u(t+1)^\top R \Delta u(t+1) + W(1 - SL(y(t+1))). \quad (3.10)$$

Eq. 3.9 and 3.10 give the cost function at one time step prediction, while MPC is predicting over a length of time horizon  $N_p$  to determine the best control candidate, so the overall cost prediction at a certain time step can be represented as Eq. 3.11.

$$\mathbf{J}^*(t) = \sum_{k=t+1}^{t+N_p} J^*(k). \quad (3.11)$$

### 3.1.8 Assessing the safety level by the contour map

At the last step in the proposed method, a concept of safety levels is built upon the normalized density distribution described by contour maps. Safety levels (SL) are directly represented by the normalized density of the geographical location. Hereupon, two dimensionless items can be further calculated to reflect different aims of evaluation: receding safety level (RSL) expressed as Eq. 3.12 and mean safety level (MSL) as Eq. 3.13.

$$RSL(t) = \frac{\sum_{N(t-\Delta T)}^{N(t)} p_i}{\Delta T}, \quad (3.12)$$

$$MSL(t) = \frac{\sum_{i=0}^{N(t)} p_i}{N(t)} \quad (3.13)$$

$N$  is the number of accumulated log data points until the moment  $t$ .  $\Delta T$  is the number of sampled data points in the receding horizon, while the receding horizon is chosen manually.

RSL calculates the mean safety level in a fixed time scale. The receding horizon for calculation is updated after each sampling. MSL calculates the mean safety level from the start to current moment  $t$ . MSL may reflect the overall safety level, hence it can be used to evaluate the performance of the human maneuvering in a sailing.

## 3.2 Results

The proposed method is implemented to the database built upon collected 16 sailings' log data. In this section, results are presented in three parts: classification results from the SVM classifier; the derived likelihood heat maps and normalized numerical contour maps, and online testing.

### 3.2.1 Classification result

The classifier is built once the first sailing's log data is added to the SVM training database. As the database evolves when new log data come into, the classifier will be updated therewith. The demonstration of the evolution result irrespective of scenarios is shown as Table 3.3.

From Table 3.3, it clearly shows that the precision of the classification result is trending to increase as the classifier evolves. As the database being larger, the precision of the classifier keeps growing. At last, the mean value of the classification precision has been developed over 96 % based on whole collected sailings' data.

After illustrating the result in a macroscope, Fig. 3.4 shows the classification precision with respect to different scenarios, and it comprehensively reveals how different scenarios correlate pairwise. In general, the performance of the classifier is improved after several evolutions.

Table 3.3: Illustration of the classifier evolution process.

Testset	Classifier		
	4	9	14
5	0.9031	-	-
10	0.9723	0.9815	-
15	0.9675	0.9578	0.9610
Mean	0.9370	0.9593	0.9684

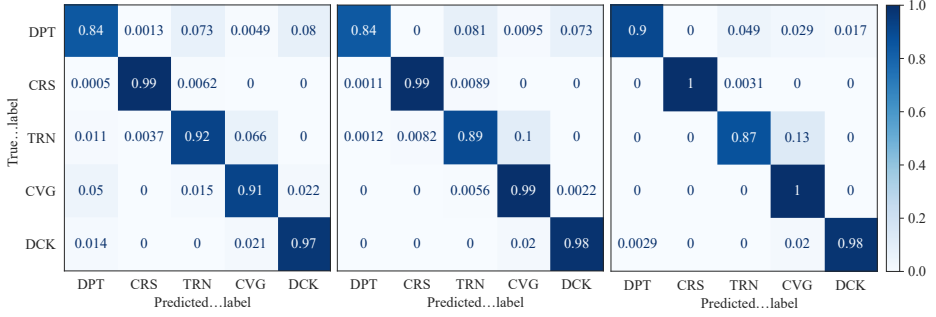


Figure 3.4: Confusion matrix reflecting precision by scenarios (left: CLF No.4; middle: CLF No. 9; right: CLF No. 14).

### 3.2.2 Likelihood heat maps and derived contours

Heat maps based on the accumulated database can be drawn, as shown in Fig. 3.5. The first five subplots show the heatmap of each scenario, while the last subplot at the right-bottom shows an overview of the complete route.

The heat maps can help the reader, e.g. captains, have a direct sense of the most travelled sites. And this feature is prominent especially in scenarios cruising, turning, and converging. However, since both the departing and docking are undergoing in a very concentrated site, the density distribution appears to be somewhat diffusion. However, it is thought to be in a tolerant extent, and can be ameliorated as the database being larger.

Based on heat maps shown in Fig. 3.5, a set of contours with respect to each scenario can be drawn as Fig. 3.6. Different from the heat maps which provide an intuitive illustration and sense of the most travelled area, the set of contours quantitatively demonstrates how the density distributes on a geographical map. Since contours are obtained by an interpolation operation, its fidelity and creditability are dependent to the quantity of data. In general, the overall trend in each scenario has been shown. For example, in the contour of cruising scenario, the closer to the center of the heat area, the larger the normalized density is.

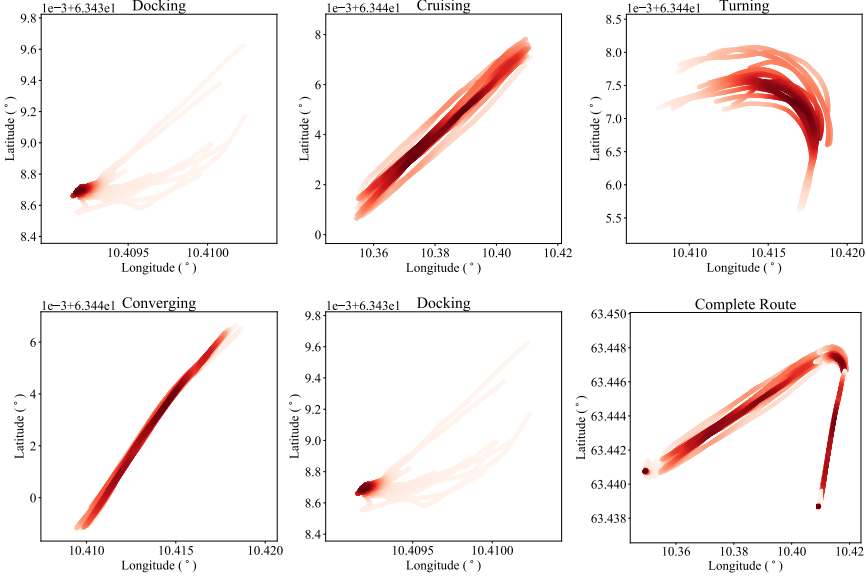


Figure 3.5: Heat maps of different scenarios.

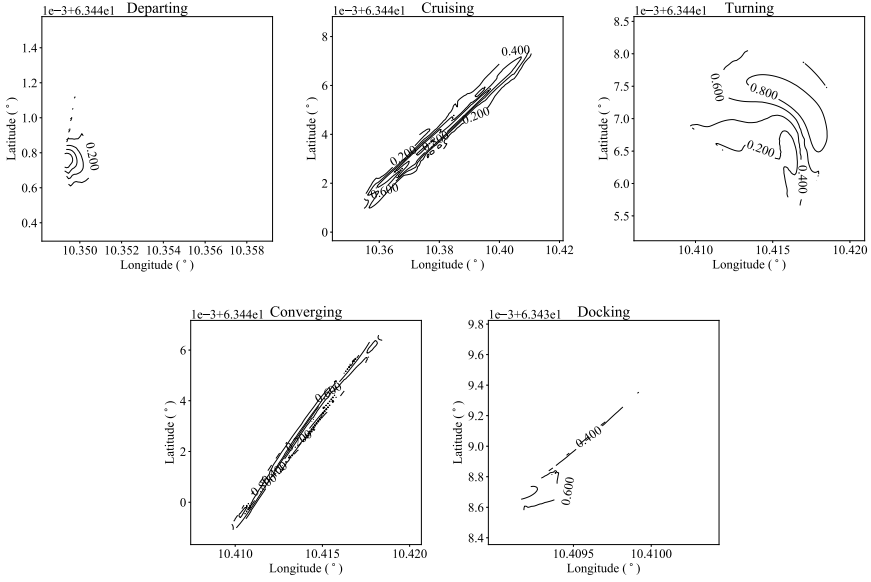


Figure 3.6: Heat maps of different scenarios.

### 3.2.3 Verification in MPC loop

In this part, the path following simulation results will be shown and assessed. Fig. 3.7 shows the path of reference (Sailing No. 6), the original MPC and the improved MPC with safety level (MPC-SL). The safety level assessment is given as Table 3.4. The prediction horizon  $N_p$  is set as 10.

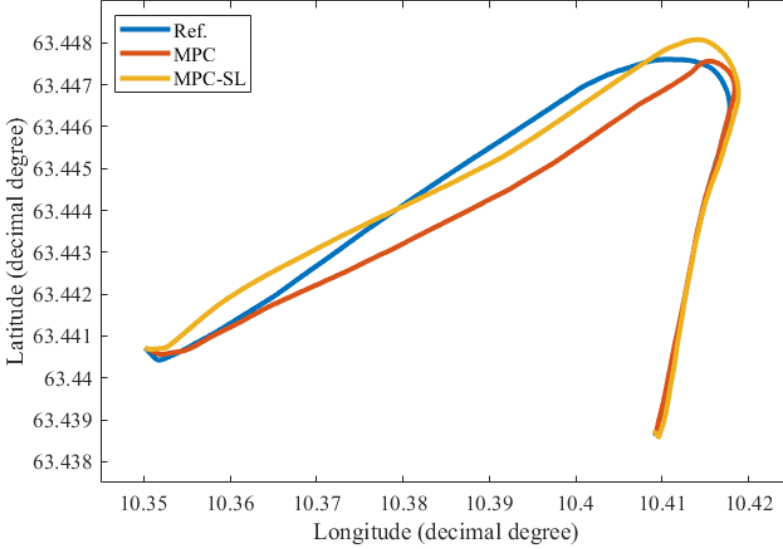


Figure 3.7: Path following simulation by MPC

Table 3.4: Verification of safety level in loop.

Scenario	Safety level		
	Ref.	MPC	MPC-SL
DPT	0.4203	0.4574	<b>0.5449</b>
CRS	0.4259	0.5135	<b>0.6743</b>
TRN	0.6851	0.6304	<b>0.6999</b>
CVG	0.5065	<b>0.5938</b>	0.5059
DCK	<b>0.6161</b>	0.4157	0.4158
Overall	0.5199	0.4574	0.5681

From the safety level statistics in Table 3.4, it can be implicitly summarized that the safety level has a strong impact on the control. After the safety level term is added into the cost function, the overall safety level increases significantly, and so as in scenario DPT, CRS and TRN.

When the vessel travels in a narrow water tunnel in CVG, where the gradient of the safety level can be very sharp, the safety level suffers a decline but in moderate level.

When the vessel is in the final bow thrusting stage, where the safety level heatmap almost concentrates to a point, it is difficult for the vessel to be strictly in the circle of high safety so that the safety level in DCK is low. In general, the safety level term improves the control in terms of safety noticeably, which suggests that the proposed methodology attains a good performance and further study can be conducted in practice.

### 3.2.4 Safety level assessment

#### Sailing status recognition:

Fig. 3.8 shows the result of the online sailing status recognition testing. The dashed lines divide the timeline into segments remarking real periods of each scenario, while the mark ‘+’ represents the recognized status at each sampling step.

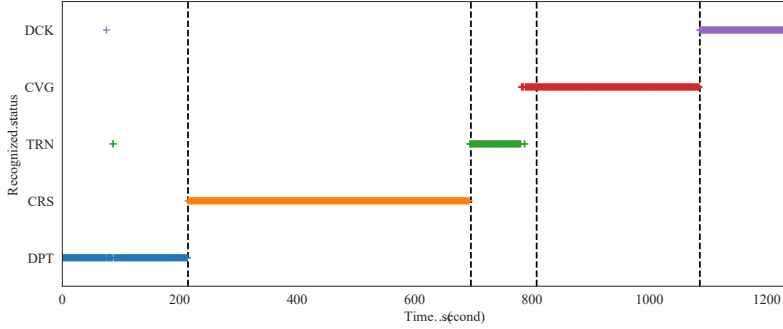


Figure 3.8: Online testing of the sailing status recognition.

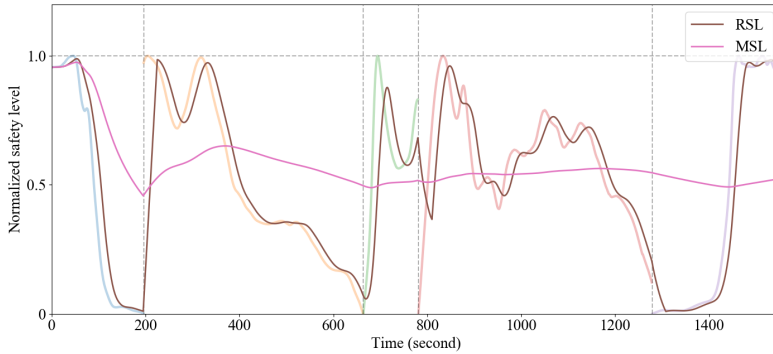


Figure 3.9: Calculated MSL and RSL (Diluted lines are the real time safe level).

**Safety level evaluation:**

According to the defined terms, RSL and MSL, and the obtained contour maps, safety level evaluation is implemented accordingly.

The two items, MSL and RSL, reflecting the safety level from different aspects, are calculated and shown as in Fig. 3.9. Since RSL calculates the average safety level at a fixed length of the past period, there is a delay to reflect the change of the safety level. This delay provides RSL the ability to reduce the effect at the start and the end during the transition time between different scenarios, which makes RSL to describe the sailing safety in a moderate way. Afterall, MSL can provide an overall evaluation of the sailing safety.

**3.3 Chapter summary**

This chapter introduces a method to utilize log data from a ferry to establish an onboard safety awareness system in order to help human to make decisions. Collected data are classified by an SVM algorithm and its results are presented as figures of heat maps and contours by statistical method. Both sets of figures together may assist to evaluate the sailing safety level. By defining new items reflecting safety levels with respect to geographical locations, the result can be used to optimize the control. MPC is designed with the safety level term integrated to verify its significance. The main idea of this chapter is to synthetically use both human expertise and objective log data to make rudiment work for autonomous navigation.



## Case study: Navigating patterns analysis and application

In this chapter, the navigating patterns (NP) of navigators when sailing in a narrow strait with intense marine traffic coming from the starboard side of the own ship (OS). This scenario is drawn from traffic environment commonly-seen in some busy straits, such as the Dover strait. In these congested waters, there are specific separation schemes to secure the safety and efficiency of the traffic. When a ship is crossing such strait, usually the target ships (TSs) are coming from either the starboard or the portboard side at a time. Navigators' NPs reflected by the recorded maneuvering data and route evaluation in such traffic environment are summarized. Then, the concluded patterns' features are used to provide on-board guidance in order to support navigators.

The following issues are addressed in this chapter:

- a data-based navigating pattern analysis method is conceived for the crossing scenario in the CA task, and three NPs, specifically conservative, moderate and aggressive modes, are concluded and interpreted;
- a guidance support system is developed based on the navigating patterns analysis (NPA) to assist navigators in making decisions on sailing routes and CA strategies selection.

This chapter presents research results from paper III.

### 4.1 Methodology

#### 4.1.1 Experimental environment

Data used in this section are collected from a Kongsberg K-Sim<sup>®</sup> maritime simulator, as shown in Fig. 4.1 - architecture of K-sim cockpit. The simulator system can provide encoded GPS (only OS) and AIS (both OS and TS) data in standard forms starting with \$GP and \$AIVD, and the decoded data selected for the research goal in this section include:

- From GPS: course, speed over ground, latitude and longitude (in WGS84), north and east (in UTM32N);
- From AIS: MMSI (Maritime Mobile Service Identity, a series of nine digits which is used to uniquely identify the ship), latitude and longitude (in WGS84), course.

#### 4.1.2 Related metrics

DCPA (distance at the closest point of approach) is one of the most important collision risk index and used as the main criterion to assess NPs. The DCPA is a synthesis index

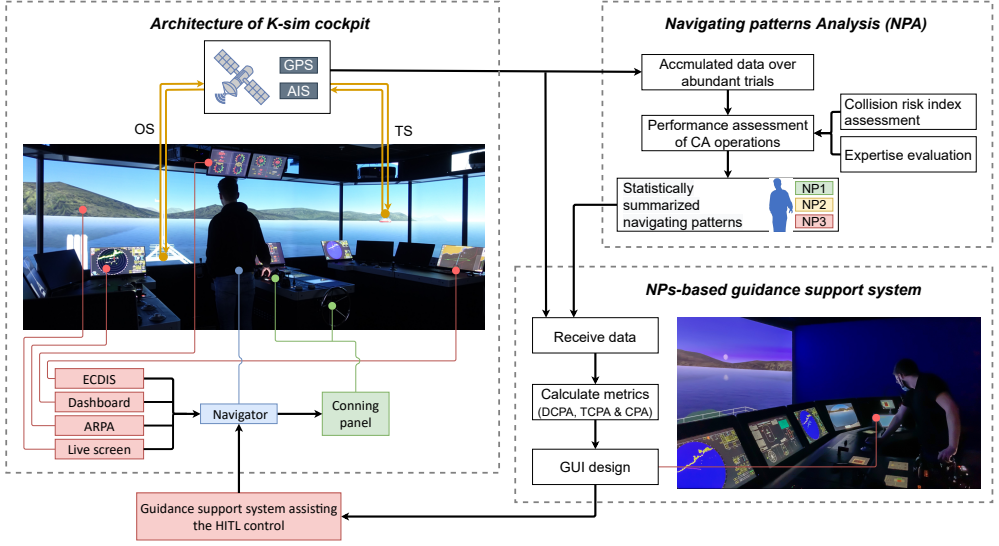


Figure 4.1: Workflow of this case study.

which is capable to reflect the motion properties of both OS and TS [78]. It is illustrated in Fig. 4.2, and calculated as:

$$DCPA = D \cdot \sin(\theta_R - \alpha_{TS}), \quad (4.1)$$

where  $D$  is the distance between OS and TS,  $\theta_R$  is the course of the relative velocity between OS and TS, and  $\alpha_{TS}$  is azimuth angle of TS to the center of OS (irrespective of the course of OS).

Considering the collected data, Eq. 4.1 can be re-write as:

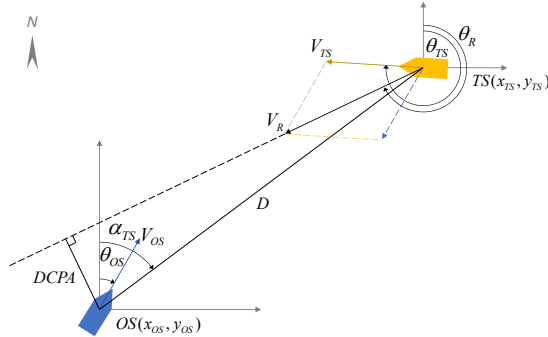


Figure 4.2: Illustration of DCPA.

$$\begin{aligned}
 \text{DCPA} &= D \cdot \sin(\theta_R - \alpha_{TS}) \\
 &= D \cdot (\sin\theta_R \cdot \cos\alpha_{TS} - \cos\theta_R \cdot \sin\alpha_{TS}) \\
 &= D \cdot \left( \frac{V_{R,x}}{\|V_R\|} \cdot \frac{D_y}{D} - \frac{V_{R,y}}{\|V_R\|} \cdot \frac{D_x}{D} \right) \\
 &= \frac{V_{R,x}}{\|V_R\|} \cdot D_y - \frac{V_{R,y}}{\|V_R\|} \cdot D_x,
 \end{aligned} \tag{4.2}$$

where  $V_R$  is the relative velocity between OS and TS. The subscript  $x, y$  represent the projected component on the east and north directions.

Since the speed over ground ( $V_{OS}, V_{TS}$  for OS and TS respectively) and course angle ( $\theta_{OS}, \theta_{TS}$  for OS and TS respectively) are collected,  $V_R(V_{R,x}, V_{R,y})$  can be calculated as:

$$\begin{aligned}
 V_{R,x} &= V_{TS,x} - V_{OS,x} \\
 &= V_{TS}\sin\theta_{TS} - V_{OS}\sin\theta_{OS},
 \end{aligned} \tag{4.3}$$

$$\begin{aligned}
 V_{R,y} &= V_{TS,y} - V_{OS,y} \\
 &= V_{TS}\cos\theta_{TS} - V_{OS}\cos\theta_{OS}.
 \end{aligned} \tag{4.4}$$

Based on the positions of OS and TS,  $D(D_x, D_y)$  can be calculated as:

$$\begin{aligned}
 D_x &= x_{TS} - x_{OS}, \\
 D_y &= y_{TS} - y_{OS}.
 \end{aligned} \tag{4.5}$$

Taking Eq. 4.3 - 4.5 into Eq. 4.2, the DCPA can then be obtained.

In addition to DCPA, the passing distance is calculated for the further interpretation. The passing distance is briefly illustrated as in Fig. 4.3. Different from DCPA which serves as a capable index for collision prediction by exploiting the kinetics information of the OS and TS, the conceptual of the passing distance can be leveraged as an index candidate for the result-oriented assessment. The passing distance, specifically for the crossing collision avoidance situation, is defined as:

**Passing Distance:** when two vessels are in a crossing collision avoidance close-encounter situation, the distance when one vessel first pass the velocity vector line of the other from the bow is defined as the passing distance.

According to the definition, passing distance is illustrated as in Fig. 4.3. It is imperative to figure out the moment  $t_{\text{passing}}$  when one vessel first pass the other. The offset from OS to the velocity vector of TS,  $e_{OS}^{TS}$ , can be calculated as:

$$\begin{aligned}
 \hat{y}_{OS} &= x_{OS} \cdot \cot\theta_{TS} + (y_{TS} - x_{TS} \cdot \cot\theta_{TS}), \\
 e_{OS}^{TS} &= |(\hat{y}_{OS} - y_{OS}) \cdot \cos\theta_{TS}|;
 \end{aligned} \tag{4.6}$$

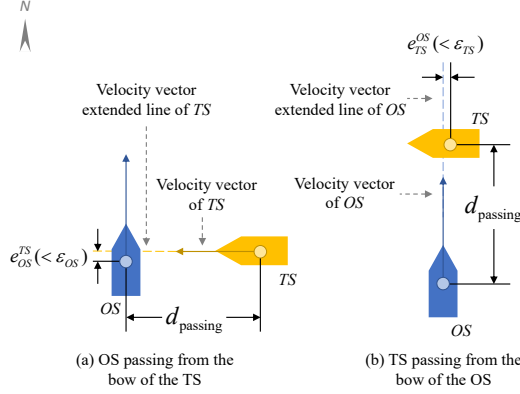


Figure 4.3: Illustration the calculation of the passing distance at  $t_{\text{passing}}$ .

while the offset from TS to the velocity vector of OS,  $e_{TS}^{OS}$ , can be calculated as:

$$\begin{aligned}\hat{y}_{TS} &= x_{TS} \cdot \cot\theta_{OS} + (y_{OS} - x_{OS} \cdot \cot\theta_{OS}), \\ e_{TS}^{OS} &= |(\hat{y}_{TS} - y_{TS}) \cdot \cos\theta_{OS}|.\end{aligned}\quad (4.7)$$

Since  $x_{OS}$  and  $x_{TS}$  can be regarded as functions of time  $t$ , the passing moment  $t_{\text{passing}}$  can be calculated as:

$$\min t_{\text{passing}}, \text{ s.t. } e_{OS}^{TS} < \varepsilon_{OS} \text{ or } e_{TS}^{OS} < \varepsilon_{TS}, \quad (4.8)$$

where  $\varepsilon_{OS}$  and  $\varepsilon_{TS}$  are small values and shall be determine according to the vessels' velocities and the sampling frequencies in practice. And the distance between the OS and TS at  $t_{\text{passing}}$  is denoted as passing distance  $d_{\text{passing}}$ .

## 4.2 Experiment I: Navigating patterns analysis

In this experiment, problems of how NPs can be conceptualized by collectable data are dealt. In general, attempts are made to seek the navigators' maneuvering logic and laws that are concealed in the data, and conclude different NPs. The significance of this experiment lies in two aspects: improving on-board decision support for the HITL-level MASS from an expertise perspective, and developing ship intelligence by rationalizing the use of data, for instance how they should be labelled.

### 4.2.1 Experiment setup and implementation

The water channel between two ports Solavågen and Festøya in Ålesund area of Norway is selected as the basis for the simulation scene. The TSs in the simulation are named as TS1, TS2 and TS3, and all of them come from the starboard side of the OS. The scenario construction is sketched in Fig. 4.4. Therefore, the simulator-based sailing task for the OS can be regarded as a complete sailing task comprised by three sub-CA tasks with different encounter details as shown in Table 4.1. The experiment implementation

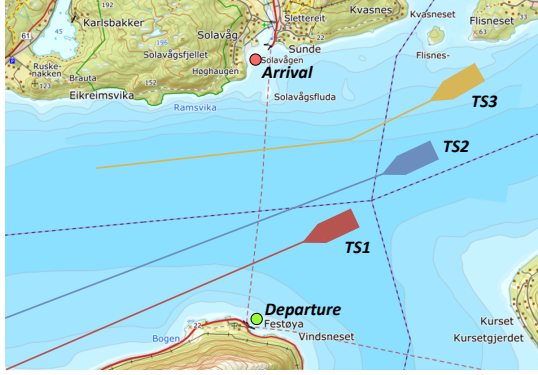


Figure 4.4: Scenario layout of the experimental CA sailing.

is carried out on K-sim<sup>®</sup> simulators at NTNU (as in Fig. 2.2b) in Ålesund. 36 trial sailings are collected in total, and the trials are labelled in the form 'F\_R\_B\_' ('\_' is a digit), where F means the experiments take place in February, while the digit following F represents the date; R is abbreviated for round, and the digit following R represents the round number; and B is abbreviated for bridge, and the digit following B represents the bridge serial number. For example, F4R2B2 means the trial takes places on February 4th, in round 2, and on the bridge No. 2.

Table 4.1: Ship information and experimental conditions setup

Property	OS	TS1	TS2	TS3
<i>Basic information about ships</i>				
length (m)	88	133	165	170
beam (m)	13.8	19.4	27.1	27.5
<i>Initial states</i>				
heading (°)	312	245	245	240
latitude (°)	62.3802	62.3882	62.3986	62.4031
longitude (°)	6.3328	6.3357	6.3569	6.3443
speed (knots)	0	14	15	10

## 4.2.2 Pattern analysis

### CA navigating schemes

In the 36 trials, navigators take 5 different CA navigating schemes when they managed to complete the trial with multiple TSs. Passing from the bow of the TS is denoted as B, while passing from the stern of the TS is denoted as S. Then the 5 schemes are S-B-B, S-S-S, S-S-B, B-S-S, and B-B-B, and they appears in 19, 11, 3, 1, and 2 trials (out of 36 trials) respectively. Theoretically, there can be another three schemes, including B-B-S, B-S-B, and S-B-S, but navigators do not select to complete the task in these schemes. It is inferred that these schemes lead to odd paths that are neither efficient nor safe.

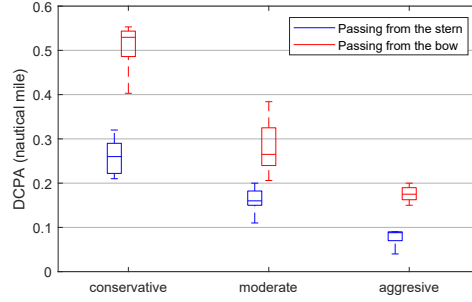


Figure 4.5: Distribution of DCPA in terms of different navigating patterns.

### Expert evaluation

The 36 trials, which includes 108 sub-CA tasks in total, are evaluated by experienced navigators rather than the navigators themselves. Three different evaluation levels are established to rate the CA performance. During evaluation, the three levels labelled with green, yellow, and red colors, were used to mark the CA performance, as no specific terminology was yet created. According to navigators, the different evaluation levels can be intuitively described as:

- **green** means the OS is operated to pass the TS at an ample distance; if passing from the bow, this distance enables the stand-on vessel to actively take action to avoid CA in some emergencies (such as OS engine failure). Meanwhile, passing in this level usually requires sparse operations on the OS control;
- **yellow** means the OS is operated to pass the TS at a sufficient distance with a certain degree of critical operations.
- **red** means the OS is operated to pass the TS at a tight distance, and the navigator needs to maneuver the vessel meticulously to safely pass the TS. If passing from the bow, sometimes such pattern may provoke the operators of the TS.

The evaluation results are listed in Table 4.2. It shows that a navigator may change his navigating strategies (the evaluation colors) in different sub-tasks.

In accordance with the expertise evaluation results, and their assessment principles, the color schemes are renamed with the terminology of the navigating patterns: the green, yellow, and red colors stand for conservative, moderate, and aggressive modes respectively.

### DCPA features

As the terminology of navigating patterns, including conservative, moderate, and aggressive, are proposed, the mapping between the patterns and the metrics are consequently investigate (DCPA and passing distance).

Fig. 4.5 depicts the DCPA distribution in terms of different navigating patterns when passing from the stern and the bow separately.

Table 4.2: Expert evaluation on each CA and its info

	Trial No.	TS1			TS2			TS3			$d_{OS}^{arrival}$ (NM)
		Evl.	DCPA (NM)	$d_{passing}$ (NM)	Evl.	DCPA (NM)	$d_{passing}$ (NM)	Evl.	DCPA (NM)	$d_{passing}$ (NM)	
S-B-B*											
1	F4R3B1		0.211	0.266		0.221	0.318		0.270	0.409	0.642
2	F4R3B2		0.181	0.235		0.251	0.396		0.403	0.612	0.583
3	F4R4B2		0.161	0.222		0.321	0.413		0.533	0.626	0.403
4	F5R1B4		0.175	0.252		0.265	0.367		0.529	0.619	0.352
5	F5R2B2		0.159	0.266		0.251	0.358		0.456	0.585	0.251
6	F5R3B2		0.149	0.256		0.341	0.441		0.536	0.638	0.346
7	F5R3B4		0.164	0.241		0.256	0.346		0.553	0.632	0.374
8	F5R4B2		0.151	0.250		0.331	0.411		0.513	0.634	0.298
9	F5R4B4		0.195	0.290		0.246	0.331		0.547	0.614	0.390
10	F4R4B1		0.174	0.224		0.245	0.356		0.379	0.520	0.528
11	F5R1B3		0.155	0.231		0.265	0.371		0.351	0.526	0.327
12	F5R2B1		0.183	0.231		0.206	0.281		0.249	0.352	0.568
13	F5R3B1		0.176	0.219		0.221	0.327		0.219	0.322	0.621
14	F5R4B3		0.131	0.201		0.222	0.343		0.349	0.459	0.231
15	F4R4B3		0.237	0.280		0.179	0.226		0.308	0.400	0.673
16	F4R2B1		0.202	0.252		0.161	0.258		0.221	0.316	0.624
17	F4R5B3		0.162	0.274		0.151	0.220		0.351	0.440	0.193
18	F4R5B4		0.112	0.181		0.201	0.340		0.321	0.428	0.173
19	F5R2B3		0.119	0.195		0.191	0.322		0.386	0.487	0.324
S-S-S											
20	F4R2B2		0.290	0.329		0.290	0.795		0.290	1.165	0.618
21	F5R2B4		0.322	0.351		0.292	0.712		0.308	0.951	0.684
22	F5R3B3		0.282	0.340		0.342	0.823		0.208	1.110	0.473
23	F5R1B2		0.222	0.334		0.142	0.343		0.308	0.323	1.158
24	F4R5B2		0.192	0.290		0.172	0.346		0.278	0.556	0.839
25	F5R1B1		0.287	0.326		0.176	0.256		0.141	0.220	0.857
26	F4R3B4		0.292	0.355		0.150	0.263		0.171	0.296	0.743
27	F4R2B3		0.190	0.262		0.190	0.501		0.200	0.704	0.598
28	F5R4B1		0.237	0.300		0.099	0.168		0.118	0.231	0.737
29	F4R5B1		0.222	0.281		0.088	0.145		0.090	0.140	0.734
30	F4R3B3		0.202	0.277		0.080	0.158		0.091	0.181	0.730
S-S-B											
31	F4R1B1		0.175	0.217		0.146	0.234		0.300	0.411	0.747
32	F4R1B4		0.070	0.125		0.111	0.172		0.428	0.519	0.623
33	F4R4B4		0.152	0.250		0.110	0.382		0.171	0.194	0.401
B-S-S											
34	F4R2B4		0.180	0.220		0.040	0.044		0.152	0.313	1.038
B-B-B											
35	F4R1B2		0.180	0.241		0.291	0.588		0.700	1.002	0.398
36	F4R1B3		0.120	0.185		0.301	0.502		0.650	0.920	0.310

\* Note: S denotes for passing from the Stern of the TS;  
B denotes for passing from the Bow of the TS.

Table 4.3: Mean DCPA for CA with different TSs

Passing from	TS1	TS2	TS3
Stern	0.191	0.161	0.197
Bow	0.160	0.242	0.405

\*The unit of values is nautical miles.

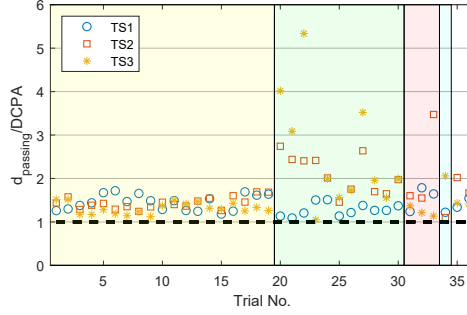


Figure 4.6: Plot of  $d_{\text{passing}}/\text{DCPA}$  values. 5 intervals on  $x$ -axis are S-B-B, S-S-S, S-S-B, B-S-S, and B-B-B. They are painted with distinguishable background colors.

From the distribution and the featured indexes, two facts can be found:

- The DCPA values selected by navigators to maneuver the OS at are distinctly different between passing from the stern and from the bow, regardless of the navigating patterns. From the collected data, the median of DCPA values for passing from the bow are 1.84, 1.68, and 1.99 times as for passing from the stern in the conservative, moderate, and aggressive pattern separately; the minimum are 1.92, 1.87, and 3.00 times; the maximum are 1.62, 1.91, and 2.03 times.
- The DCPA values between different patterns are clearly scattered on different scales, i.e. the DCPA can reveal the navigating patterns to a certain extent.

Table 4.3 gives the mean DCPA values of passing from the stern/bow in each sub-tasks. It shows that DCPA is less influenced by the CA-scenario difference in encounters with different TSs when passing from the stern, while the mean DCPA inclines to be larger when passing from the bow than from the stern. When passing from the stern, navigators prefer keeping the vessel to the original sailing route (without TSs on the route) as close as possible to achieve the least deviation and detour from the original route. To realize it, navigators usually keep a moderate speed to the course direction pointing to the stern of the TS.

#### Passing distance $d_{\text{passing}}$

Based on data in Table 4.2,  $d_{\text{passing}}/\text{DCPA}$  values are calculated accordingly, and results are plotted as in Fig. 4.6. The  $x$ -axis is divided into 5 intervals in terms of navigating



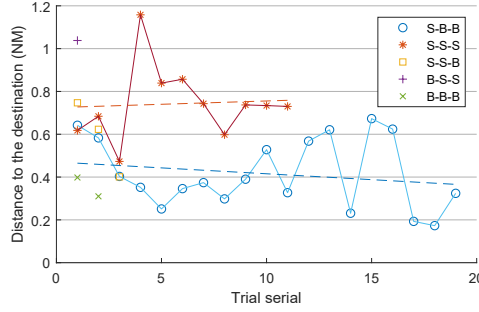


Figure 4.7: Distance to the destination at T=550 s. The dash lines in red and blue are trendlines of datasets S-S-S and S-B-B.

schemes (see in Table 4.2). The most important fact concluded from Fig. 4.6 is that all values are greater than 1, i.e.  $d_{\text{passing}}$  is always greater than the DCPA. From the definition of  $d_{\text{passing}}$ , it is strict the distance when one ship passes the center line (extended) of another.  $d_{\text{passing}}/\text{DCPA}$  greater than 1 means the strict passing distance is always larger than the principal metric DCPA. This guarantees the DCPA to be eligible as the collision risk assessment candidate for designing a guidance support system in the further step, which means as long as DCPA is selected in a proper way,  $d_{\text{passing}}$  is secured.

#### Distance to the destination $d_{OS}^{\text{arrival}}$

In order to investigate the efficiency of different CA schemes and navigating patterns, the distance to the destination at T = 550 s is calculated and given in Table 4.2, and is depicted in Fig. 4.7. Considering the OS has finished the CA sub-tasks with all the three TSs before T = 550 s in all trials, it is a proper time for efficiency assessment.

In terms of different CA scheme, most trial select S-B-B or S-S-S as the CA scheme, and other types are so rarely selected that they are not discussed statistically in this part. From the figure, it shows that the distance to the destination is farther in general when the S-S-S scheme is taken. The S-S-S scheme means that the OS operated strictly under the CA operational requirements according to the COLREGs, while the S-B-B scheme means that the OS only follows the COLREGs in the first CA sub-task, and violates the COLREGs in the rest two sub-tasks. It can be inferred that the violation of the COLREGs is at the aim of increasing the sailing efficiency. This is a balanced decision made by the navigator between the efficiency and the safety.

#### 4.2.3 Summary

Based on the calculation of key metrics DCPA and the expertise evaluation upon scenario reconstruction, three different navigating patterns in terms of the DCPA for passing the TS from the stern and the bow separately. In addition to the DCPA, two additional calculated figures, the passing distance and the distance to the destination (at T = 550 s), are used to comprehensively interpret navigators' rationality in CA operations. Finally the DCPA scales for the different patterns are concluded:

Table 4.4: DCPA scales of different navigating patterns

Passing from	Aggressive	Moderate	Conservative
Stern	$< 0.100$	$[0.100, 0.200)$	$\geq 0.200$
Bow	$< 0.200$	$[0.200, 0.400)$	$\geq 0.400$

\*The unit of values is nautical miles.

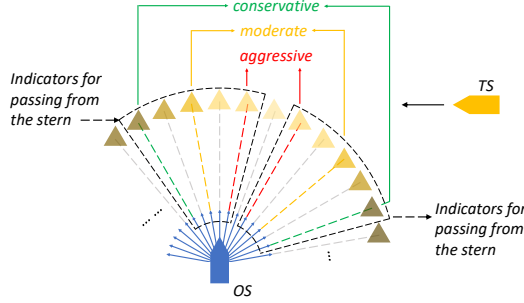


Figure 4.8: Illustration of the GUI of the developed system.

### 4.3 Experiment II: guidance support system testing

In this section, a real-time on-board decision support system for human-centered navigation based on the NPA results from Section 4.2 is developed.

#### 4.3.1 Description of the guidance support system

The guidance support system is developed in order to support navigators in making decisions in the CA scenario. Similar as the existing ECDIS, the system to be developed should be concise, informative, and functional. To be concise, it requires that no irrelevant information are shown on the graphic user interface (GUI), which helps navigators focus on key elements. To be informative, it requires the GUI to provide as much information as possible in a wise manner. To be functional, it requires the system can be easily understood for decision making and operation reacting at navigators' favors.

Taking the calculated items as the basis, a GUI of the navigating support system is developed and illustrated in Fig. 4.8.

#### Validation on simulator and statistical analysis

The developed system is validated in 4 trials in the same scenario as in Section 4.1 on the simulator. Among these trials, S-B-B CA scheme is taken in 2 trials, S-S-S and B-B-B CA scheme is taken in 1 trial for each.

The key features of the testing trials are listed in Table 4.5. Regarding the navigating pattern selection, it can be found that with the developed system, in all four trials, the OS is navigated to pass the TS in the moderate pattern in 15 sub-tasks, and 1 in the conservative pattern (according to its DCPA, and the definition given in Section 4.2). It is concluded the system has a positive performance in assisting the navigator to take a moderate pattern to navigate the OS.

Table 4.5: Test results with the developed system

Trial No.	TS1		TS2		TS3		$d_{OS}^{arrival}$
	NP	DCPA	NP	DCPA	NP	DCPA	
S-B-B							
MR1		0.142		0.285		0.297	0.517
MR2		0.133		0.237		0.281	0.345
S-S-S							
MR3		0.239		0.146		0.117	0.574
B-B-B							
MR4		0.203		0.328		0.394	0.494

\*The unit of values is nautical miles.

#### 4.3.2 Summary

From the statistical analysis and the realization of an example, the developed system has a positive influence on navigators' navigating manners. It reduces the navigators' brainwork on calculation and plan of the sailing route to some extent by providing some indicating information.

#### 4.4 Chapter summary

In this chapter, it is aimed to solve pragmatic industrial issues of maritime traffic that are often found in narrow water channels. Navigating patterns of navigators are proposed and conceptualized, and a scenario is designed that imitates the traffic situation as an attempt to find the best navigation solution. Three navigating patterns, namely aggressive, moderate, and conservative modes, were classified with the help of expertise knowledge from experienced navigators. They are further quantified for collision avoidance tasks in terms of the DCPA, an imperative collision risk index. Based on detected navigating patterns, a guidance support system with GUI was developed for the one-direction multi-ship collision avoidance scenario. The developed system was also tested on the simulator.



## Case Study: Visual-attention analysis and measurement

Human visual system reflects navigators' concentration [62], fatigue status [79], maneuvering interests [80], among other factors that are closely related to sailing safety and efficiency. Conducting research on navigators' visual attention and eye movement, therefore, enables us to understand the logic and mechanism of how navigational decisions and commands are made. It also helps to learn sailing patterns and detect anomalies, which in return provides practical information for both on-board navigators and remote surveillance personnel.

In this chapter, the following issues are discussed:

- how can navigators' response and action in critical operations reflected by visual-attention analysis?
- how can advanced functions displayed on the ECS be validated by visual-attention analysis?
- how can the method of visual-attention measurement be improved by and benefited from machine learning techniques?

The works presented in this chapter are from papers IV, V, and VI.

### 5.1 Eye-tracker-based visual attention analysis

#### 5.1.1 Metrics

- area of interest (AOI) is a manually selected region within the tracked map, and researchers can extract metrics to their need and interest specifically for this selected region. The AOIs in this section are (as illustrated in Fig. 5.1):
  - AOI-I: scene-projection wall;
  - AOI-II: the ECS screen;
  - AOI-III: the dashboard screen.
- Transition frequency  $f$ : the visual transition times between different AOIs in a specific time spell. The transition frequency reveals the activity level of the eye movement, i.e., a higher transition frequency implies that the navigator is fastly transitting his/her visual attention between different AOIs to closely monitor information from multiple channels so that the navigator gets aware of the situation in a big picture.

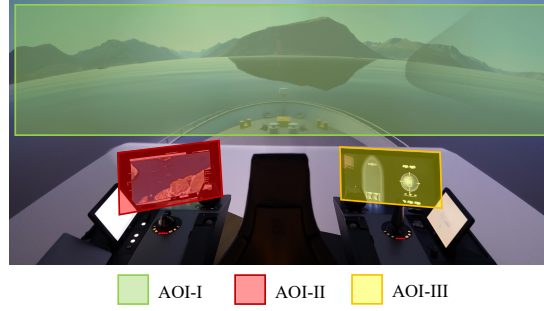


Figure 5.1: Area of interest (AOI) on the simulator.

- Duration of fixation  $t$ : the gaze duration on a specific AOI. The length of the duration of fixation reflects how much the navigator is interested in an AOI at a specific gaze. The longer duration time means it takes longer time for the navigator to obtain information from the AOI and calculate the situation upon it.
- Total duration time  $T$ : which is the total time the navigator keeps attention on a specific AOI during a complete experimental session. It can be calculated as  $T_{\text{AOI-j}} = \sum_{i=1}^n t_i$ , where  $n$  represents the total times that AOI-j is visually visited in a complete experimental session.

### 5.1.2 Experimental Design

#### Experimental Site & Equipment Setup

The experiment is conducted on the immersive ship-bridge simulator (Fig. 2.2c). The interface to the ship bridge simulator mainly contains three screens: the control panel, the customized ECS which provides the map-based navigational information, and the scene screen where the designed navigational scenario is displayed. These three screens are shown as Fig. 5.1 and their AOIs are framed accordingly: AOI-I, II, and III locate on respectively the scene screen, the ECDIS screen, and the control panel screen.

The eye tracker used in this experiment is Tobii Pro Glasses 2 which is a one-point calibrated and 3D-eye-modelling eye tracker. More specifications can be found in the official user's manual [81].

#### Scenario Design

The designed scenario to be implemented on the simulator is illustrated as in Fig. 5.2. According to the COLREGs [82], the OS shall give way to the TSs coming from its starboard. Therefore, in the designed scenario, the OS shall give ways to TS<sub>1</sub> - TS<sub>4</sub>, however the regulation is not necessary to apply if the distance is far enough to guarantee traffic security. Though TS<sub>5</sub> which is from the OS's portboard side yields to give way, it still might attract the navigator's (on the OS) attention to synthetically analyze the traffic situation. It means the existence of TS<sub>5</sub> increase the complexity of the situation and requires more consideration and calculation from the navigator.

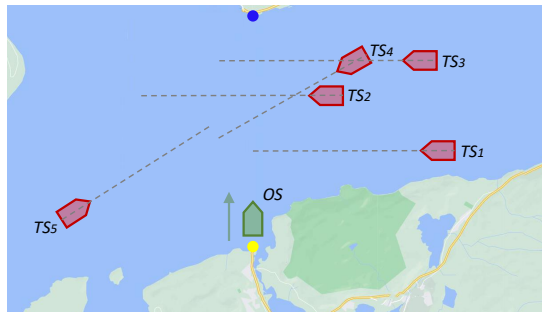


Figure 5.2: Designed scenario on the map.

### 5.1.3 Visual attention in critical operations

#### Workflow

The workflow for analyzing navigators' visual attention in critical operations is shown in Fig. 5.3 and contains 4 steps.

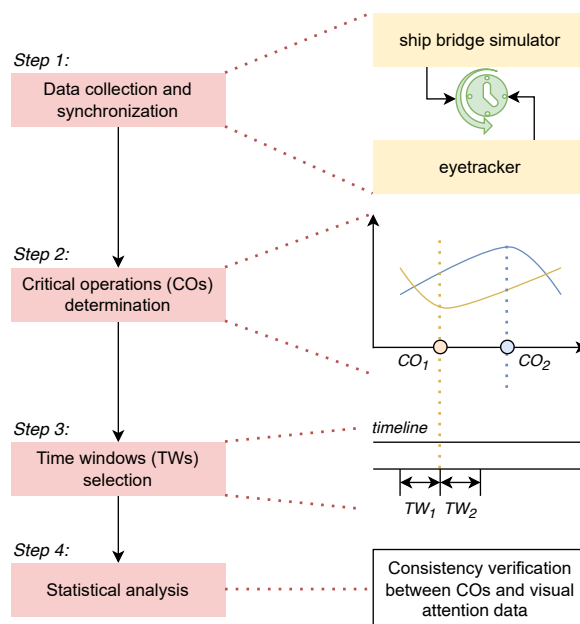


Figure 5.3: Illustration of the workflow to this research.

**Step 1 - data collection and synchronization** Experimental data are collected in two ways: eye-tracker-based visual attention data collected from the participated navigators to the experiment; ship motion data including position, speed, and course are

exported and collected through the simulator system. Since the eye-tracker system is independent of the ship-bridge simulator, data from the two portals need to be synchronized according to their timestamps.

**Step 2 - critical operations (CO) determination** Critical operations (CO) are mainly determined by the change rate of speed and course to the ship, while also referred to the expertise (the participated navigators) recommendation.

**Step 3 - time window (TW) selection** Time windows (TW) are spells where the visual attention and transition are deemed to be closely relevant to assess how they relate to the COs. TVs can be prior, during, and post the COs.

**Step 4 - statistical analysis** After COs and TWs are settled, some features are counted for further analysis and comparison between different TWs. Before explaining the features, a commonly used concept - the area of interest (AOI) - should be clarified in advance:

### Result

**Transition Times** Fig. 5.4 shows the counted transition times of each AOI. There is a clear trend that the visual transition is less active as all AOI are less frequently visited after the COs take place. AOI-I is visited more often by the navigator than the other two AOIs.

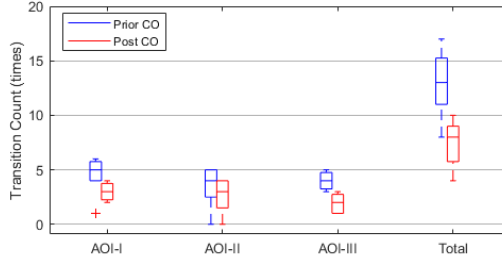


Figure 5.4: Transition times of each AOI and the total count.

**Duration of Fixation** The two data features, average and median values, are used to evaluate the duration of fixation shown in Fig. 5.5. Both features significantly increase in all AOIs. According to Section 5.1.3, the visual transition frequency declines, which results in a great increment in the duration of fixation in every individual fixation.

**Total Fixation Time** Fig. 5.6 reveals that after the CO takes place, the fixation time on AOI-I increases while incline to go down on AOI-II and III. Since the CO is defined as critical operations, it can be inferred that after CO happens, the navigator regards the ship in a safe state and is more relaxed than in the spell of prior-CO when the navigator is demanded to be aware of the situation from the ECDIS (AOI-II) and tightly from the control command (AOI-III), the navigator prefers to put more attention on the vivid scene screen (AOI-I) to visually explore new situations to be handled.

In summary, the statistical results show clear discrimination between the prior-



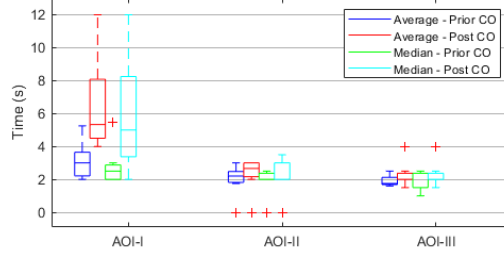


Figure 5.5: Features to the duration of fixation for each AOI.

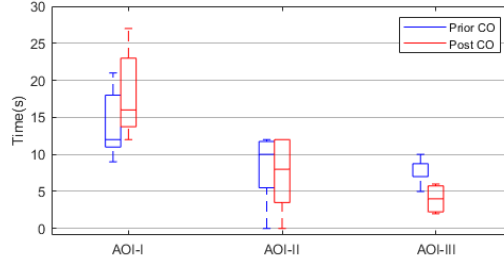


Figure 5.6: Total fixation time for each AOI.

and post- CO spells. In the spell prior to CO, the navigator visual attention transit fast between different AOIs to obtain information as completed as possible from every channel to make a synthetically optimal solution to handle the collision avoidance. After the CO, navigators prefer to keep visual outlook (AOI-I) than scrutinizing the information on the smaller screens (AOI-II and III).

#### 5.1.4 Usability evaluation of electronic chart system

The workflow of this work is illustrated as shown in Fig. 5.7.

##### Risk metric

In this study, a CRI is used as the risk metric, and it is calculated as:

$$\text{CRI} = W_{\text{DIF}} \cdot \text{DIF} + W_{\text{dv}} \cdot d_v + W_{\text{rr}} \cdot \text{rr}, \quad (5.1)$$

where DIF,  $d_v$ , and rr are denoted for the domain intersection factor, closest predicted distance, and risk radius factor, while  $W_{\text{DIF}}$ ,  $W_{\text{dv}}$ , and  $W_{\text{rr}}$  represents the corresponding empirical weight. The details of the CRI explanation can be found in [83].

##### Statistics on visual attention

In total, six sets of two-trial sailings are collected and the global statistical results are given as follows.

In Table 5.1, three featured values' scales, including median, maximum, and total

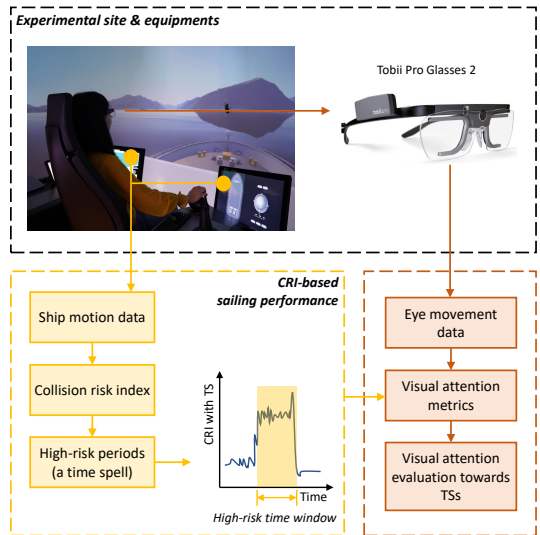


Figure 5.7: Workflow of this work (Picture of Tobii Pro glasses 2 is credited to the official website to Tobii Pro®).

Table 5.1: Statistics scales on duration of fixation features for complete sailings

	Median (s)	Maximum (s)	Total (s)
<i>AOI-I</i>			
wo.	[4.3, 5.2]	[18.0, 24.0]	[278.0, 310.5]
w.	[4.4, 4.9]	[16.0, 23.5]	[240.7, 280.4]
<i>AOI-II</i>			
wo.	[0.5, 1.1]	[2.5, 5.5]	[5.0, 20.0]
w.	[2.8, 3.9]	[7.5, 9.0]	[98.5, 125.6]
<i>AOI-III</i>			
wo.	[3.7, 4.4]	[8.5, 10.2]	[225.8, 245.0]
w.	[3.8, 4.2]	[8.2, 12.0]	[196.8, 254.5]

duration, are listed. The statistics show a compliant result in line with the findings in the individual case: when ECS is partly disabled, the navigator prefers to use visual sight to percept the environment directly, instead of getting the imperfect information from the partial ECS. The maximum in AOI-I can last very long, as the maximum usually happens at the tail of the sailing where the evasion of TSs has been addressed, and a distance remains to the destination; in this time spell, the navigator usually keeps the target their attention on AOI-I to percept the situation visually. An essential reason that may account for it is that not all types of ships are equipped with communication and positioning devices, which means the eye vision is the only reliable detector in this situation (for example, small fishing boats are usually not equipped with AIS, then it requires the navigator to detect, locate, and calculate it only rely on their own eye vision).

Table 5.2: Statistics on transition frequencies in complete sailings

No.	I-II	I-III	II-III
wo.	3.5	10.4	-
w.	5.5	12.0	0.5

\* times per minute

The values in Table 5.2 are the overall average from all collected sailings in their classes. The overall trend corresponds to the individual case that the eye movement activity level is higher when the ECS is fully enabled. The transition between AOI-I and III is the most frequent, and direct transition between AOI-II and III rarely happens.

## 5.2 Camera-based deep learning model for visual attention measurement

The solution of eye-tracker glasses has brought the research forward, but the low feasibility and high cost of equipment for recording visual attention have hindered collecting data from navigators on either real ships or simulators. With the rapid development of image technology and artificial intelligence (especially computer vision and pattern recognition algorithms), the authors are committed to providing a low-cost and non-intrusive visual attention recognition solution by developing an integrated system that consists of a consumer sports camera and a CNN deep-learning algorithm. This framework enables to trace navigators' visual attention at a high frequency (up to 120 Hz) to specific visual attention zones (VAZs).

### 5.2.1 Methodology & Setup

The workflow is divided into two parts: training flow which includes the database formation and the details of the designed CNN-based deep-learning algorithm; and the testing flow which includes how the trained model is applied in trial sailings and how the performance is evaluated.

#### Training flow

Training flow forms the base of the developed solution (the upper in Fig. 5.8). The first step is to invite navigators to perform random trials in the ship-bridge simulator,

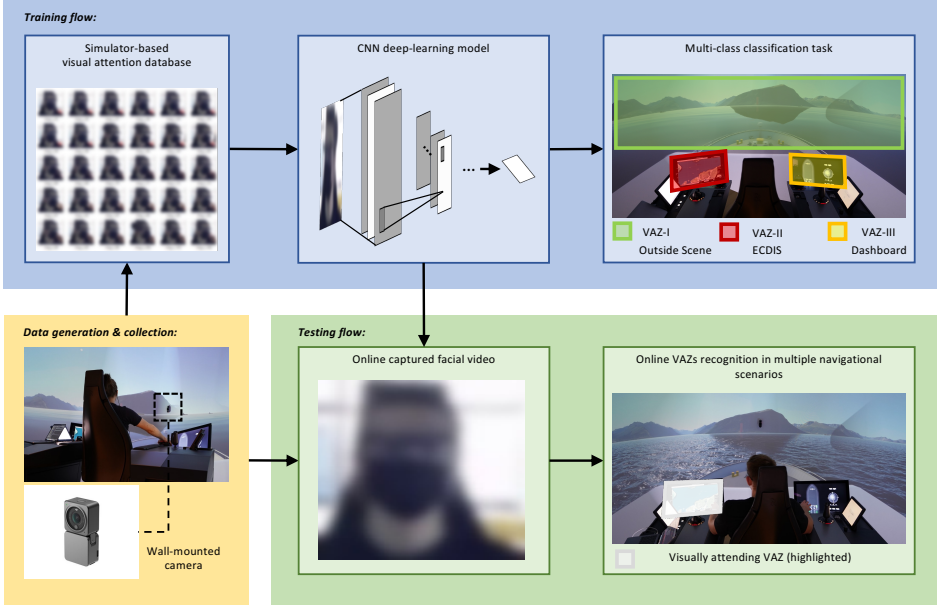


Figure 5.8: Workflow of the CaBDeeL solution (images containing facial identity have been blurred for demonstration in the figure according to the General Data Protection Regulation (GDPR)).

from which the data build up the primary database. A wall-mounted sports camera is used to capture navigators' head and eye movements from their front view (as shown in Fig. 5.8). In this step, the eye-tracker glasses are used only to sort the collected images into different classes in the database. According to the configuration of the ship-bridge simulator, as shown in the top-right embedded chart in Fig. 5.8, there are three VAZs included which corresponds to the AOIs in the former section.

The database continues to expand as trials accumulate. The second step is then to train the deep-learning model with such a database. After the model is well-trained, it is able to classify navigators' visual attention into corresponding VAZs correctly.

**Database formation** We collected around 40 minutes of video to establish the primary database, and the video was recorded with a resolution of 1080P and at a rate of 60 frames per second. Applying the eye-tracker glasses' data as reference and after necessary data pruning, the distribution of the collected data in each class is 50.0 %, 16.7 %, and 33.3 % for VAZ-I, II, and III, respectively.

**Algorithm** In this study, we developed a CNN deep-learning model whose structure is shown in Fig. 5.9. In general, it contains three convolutional layers, three max-pooling layers, one flatten layer, and two fully-connected layers.

Each convolutional layer in this network includes two operations:

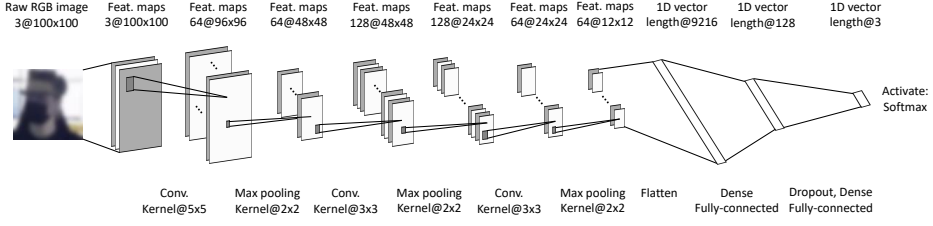


Figure 5.9: Structure of CNN-based deep-learning algorithm.

$$\begin{aligned} \mathbf{s} &= \text{Conv}(\mathbf{x}) \\ \mathbf{s} &= \text{ReLU}(\mathbf{s}) \end{aligned} \quad (5.2)$$

where  $\mathbf{x}$  is the input; *Conv* denotes the convolutional operation and its weight is to be learned by training; *ReLU* is selected as the activation function to solve this image classification problem [84]. In the three convolutional layers, their corresponding kernels are selected with sizes of  $5 \times 5$ ,  $3 \times 3$ , and  $3 \times 3$ .

Max pooling layers (sub-sampling layers) are performed after each convolutional layer to compress the image data, reduce the number of the weights and avoid over-fitting. In this network, all max-pooling layers have the same kernel size at  $2 \times 2$ . After the convolutional and max-pooling layers, the multi-channel maps are flattened to a 1D vector. Then two fully-connected layers follow up to weigh and rectify features. The dropout operation in the last fully-connected layer also prevents over-fitting. Finally, the features map is dense to a 1D vector with a length of 3; and as we are about to solve a multi-class single-label problem, *softmax* is chosen as the activation function to produce the probability of each class.

### Testing flow

Testing flow is downstream when the model is trained and ready to use. Navigators are invited to maneuver on the ship-bridge system again to generate videos for testing. The videos are exported and decomposed into frames, and then the trained deep-learning model is applied to the frames to recognize the VAZ of the navigator in the image. When collecting data in this flow, navigators are also asked to wear the eye-tracker glasses, and it is only to verify the results and performance of the deep-learning model.

### 5.2.2 Results & Discussion

The verification of the trained model in some trial sailings is illustrated and compared with the eye-tracker glasses to demonstrate the significance of maritime application.

### Training result

Table 5.3 compares the sampling rate of the eye-tracker glasses and the accuracy of CaBDeeL. The glasses can precisely locate the gaze zone when eye movement is sampled effectively. However, the sampling process can be unstable, especially when navigators squint over the edge of the glasses frame. The glasses cannot properly predict the gaze

Table 5.3: Comparison on sampling rate/accuracy

No.	Duration (mm:ss)	Sampling rate/accuracy
<i>Eye-tracker glasses</i>		
Trial 1	16:44	93 %
Trial 2	5:47	90 %
Trial 3	12:02	84 %
Trial 4	5:16	83 %
<i>CaBDeeL</i>		
Overall	-	95 %

estimation if the eye movement fails to be sampled. Compared to the glasses, CaBDeeL shows more robustness as long as the camera functions normally. Accuracy over 95 % has already outperformed the eye-tracker glasses in this VAZs recognition task on the ship-bridge simulator.

#### Test in two trials

**Scenario setup** Two different scenarios are designed (as shown in Fig. 5.10) to test the performance of the trained model, including in heavy traffic conditions where collision avoidance operations are needed as well as in light traffic conditions where the navigator freely maneuvers the ship to cruise on the sea.

**Classification accuracy** The classification accuracy is plotted in Fig. 5.11. In Fig. 5.11(a), the prediction accuracy has overall satisfactory performance. It is the most accurate when predicting the VAZ-III while the least accurate when predicting the VAZ-I. The fact that VAZ-I is the scene screen with broad coverage within eyesight may explain this. In Fig. 5.11(b), it is interesting to find that VAZ-II is never visually visited by the navigator, which implies that the navigator prefers to use pure visual sight to observe the environment on VAZ-I when the traffic situation is less demanding. In this scenario, the prediction accuracy is even higher when training the model (95 %). A reason to explain it is that since one of the VAZs is never paid attention to by the navigator, it reduces the probability of incorrectly sorting the frame into that class.

In general, CaBDeeL (500 epochs) scores overall accuracy at 93.5 % and 95.9 %

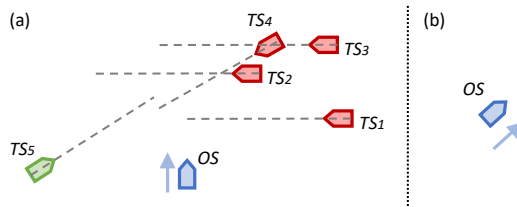


Figure 5.10: Two scenarios: (a) heavy traffic with collision avoidance demand; (b) cruise in light traffic.

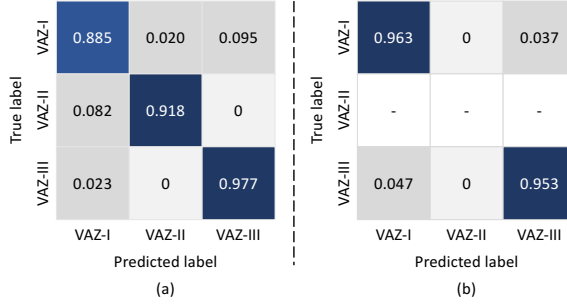


Figure 5.11: Confusion matrices in the two scenarios of CaBDeeL (500 epochs).

Table 5.4: Sampling rate/accuracy comparison in the two scenarios

Scenario	CaBDeeL-500	Eye-tracker
(a)	93.5 %	69.0 %
(b)	95.9 %	95.0 %

as in Table 5.4 for the Scenario (a) and b respectively. While the sampling rate of the eye-tracker glasses meets some critical issues which result in a low rate in Scenario (a), it can be caused by an improper way of wearing the glasses, failure in eyes location calibration, swift eye sweeping, and extreme glare.

**Visualization & Comparison** Fig. 5.12 shows three subfigures when the navigator looks at different VAZs. The bottom-left of each subfigure in Fig. 5.12 shows that eye-tracker glasses can locate the gaze to an exact point, although they fail to track eye movement in some cases. While CaBDeeL can recognize different VAZs, which means an approximate area of visual attention. Fig. 5.12 proves the accuracy of the CaBDeeL in the trial sailings in the designed scenarios.

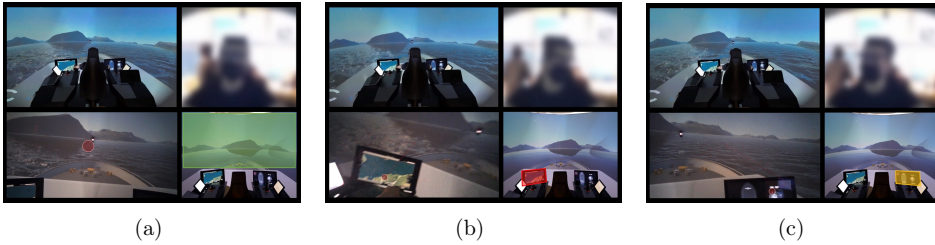


Figure 5.12: Matts plot of (1) top-left: back-view (only used for demonstration, not relevant to CaBDeeL); (2) top-right: front-view (input image to CaBDeeL; the facial image shown here is blurred according to GDPR); (3) bottom-left: eye-tracker glasses marked video; (4) bottom-right: CaBDeeL recognized VAZ is highlighted.

### Applicable function

Like the eye-tracker glasses, CaBDeeL is capable of realizing pragmatic visual attention analysis by providing commonly used metrics, such as transition frequency, duration of fixation, and the total duration time of fixation.

**Transition frequency** Fig. 5.13 depicts the transition frequency between every two VAZs. In Scenario (a), the navigator transits their visual attention between VAZ-I and III at the highest frequency, although it is hard to distinguish direct transits between VAZ-II and III. To handle collision risks, the navigator needs to gather information from the ECDIS, for example, the distance/time to the closet point of approach, speeds of TSs, route prediction, and other traffic information, and they have to assess the situation from the ECDIS and with direct observation of the situation and traffic. While In Scenario (b), VAZ-II never captures any attention of the navigator, which implies that the navigator tends to fully rely on his own observation when sailing in light traffic. Moreover, the total transition frequencies in Scenario (a) and (b) are 15.9 and 13.6 transitions per minute. This difference also demonstrates that attention activeness is lower when sailing under ordinary circumstances than in complicated ones.

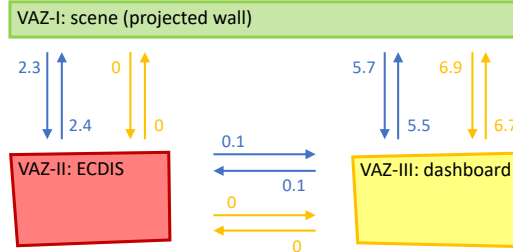


Figure 5.13: Transition frequency between every two VAZs in the two scenarios (transitions per minute). The blue lines depicts for Scenario (a) and the yellow lines depicts for Scenario (b).

Table 5.5: Duration of fixation features

No.	Scale (s)	Median (s)	Mean (s)
<i>Scenario (a): heavy traffic</i>			
VAZ-I	[0.3, 13.8]	1.5	2.0
VAZ-II	[0.2, 10.3]	1.8	2.6
VAZ-III	[0.1, 8.5]	3.0	4.0
<i>Scenario (b): light traffic</i>			
VAZ-I	[0.4, 24.0]	4.0	5.6
VAZ-II	-	-	-
VAZ-III	[0.6, 8.4]	2.2	2.8

**Duration of fixation** Table 5.5 lists the features in the duration of fixation. In Scenario (a), VAZ-III has the highest mean and median, i.e., more information on the



dashboard to be read at each time. When the navigator receives such information, their attention shifts away only shortly as it is dangerous to leave the situation unattended. Both scenarios yield interesting results when comparing their features. In Scenario (b), the maximum on VAZ-I reaches 24.0 seconds which is much higher than any maximums in Scenarios (a). Light traffic requires fewer operations and consequently demands less attention on the dashboard that provides maneuvering and machinery information. In addition, the lower threshold of the scale in Scenario (b) is much higher, which also proves that the navigator is less visually active.

**Total duration proportion** Fig. 5.14 plots the total duration time spent on each VAZ in the two scenarios. In Scenario (a), according to Fig. 5.14(a), VAZ-III dominates the navigator's attention. From the proportion distribution, it can be inferred that navigators are more sensitive to the machinery commands (such as propulsion rate, speed, and rudder angle) to achieve fine maneuvering when sailing in a congested water channel. Meanwhile, the navigator also needs to obtain information and receive decision support from the ECDIS system to select a collision avoidance scheme. Different from the heavy traffic situation, Fig. 5.14(b) reveals that the navigator places their visual sight over the window to observe the environment and become aware of the situation. This is in accordance with to the discovery in Section 5.2.2.

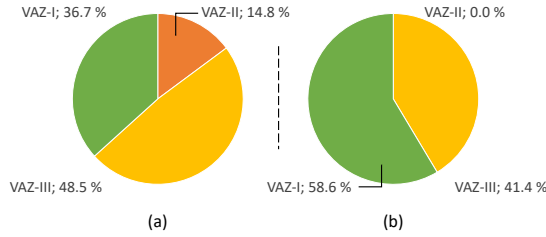


Figure 5.14: Total duration proportion of each VAZ in the two scenarios.

### Chapter summary

In this chapter, both traditional eye-tracker-glasses based visual attention analysis and novel camera-based deep learning method for visual attention tracking are contained. Visual attention directly reflects the traces of human willings and contains much information in navigators' physical and psychological status. Navigators' visual attention in critical operations (e.g., collision avoidance) is studied while the integrated decision support functions on specific screen is also verified of usability. To cope with the limitation of the traditional eye-tracker glasses, a non-intrusive and lost cost camera-based visual attention tracking method using machine learning algorithm is developed and tested as well.



## Conclusion and Further Work

This dissertation has proposed the synthesis study of HITL navigational operations towards MASS. Research findings in three case studies concerning expertise knowledge and navigational behaviors are presented. All contributions in this dissertation target to understand the human logic, attempt to concrete the knowledge, and apply the expertise into the operational loop to promote HITL navigational safety. Most of the platforms, equipment, and algorithms used in this dissertation are not new, but it lacks a systematic framework to integrate them together for the HITL navigational operations study. The work illustrated in this dissertation is expected to provide a perspective and implementation on how a systematic research routine on human navigators can be established as the basis for MASS.

### 6.1 Summary of contributions

Constructing the experimental design and implementation scheme based on different ship-bridge facilities to provide decision support in terms of guidance, navigation, and control, as stated in RO1, is the primary goal of this dissertation. To achieve it, developing a novel monitoring method for the navigators' operational behaviors with higher feasibility, versatility, and economic efficiency is the first to be concerned, as clarified in RO2. After the monitoring and data collection, the following work is to handle the data with different analysis methods, which is stated as a goal in RO3, and this is covered in all three case studies. Case studies in chapters 3 and 4 interpret collected data by human expertise and use the concluded results to provide onboard support; the case study in chapter 5 analyzes the visual attention data statistically by eye-tracking metrics. As data are addressed, and knowledge is obtained, the next is to propose onboard decision support tools to promote HITL navigational performance as stated in RO4. Case studies in chapters 3 and 4 contain this topic. In chapter 3, novel terms of safety levels are defined and verified with the MPC method in the path routing loop; in chapter 4, the concluded NPs are used to develop a decision support system dealing with the collision avoidance task.

The main contributions of this dissertation are summarized as follows:

- Present the fundamentals to use different experimental platforms, facilities, and equipment to support HITL navigational operations research towards MASS. The experimental implementation is demonstrated in three different case studies.
- Propose a new ship-bridge monitoring solution with higher usability to improve the feasibility of navigational data collection.
- Propose a framework on how human expertise can be used to supervise the data

interpretation and their usage in onboard decision support in terms of path optimization and collision avoidance.

- Present a set of navigators' visual attention interpretation methods to assess their response in critical operations and usage of specific displays.

## 6.2 Summary of publications

The summary of publications is as follows:

Paper I presents a method to interpret the log data from a commuter ferry. The proposed method aims to construct the mechanism of how human expertise steers a ferry and then model the mechanism as the criterion to judge the status of the ship during sailing. The model criteria can thus be used to support onboard decisions. As the commuting route is considered a promising application for ship intelligence, the method is implemented on a customized commuting route in Trondheim. In order to establish the empirical criteria model, human experts' advice is taken into account to define different sailing scenarios in the commuting route. At last, the decomposition result is demonstrated by statistical method to help better understand the mechanism of operating a commuting ferry.

Paper II is a continuation of the work in paper I and introduces a framework for how log data can be comprehensively used to provide onboard support and enhance sailing route safety. The main idea of this paper is to synthetically use both human expertise and objective log data to make rudiment work for autonomous navigation.

Paper III proposes and conceptualizes navigating patterns of navigators and designs a scenario that imitates the traffic situation as an attempt to find the best navigation solution. Through simulator-based experiments, we collected 36 trials' data for analyzing navigating patterns. Three navigating patterns, namely aggressive, moderate, and conservative modes, were classified with the help of expertise knowledge from experienced navigators. They are further quantified for collision avoidance tasks in terms of the DCPA, an imperative collision risk index. Based on detected navigating patterns, a guidance support system with GUI was developed for the one-direction multi-ship collision avoidance scenario. The developed system was also tested on the simulator.

Paper IV suggests an approach by applying an eye-tracker-based visual attention assessment to evaluate the performance of how navigators handle the collision avoidance tasks in maritime traffic. The statistical results reveal that the visual activities change between different patterns during the whole process of handling collision avoidance.

Paper V develops a camera-based deep-learning (CaBDeeL) solution that solves the VAZs recognition problem in this letter. The developed framework attains excellent results in achieving the goal. When CaBDeeL is applied to trial sailings, it scores overall accuracy beyond 95 %. This solution outperforms the traditional visual attention tracking method given its high robustness, low cost, and non-intrusive feasibility.

Paper VII introduces the experimental platforms to carry out HITL research in the maritime navigation domain. The difference and applicable scenes to each platform are discussed, and simulator and research vessel-based HITL experimental design and implementation routines are consolidated by clarifying the roles of each involved party of interests. This framework has brought systematic routines in conducting HITL navigational operations research in various experimental environments.

Paper VI implements an evaluation of the effectiveness of Electronic chart system (ECS) maritime navigators by utilizing collision risk analysis and visual attention assessment. Some interesting results from the eye-tracker glasses are presented, and some particular behaviors are demonstrated with respect to professional domain knowledge in nautical science. The content of the result and discussion is expected to enhance comprehending navigators' maritime operations and behavior, which can be used as the fundamental knowledge for developing specific intelligent decision support for MASS at HITL levels.

### 6.3 Future work

This dissertation has mainly focused on the synthesis study of HITL navigational operations towards MASS. As this is a big topic that is related to every section of the maritime navigation and transportation system, the works in this dissertation are made to cover as comprehensive and systematic the range as possible. The below bullet points provide suggestions for how the presented research may be extended.

- For the monitoring, the camera-based solution developed in this dissertation can only handle the navigators operating at a fixed position. The solution shall be improved to cope with different ship-bridge environments. An additional camera sensor shall be added to the loop for image collection and position calibration. Furthermore, visual attention is not the only object to be monitored for understanding navigators' operations, but also body movement and gesture motion are also of research interest and shall make the monitoring system more comprehensive.
- For the data collection, it is expected to collect more data in different scenarios, including other CA situations, as well as other scenarios in ship maneuvering and sailing, such as departing and docking. More data input is to better understand the navigating logic of human navigators in the hope of shedding light on both the development of MASS and human-machine interaction performance as the MASS is still at the HITL level
- For the visual attention analysis, as a result, describe the visual attention with respect to transition frequency and fixation duration in general; the details in each AOI in terms of fixation points and distribution can be studied further to understand the navigators' logic more precisely. It is expected to develop a quantitative empirical mathematical model as the evaluation leverage instead of human interpretation.
- The decision support system developed with human expertise supervision in the first two case studies is specifically for two scenarios: commuter route in Trondheim and ferry route near Ålesund. It is expected to propose a more intelligent way, such as by intaking and testing different algorithms and optimization methods in path planning, situation awareness, and human status assessment, to promote the universality of usage of the developed systems.



## References

- [1] Review of maritime transport 1968. UNCTD (United Nations Conference on Trade and Development), United Nations Publications, New York, USA, 1968.
- [2] Review of maritime transport 2021. UNCTD (United Nations Conference on Trade and Development), United Nations Publications, New York, USA, 2021.
- [3] Manning annual review and forecast 2021/22. Drewry Maritime Research, London, UK, 2021.
- [4] Maritime outlook 2021. Norwegian Shipowners' Association, Oslo, Norway, 2021.
- [5] Sercan Erol and Ersan Başar. The analysis of ship accident occurred in turkish search and rescue area by using decision tree. *Maritime Policy & Management*, 42(4):377–388, 2015.
- [6] Raluca Apostol-Mates and Alina Barbu. Human error—the main factor in marine accidents. *Naval Academy Scientific Bulletin*, 19(2):451–454, 2016.
- [7] Javier Sánchez-Beaskoetxea, Imanol Basterretxea-Iribar, Iranzu Sotés, and María de las Mercedes Maruri Machado. Human error in marine accidents: Is the crew normally to blame? *Maritime Transport Research*, 2:100016, 2021.
- [8] European Maritime Safety Agency. Annual overview of marine casualties and incidents 2015. EMSA Lisbon, 2015.
- [9] European Maritime Safety Agency. Annual overview of marine casualties and incidents 2020. EMSA Lisbon, 2020.
- [10] Nader R Ammar and Ibrahim S Seddiek. Eco-environmental analysis of ship emission control methods: Case study ro-ro cargo vessel. *Ocean Engineering*, 137:166–173, 2017.
- [11] Dongfang Ma, Weihao Ma, Sheng Jin, and Xiaolong Ma. Method for simultaneously optimizing ship route and speed with emission control areas. *Ocean Engineering*, 202:107170, 2020.
- [12] Walter Lhomme and João P Trovão. Zero-emission casting-off and docking maneuvers for series hybrid excursion ships. *Energy Conversion and Management*, 184:427–435, 2019.
- [13] Ruoli Tang, Qing An, Fan Xu, Xiaodi Zhang, Xin Li, Jingang Lai, and Zhengcheng Dong. Optimal operation of hybrid energy system for intelligent ship: An ultrahigh-dimensional model and control method. *Energy*, 211:119077, 2020.

- [14] Marco Gianni, Andrea Pietra, and Rodolfo Taccani. Outlook of future implementation of pemfc and sofc onboard cruise ships. In *E3S Web of Conferences*, volume 238. EDP Sciences, 2021.
- [15] Tongtong Wang, Guoyuan Li, Baiheng Wu, Vilmar Æsøy, and Houxiang Zhang. Parameter identification of ship manoeuvring model under disturbance using support vector machine method. *Ships and Offshore Structures*, pages 1–9, 2021.
- [16] Xu Han, Bernt Johan Leira, Svein Sævik, and Zhengru Ren. Onboard tuning of vessel seakeeping model parameters and sea state characteristics. *Marine Structures*, 78:102998, 2021.
- [17] Luman Zhao and Myung-Il Roh. Colregs-compliant multiship collision avoidance based on deep reinforcement learning. *Ocean Engineering*, 191:106436, 2019.
- [18] Tor A Johansen and Thor I Fossen. Control allocation—a survey. *Automatica*, 49(5):1087–1103, 2013.
- [19] Thor I Fossen. *Handbook of marine craft hydrodynamics and motion control*. John Wiley & Sons, 2011.
- [20] Remote and autonomous ships: The next steps. Advanced Autonomous Waterborne Applications (AAWA) Project, Rolls-Royce, London, UK, 2016.
- [21] Colling Kooij, Alina P Colling, and CL Benson. When will autonomous ships arrive? a technological forecasting perspective. In *Proceedings of the International Naval Engineering Conference and Exhibition (INEC)*, volume 14, 2019.
- [22] Regulatory scoping exercise on maritime autonomous surface ships. In *Maritime Safety Committee, 100th session*. International Maritime Organization, 2018.
- [23] Chenguang Liu, Xiumin Chu, Wenxiang Wu, Songlong Li, Zhibo He, Mao Zheng, Haiming Zhou, and Zhixiong Li. Human-machine cooperation research for navigation of maritime autonomous surface ships: A review and consideration. *Ocean Engineering*, 246:110555, 2022.
- [24] Anete Vagale, Rachid Oucheikh, Robin T Bye, Ottar L Osen, and Thor I Fossen. Path planning and collision avoidance for autonomous surface vehicles i: a review. *Journal of Marine Science and Technology*, pages 1–15, 2021.
- [25] Imran Ashraf, Yongwan Park, Soojung Hur, Sung Won Kim, Roobaea Alroobaea, Yousaf Bin Zikria, and Summera Nosheen. A survey on cyber security threats in iot-enabled maritime industry. *IEEE Transactions on Intelligent Transportation Systems*, 2022.
- [26] LR code for unmanned marine systems. In *ShipRight Design and Construction, Additional Design Procedures*. Lloyd’s Register, 2017.
- [27] DNVGL-CG-0264 class guideline: Autonomous and remotely operated ships. DNVGL, 2018.
- [28] R Glenn Wright. Unmanned and autonomous ships: An overview of mass. 2020.



- [29] Mehrangiz Shahbakhsh, Gholam Reza Emad, and Stephen Cahoon. Industrial revolutions and transition of the maritime industry: The case of seafarer’s role in autonomous shipping. *The Asian Journal of Shipping and Logistics*, 38(1):10–18, 2022.
- [30] Toshiyuki Miyoshi, Shoji Fujimoto, Matthew Rooks, Tsukasa Konishi, and Rika Suzuki. Rules required for operating maritime autonomous surface ships from the viewpoint of seafarers. *The Journal of Navigation*, 75(2):384–399, 2022.
- [31] Hristos Karahalios. Evaluating the knowledge of experts in the maritime regulatory field. *Maritime Policy & Management*, 44(4):426–441, 2017.
- [32] Thiago Gabriel Monteiro, Charlotte Skourup, and Houxiang Zhang. Optimizing cnn hyperparameters for mental fatigue assessment in demanding maritime operations. *IEEE Access*, 8:40402–40412, 2020.
- [33] Runze Mao, Guoyuan Li, Hans Petter Hildre, and Houxiang Zhang. A survey of eye tracking in automobile and aviation studies: Implications for eye-tracking studies in marine operations. *IEEE Transactions on Human-Machine Systems*, 51(2):87–98, 2021.
- [34] Frøy Birte Bjørneseth, Mark D Dunlop, and Eva Hornecker. Assessing the effectiveness of direct gesture interaction for a safety critical maritime application. *International journal of human-computer studies*, 70(10):729–745, 2012.
- [35] Ik-Hyun Youn, Deuk-Jin Park, and Jeong-Bin Yim. Analysis of lookout activity in a simulated environment to investigate maritime accidents caused by human error. *Applied Sciences*, 9(1):4, 2019.
- [36] Thiago Gabriel Monteiro, Guoyuan Li, Charlotte Skourup, and Houxiang Zhang. Investigating an integrated sensor fusion system for mental fatigue assessment for demanding maritime operations. *Sensors*, 20(9):2588, 2020.
- [37] Marilia Abilio Ramos, Ingrid Bouwer Utne, and Ali Mosleh. Collision avoidance on maritime autonomous surface ships: Operators’ tasks and human failure events. *Safety science*, 116:33–44, 2019.
- [38] Lokukaluge P Perera, Brage Mo, Leifur Arnar Kristjánsson, PC Jonvik, and JO Svardal. Evaluations on ship performance under varying operational conditions. In *Proceedings of the 34th International Conference on Ocean, Offshore and Arctic Engineering (OMAE 2015), Newfoundland, Canada, (OMAE2015-41793)*, 2015.
- [39] Wei Chian Tan, Ching-Yen Weng, Yu Zhou, Kie Hian Chua, and I-Ming Chen. Historical data is useful for navigation planning: Data driven route generation for autonomous ship. In *2018 IEEE International Conference on Robotics and Automation (ICRA)*, pages 7478–7483. IEEE, 2018.
- [40] Shangbo Mao, Enmei Tu, Guanghao Zhang, Lily Rachmawati, Eshan Rajabally, and Guang-Bin Huang. An automatic identification system (ais) database for maritime trajectory prediction and data mining. In *Proceedings of ELM-2016*, pages 241–257. Springer, 2018.

- [41] André Listou Ellefsen, Xu Cheng, Finn Tore Holmeset, Vilmar Æsøy, Houxiang Zhang, and Sergey Ushakov. Automatic fault detection for marine diesel engine degradation in autonomous ferry crossing operation. In *2019 IEEE International Conference on Mechatronics and Automation (ICMA)*, pages 2195–2200. IEEE, 2019.
- [42] André Listou Ellefsen, Vilmar Æsøy, Sergey Ushakov, and Houxiang Zhang. A comprehensive survey of prognostics and health management based on deep learning for autonomous ships. *IEEE Transactions on Reliability*, 68(2):720–740, 2019.
- [43] Guoyuan Li, Runze Mao, Hans Petter Hildre, and Houxiang Zhang. Visual attention assessment for expert-in-the-loop training in a maritime operation simulator. *IEEE Transactions on Industrial Informatics*, 16(1):522–531, 2019.
- [44] Rami Zghyer and Runar Ostnes. Opportunities and challenges in using ship-bridge simulators in maritime research. *Proceedings of Ergoship 2019*, 2019.
- [45] Deuk-Jin Park, Jeong-Bin Yim, Hyeong-Sun Yang, and Chun-ki Lee. Navigators’ errors in a ship collision via simulation experiment in south korea. *Symmetry*, 12(4):529, 2020.
- [46] Yang Zhou, Winnie Daamen, Tiedo Vellinga, and Serge Hoogendoorn. Review of maritime traffic models from vessel behavior modeling perspective. *Transportation Research Part C: Emerging Technologies*, 105:323–345, 2019.
- [47] Jørgen Ernstsens and Salman Nazir. Performance assessment in full-scale simulators—a case of maritime pilotage operations. *Safety Science*, 129:104775, 2020.
- [48] Luman Zhao, Guoyuan Li, Knut Remøy, Baiheng Wu, and Houxiang Zhang. Development of onboard decision supporting system for ship docking operations. In *2020 15th IEEE Conference on Industrial Electronics and Applications (ICIEA)*, pages 1456–1462. IEEE, 2020.
- [49] Thiago Gabriel Monteiro, Charlotte Skourup, and Houxiang Zhang. Using eeg for mental fatigue assessment: A comprehensive look into the current state of the art. *IEEE Transactions on Human-Machine Systems*, 49(6):599–610, 2019.
- [50] Thiago Gabriel Monteiro, Houxiang Zhang, Charlotte Skourup, and Eduardo Aoun Tannuri. Detecting mental fatigue in vessel pilots using deep learning and physiological sensors. In *2019 IEEE 15th international conference on control and automation (icca)*, pages 1511–1516. IEEE, 2019.
- [51] Thiago Gabriel Monteiro, Charlotte Skourup, and Houxiang Zhang. A task agnostic mental fatigue assessment approach based on eeg frequency bands for demanding maritime operation. *IEEE Instrumentation & Measurement Magazine*, 24(4):82–88, 2021.
- [52] Odd Sveinung Hareide and Runar Ostnes. Scan pattern for the maritime navigator. *TransNav: International Journal on Marine Navigation and Safety of Sea Transportation*, 11(1), 2017.

- [53] Baiheng Wu, Luman Zhao, Sai Rana Thattavelil Sunikumar, Hans Petter Hildre, Houxiang Zhang, and Guoyuan Li. Visual attention analysis for critical operations in maritime collision avoidance. In *2022 17th International IEEE Conference on Control and Automation (ICCA)*. IEEE, 2022.
- [54] Baiheng Wu, Guoyuan Li, Luman Zhao, Hans Petter Hildre, and Houxiang Zhang. A human-expertise based statistical method for analysis of log data from a commuter ferry. In *2020 15th IEEE Conference on Industrial Electronics and Applications (ICIEA)*, pages 1471–1477. IEEE, 2020.
- [55] Baiheng Wu, Guoyuan Li, Luman Zhao, Hans-Ingar Johansen Aandahl, Hans Petter Hildre, and Houxiang Zhang. Navigating patterns analysis for onboard guidance support in crossing collision-avoidance operations. *IEEE Intelligent Transportation Systems Magazine*, 2021.
- [56] Baiheng Wu, Guoyuan Li, Tongtong Wang, Hans Petter Hildre, and Houxiang Zhang. Sailing status recognition to enhance safety awareness and path routing for a commuter ferry. *Ships and Offshore Structures*, 16(sup1):1–12, 2021.
- [57] Specifications of ntnu’s research vessel r/v gunnerus, 2006.
- [58] Peihua Han, Guoyuan Li, Robert Skulstad, Stian Skjong, and Houxiang Zhang. A deep learning approach to detect and isolate thruster failures for dynamically positioned vessels using motion data. *IEEE Transactions on Instrumentation and Measurement*, 70:1–11, 2020.
- [59] Tongtong Wang, Guoyuan Li, Lars Ivar Hatledal, Robert Skulstad, Vilmar Æsøy, and Houxiang Zhang. Incorporating approximate dynamics into data-driven calibrator: A representative model for ship maneuvering prediction. *IEEE Transactions on Industrial Informatics*, 18(3):1781–1789, 2021.
- [60] F Di Nocera, S Mastrangelo, S Proietti Colonna, A Steinhage, M Baldauf, and A Kataria. Mental workload assessment using eye-tracking glasses in a simulated maritime scenario. *Proceedings of the human factors and ergonomics society europe*, pages 235–248, 2016.
- [61] Hardeep Singh, Jagjit Singh Bhatia, and Jasbir Kaur. Eye tracking based driver fatigue monitoring and warning system. In *India International Conference on Power Electronics 2010 (IICPE2010)*, pages 1–6. IEEE, 2011.
- [62] Omer Arslan, Oguz Atik, and Serkan Kahraman. Eye tracking in usability of electronic chart display and information system. *The Journal of Navigation*, 74(3):594–604, 2021.
- [63] Oguz Atik. Eye tracking for assessment of situational awareness in bridge resource management training. *Journal of Eye Movement Research*, 12(3), 2019.
- [64] Odd Sveinung Hareide and Runar Ostnes. Maritime usability study by analysing eye tracking data. *The Journal of Navigation*, 70(5):927–943, 2017.

- [65] HR Chennamma and Xiaohui Yuan. A survey on eye-gaze tracking techniques. *arXiv preprint arXiv:1312.6410*, 2013.
- [66] Amer Al-Rahayfeh and Miad Faezipour. Eye tracking and head movement detection: A state-of-art survey. *IEEE journal of translational engineering in health and medicine*, 1:2100212–2100212, 2013.
- [67] Hyeon Chang Lee, Duc Thien Luong, Chul Woo Cho, Eui Chul Lee, and Kang Ryoun Park. Gaze tracking system at a distance for controlling iptv. *IEEE Transactions on Consumer Electronics*, 56(4):2577–2583, 2010.
- [68] Yiu-ming Cheung and Qinmu Peng. Eye gaze tracking with a web camera in a desktop environment. *IEEE Transactions on Human-Machine Systems*, 45(4):419–430, 2015.
- [69] Jiannan Chi, Zuoyun Yang, Guosheng Zhang, Tongbo Liu, and Zhiliang Wang. A novel multi-camera global calibration method for gaze tracking system. *IEEE Transactions on Instrumentation and Measurement*, 69(5):2093–2104, 2019.
- [70] Amogh Gudi, Xin Li, and Jan van Gemert. Efficiency in real-time webcam gaze tracking. In *European Conference on Computer Vision*, pages 529–543. Springer, 2020.
- [71] Lihong Dai, Jinguo Liu, and Zhaojie Ju. Binocular feature fusion and spatial attention mechanism based gaze tracking. *IEEE Transactions on Human-Machine Systems*, 2022.
- [72] Lan Anh Nguyen, Minh Duc Le, Si Hiep Nguyen, Thi Hoang Hoa Nghiem, et al. A new and effective fuzzy pid autopilot for ships. In *SICE 2003 Annual Conference (IEEE Cat. No. 03TH8734)*, volume 3, pages 2647–2650. IEEE, 2003.
- [73] LP Perera, JP Carvalho, and C Guedes Soares. Fuzzy logic based decision making system for collision avoidance of ocean navigation under critical collision conditions. *Journal of marine science and technology*, 16(1):84–99, 2011.
- [74] Michael R Benjamin, John J Leonard, Joseph A Curcio, and Paul M Newman. A method for protocol-based collision avoidance between autonomous marine surface craft. *Journal of Field Robotics*, 23(5):333–346, 2006.
- [75] MS Tannum and JH Ulvensøen. Urban mobility at sea and on waterways in norway. In *Journal of Physics: Conference Series*, volume 1357, page 012018. IOP Publishing, 2019.
- [76] G Hinton and L van der Maaten. Visualizing data using t-sne journal of machine learning research. 2008.
- [77] Mohamed Aly. Survey on multiclass classification methods. *Neural Netw*, 19(1):9, 2005.
- [78] Yingjun Hu, Anmin Zhang, Wuliu Tian, Jinfen Zhang, and Zebei Hou. Multi-ship collision avoidance decision-making based on collision risk index. *Journal of Marine Science and Engineering*, 8(9):640, 2020.

- 
- [79] Mateus Sant’Ana, Guoyuan Li, and Houxiang Zhang. A decentralized sensor fusion approach to human fatigue monitoring in maritime operations. In *2019 IEEE 15th International Conference on Control and Automation (ICCA)*, pages 1569–1574. IEEE, 2019.
  - [80] Odd Sveinung Hareide. The use of eye tracking technology in maritime high-speed craft navigation. *Doktoravhandlingar ved NTNU*, 2019.
  - [81] Tobii Pro AB. Tobii pro glasses 2 user’s manual version 1.1.3, 2020.
  - [82] International Maritime Organization. COLREGs: Convention on the international regulations for preventing collisions at sea. London, 1972.
  - [83] Sai Rana Thattavelil Sunilkumar. Development of close range real-time decision support system for ship guidance and navigation. *Master thesis, Norwegian University of Science and Technology*, 2021.
  - [84] Vinod Nair and Geoffrey E Hinton. Rectified linear units improve restricted boltzmann machines. In *Icml*, 2010.



# Appendix





*A*





**Paper I**

This paper is not included due to copyright

*B*

Paper II

## Sailing status recognition to enhance safety awareness and path routing for a commuter ferry

Baiheng Wu , Guoyuan Li , Tongtong Wang, Hans Petter Hildre  and Houxiang Zhang 

Department of Ocean Operations and Civil Engineering, Norwegian University of Science and Technology (NTNU), Ålesund, Norway

### ABSTRACT

This paper suggests a framework about how log data are used to develop a classifier to recognise the sailing status of a commuter ferry, which, in turn, serves as a tool of safety awareness. Several sailing scenarios are defined under the expertise's interpretation based on log data. A classifier is developed by support vector machine algorithm to recognise different scenarios. The classifying precision is getting improved as the database getting larger. Heat maps are drawn statistically to obtain the likelihood site of each sailing status. Contour maps are drawn by interpolation according to heat maps. Based on contour maps, two evaluation items are proposed to reflect the safety level. The safety level term is used for optimising the control. The established classifier has a recognition precision over 96 percent. A path following simulation is executed to verify the effectiveness of the safety level for enhancing sailing safety.

### ARTICLE HISTORY

Received 1 December 2020  
Accepted 18 March 2021

### KEYWORDS

Commuter ferry; support vector machine; ship intelligence; decision support system; safety awareness



### 1. Introduction

In the last decade, the artificial intelligence has been extensively studied by researchers from different academic fields of interests, and at the same time, it has also attracted practitioners occupied in various industrial fields to put efforts in, e.g. graphical/semantic recognition, autopilot system for automobiles. There have been scholars introducing the artificial intelligence to marine research and applications, but compared with the prosperity in the mentioned fields, this bundle of techniques still draws less attention in the maritime industry. Multiple reasons may account for the current situation. One of them is the artificial intelligence is not yet well studied, which means its performance cannot be guaranteed in real on-board operations, especially in some critical scenarios at high risk. In other words, we cannot substitute the human expertise on-board by an immature technology. Nevertheless, this reason should not prevent the maritime industry from exploring advanced technologies since the pragmatic value will emerge only after substantial and enough research and tests are proceeded. From another respect, it has been statistically stated that human errors have been the dominant factor for causing shipwrecks (Islam et al. 2017; Wiegmann and Shappell 2017). Even though the current progress in artificial intelligence is thought to be ineligible to replace the role of captains, it can at least assist them to avoid making mistakes so that the risk of human errors can be reduced at a large extent. With the rapid development in some minor subjects, including sensor fusion, data mining, and machine learning, constructing an on-board safety awareness system seems to be worth a shot (Elkins et al. 2010). In this paper, we develop

a framework how on-board log data can be utilised to enhance path routing and sailing safety, and to reflect human expertise as well. We also find a realisable application for this framework: commuter ferries with fixed route and certain number of critical operations in a sailing.

Data are necessary to implement artificial intelligence in any fields, including the maritime industry. As the hardware facility cost decreased remarkably in recent years, basic sensors are commonly equipped on most vessels (even the civil ships), which makes log data more accessible to be collected for research aims (Borkowski 2012; Ren et al. 2021). Besides the accessibility of the data, another concern for the data to be credited for further use is the data quality. Since the wrong data can contaminate the database, and thereby affect the performance of the artificial intelligence in a negative way, the data should be collected and selected meticulously. In this respect, human expertise can give sufficient supply. Therefore, it is believed that log data from any successful and safe sailings are with good quality for further utilisation.

Although it is said that on-board log data are getting more accessible, it is still at a small quantity compared with its counterpart in the automotive field. To ensure that enough data can be obtained to establish an intelligent system, we notice the application of commuter ferry which usually travels between two or more designated ports with a fixed sailing route. Repeated sailings guarantee the quantity of log data. Moreover, such type of routes usually contains countable critical operations at certain areas, which makes it possible to develop an algorithm to recognise different sailing status. With the accumulation of data and a proper utilisation of

**CONTACT** Guoyuan Li  [guoyuan.li@ntnu.no](mailto:guoyuan.li@ntnu.no)  Department of Ocean Operations and Civil Engineering, Norwegian University of Science and Technology (NTNU), Larsgårdsvegen 2, 6009 Ålesund, Norway

© 2021 The Author(s). Published by Informa UK Limited, trading as Taylor & Francis Group  
This is an Open Access article distributed under the terms of the Creative Commons Attribution-NonCommercial-NoDerivatives License (<http://creativecommons.org/licenses/by-nc-nd/4.0/>), which permits non-commercial re-use, distribution, and reproduction in any medium, provided the original work is properly cited, and is not altered, transformed, or built upon in any way.

them, we can learn the safety laws from the successful experience of human operations.

In this paper, a safety awareness system is designed for the commuter ferry. The system is developed mainly in two stages: designing a classifier to automatically sort the log data; constructing maps which reflect the sailing safety level based on the sorted data. The classifier predicts the sailing status online and the safety awareness can be given in a quantitative way; it is involved in the control loop to optimise the control input for verification.

Although relevant study is not prevalent in the research in maritime fields, such research has been extensively studied in the automobile field and has been applied in reality. Li et al. (2017, 2019a, 2019b, 2020) studied the classification and recognition of driving style and behaviours in different conditions with popular learning algorithm and different experimental methods. Compared with the pattern recognition, the concept of on-board decision support system is more acquainted with the maritime industry, and the safety awareness system developed in this paper can be seen as a component of such an on-board decision support system. There are different ways to develop on-board decision support systems. For example, some scholars build knowledge-based expert systems to support on-board decision (Perera et al. 2012; Calabrese et al. 2012); some use classical and/or novel control theories and tools to improve the manoeuvrability under particular conditions (Pietrzykowski et al. 2010; Nielsen and Jensen 2011); some introduce advanced algorithms to optimise the path planning and navigation (Lazarowska 2012; Simsir et al. 2014; Vettor and Soares 2015; Pietrzykowski et al. 2017); and some use data from automatic identification system (AIS) to support trajectory reconstruction and path following navigation (Zhang et al. 2018; Xu et al. 2019). From another view, such a safety awareness system is within the issue of situation awareness which has attracted researchers to focus on for aiding on-board operation (Chauvin et al. 2008; Nilsson et al. 2008; Fossdal 2018; Li et al. 2019; Nisizaki 2019). However, most research items stay in a conceptual stage without mathematical calculation and applicable data utilisation framework.

The novelty of the work in this paper locates mainly on two points: (1) Using real log data collected from a commuter ferry, instead of the data from simulators or other types of publishable data (AIS data), to analyse the ship manoeuvring status. Log data outperform other sources by directly reflecting captains' navigating behaviours and logics; (2) interpreting the log data by splitting the sailing route into different scenarios with featured particularity, instead of arbitrarily analysing the entire sailing route as a whole. The proposed safety awareness system is verified in a model predictive control loop which has been a popular control algorithm in the research for the auto-piloting car and autonomous vessel (Tøndel et al. 2003; Hagen et al. 2018; Tengesdal et al. 2020).

The paper is organised as follows: Section 2 introduces the proposed method in detail, including data collection and pre-processing, definition of split scenarios, pre-check before applying machine learning algorithm, the design of SVM and how the result can be interpreted by heat maps and

used to assess the safety level; Section 3 illustrates the result in three parts, including the classification result by SVM, the two types of figures demonstrating the classification result, the online testing and the verification in the control loop. At last, a conclusion of the paper is given as a sum and prospect.

## Nomenclature

CLF	classifier
CRS	cruising (scenario)
CVG	converging (scenario)
DCK	docking (scenario)
DPT	departing (scenario)
KDE	kernel density estimation
$L$ ; $L'$	label set; label set in each binary classifier
MPC	model predictive control
MSL	mean safety level
OH	optimal hyperplane or maximum margin hyperplane
$\hat{p}$ ; $\hat{p}_N$	estimated density; normalised estimated density
RPM	revolutions per minute
RSL	receding safety level
SL	safety level
SVM	support vector machine
TRN	turning (scenario)
$t$ -SNE	$t$ -distributed stochastic neighbour embedding

## 2. Methodology

The framework for sailing status recognition is shown as Figure 1. It includes several key steps: data collection and pre-processing, the design of SVM and its implementation on log data, interpretation of the classification result and its visualisation, and at last, a quantitative evaluation function is proposed to assess the level of sailing safety of the ferry based on the classification result of the accumulated historical log data. The contents included in Figure 1 will be extendedly explained in the following subsections.

### 2.1. Data collection and pre-processing

Log data used in this paper are from a customised commuting route between Trondhjem Biological Station and the berthing port at the estuary of the Nidelva river located in Trondheim, Norway (the white curve in the map in Figure 1 conceptually illustrates the route). The sailings on the commuting route are executed by R/V Gunnerus, a Research and survey Vessel owned by NTNU. The mileage of this commuting route is around 5 kilometres. The vessel is equipped with a 200 kW bow thruster at front for the positioning operation, two 500 kW main azimuth thrusters for the propulsion and course.

The database is constructed by log data from 16 sailings from September 2016 to June 2017 in a traffic-free environment. The sampling frequency of log data is 1 Hz. The information contained by the database can be sorted into three groups: geographical information, ship motions in different degrees of freedom and on-board machinery status. Since the geographical information is distinctly related to different scenarios (which will be defined in a later part), while we want to seek the laws from the ship status itself, items in the

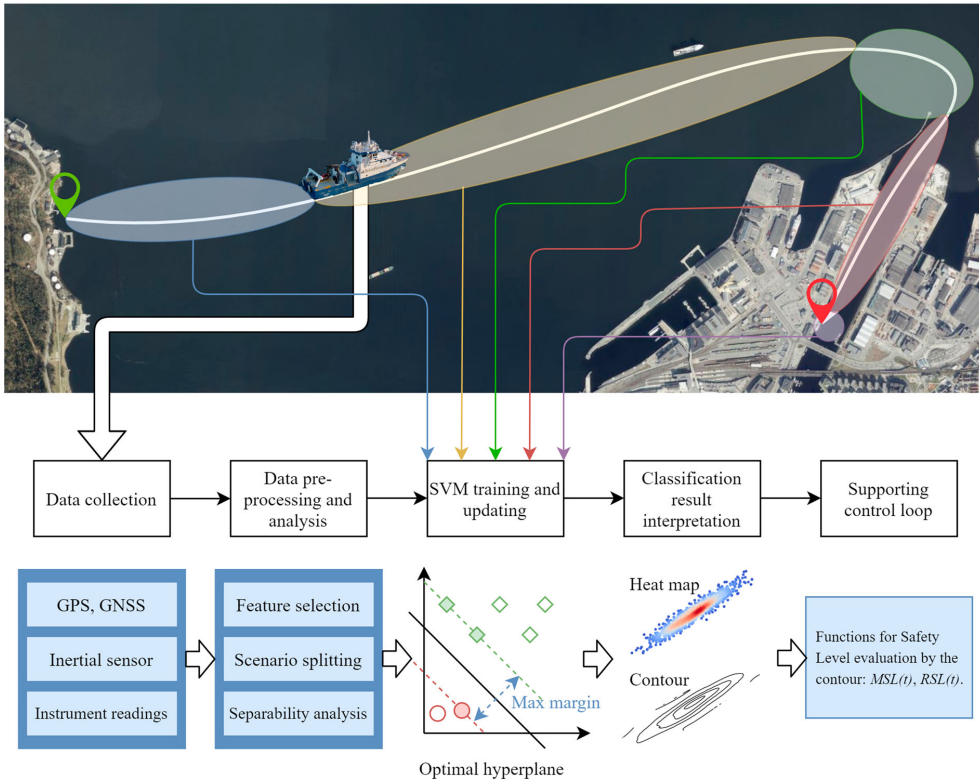


**Figure 1.** Framework of the proposed decision support system for sailing status recognition and safety evaluation (map resource: the Norwegian Mapping Authority). (This figure is available in colour online.)

database reflecting the geographical information are excluded. According to the navigation and manoeuvring habits of captains, featured items are selected from collected data (Wu et al. 2020). They are listed and sorted as in Table 1. All eight featured items in Table 1 are designated as variables for training the scenario recognition algorithm (support vector machine in Section 2.4).

## 2.2. Definition for scenarios by human expertise

According to human expertise, a commuting sailing route can be divided into different scenarios in terms of manoeuvring commands and the vessel response which can be reflected by collected log data. In this customised commuting route, five scenarios are separated from the whole sailing, which are described in detail as follows:

- Departing: the ferry sets off from the port and keeps accelerating.
- Cruising: the ferry usually reaches the rated RPM and travels on the route smoothly.
- Turning: the ferry adjusts its course towards another direction. Deceleration and angular speed increase in this phase.
- Converging: the ferry moves in the narrow channel at a speed lower than the rated, and it finally gets parallel to the coastline with a short distance.
- Docking: the ferry is with no surge speed but only sway, by using the bow thruster to push itself into the berthing point.

The rough illustration of the separation is shown in the map in Figure 1, as five scenarios are marked with ovals in different colours.

Hereupon, the original database is constructed as Equation (1), where  $X$  represents for a database consisted of  $n$  items described by eight variables mentioned in Table 1.

$$\log \text{ data} = \{X; L\}, X \in \mathbb{R}^{n \times 8}, L \in \mathbb{R}^{n \times 1}$$

$$L = \{l_1, l_2, \dots, l_n\}$$

$$\forall l_i \in L, l_i \in \{\text{departing, cruising, turning, converging, docking}\}$$

**Table 1.** Groups of featured log data items.

Groups	Ship motion	Machineries
Data items	Heading (°) Speed (knots) Pitch (°)	Bow thruster-RPM feedback (%) Port board-RPM feedback (%) Starboard-RPM feedback (%) Port board-azimuth feedback (°) Starboard-azimuth feedback (°)

### 2.3. Separability pre-check

Before designing the algorithm for the classifier, it is proper to have a preview of the data to check whether the database is separable. If it is, we may check at a further step to have a sense whether it is linearly separable, approximate linearly separable or not, so that we may determine some properties of the classifier to be designed later.

Firstly, the database is examined by the  $t$ -distributed stochastic neighbour embedding ( $t$ -SNE) algorithm (Maaten and Hinton 2008). By the algorithm, the high-dimensional database is converted into a visualisable low-dimensional database:

$$\begin{aligned} X &= \{x_1, x_2, \dots, x_n\} \in \mathbb{R}^{n \times 8} \xrightarrow{t\text{-SNE}} \\ Y &= \{y_1, y_2, \dots, y_n\} \in \mathbb{R}^{n \times 2} \end{aligned} \quad (2)$$

The  $t$ -SNE result is shown as in Figure 2. From the visualised result, it can be clearly found that there is a trend for each scenario to get clustered, hence it can be inferred that the sailing route can be separated into different scenarios based on the selected data.

Besides  $t$ -SNE, pair plots can be used to reflect the independency of each class. Here, two pair plots are selected and shown in Figure 3. From the self-correlation of port thruster RPM, heading and speed, it shows that there is independency between different scenarios. And bow thruster RPM also gives useful information to tell scenarios apart, e.g. docking data points are explicitly away from other scenarios when the bow thruster is in correlation with port thruster RPM. It should be noted that the power density function (PDF) value of the bow thruster self-correlation at 0 is dominant over the scale. This results from that the bow thruster is strictly kept turned off in almost whole period over scenarios including cruising, turning and converging. While in departing and docking scenarios, the bow thruster is not kept at a fixed running rate, the scattering makes the PDF at each value to be trivial against the counterpart at 0.

Since the database is with a dimensionality at 8, which can be considered as a high dimensional database. From the pre-

check of  $t$ -SNE dimension reduction and the pair plots, we may putatively assume scenarios in the sailing route described by log data are approximate linearly separable.

### 2.4. Support vector machine

SVM algorithm is chosen to build a classifier to solve the classification problem. The SVM algorithm is trained with collected log data according to eight features in Table 1. In practice, we convert the multiclass classification problem into several binary classification problems (Aly 2005). Then, there will be a specific classifier  $\text{CLF}_k$  for scenario  $k$ , and 5 in total for all scenarios. Taking scenario  $k$  as an example, for the data points whose original labels are the same as scenario  $k$ , they will be given new labels 1; otherwise, they will be given new labels  $-1$ . Then a new vector  $L'$  will be created by updated labels, and the vector will substitute the original label  $L$ . This process can be expressed as follows:

$$\text{CLF}_k: \begin{cases} l'_i = 1, & \text{if } l_i = k \\ l'_i = -1, & \text{otherwise} \end{cases} \quad (3)$$

For each binary classifier, there is a specific optimal hyperplane:

$$\text{OH}_k: W_k X + b_k = 0 \quad (4)$$

where  $W_k$  is the normal vector to the hyperplane. The optimal hyperplane lies between two parallel hyperplanes:

$$\begin{aligned} \text{OH}_k^+: W_k X + b_k &= 1 \\ \text{OH}_k^-: W_k X + b_k &= -1 \end{aligned} \quad (5)$$

Points on and above hyperplane  $\text{OH}_k^+$  will be assigned label 1, and finally turns into label  $k$ . And points on and below hyperplane  $\text{OH}_k^-$  will be assigned label  $-1$ , and finally will not be classified into the dataset of scenario  $k$ .

While the SVM algorithm is designed, the database is updated after every sailing so that the classifier built by SVM evolves simultaneously. And the updated classifier can be used to recognise the scenario status in subsequent sailings. The idea of this training process is mainly borrowed from

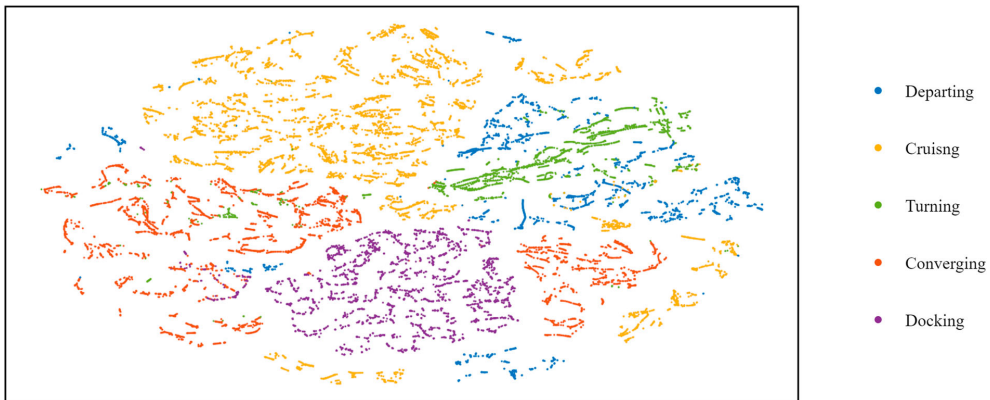


Figure 2. Visualisation of dimension reduction result by  $t$ -SNE. (This figure is available in colour online.)

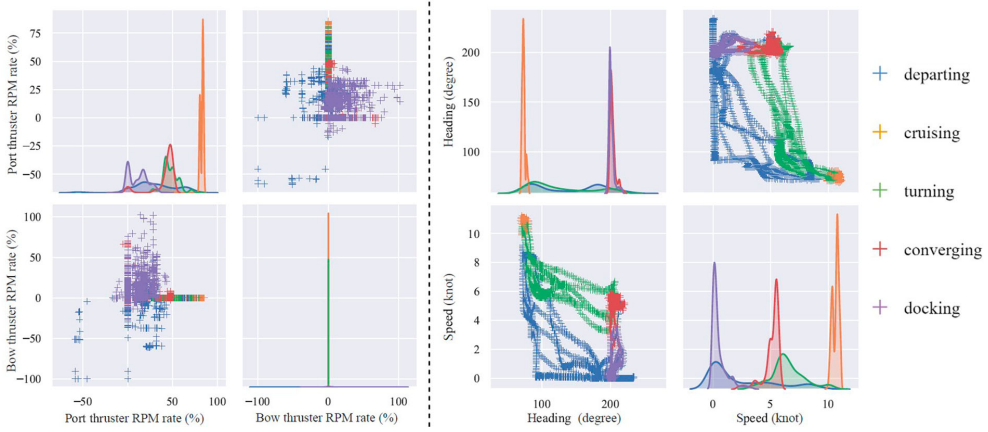


Figure 3. Selected pair plots. (This figure is available in colour online.)

Hold-out validation (Berrar 2019). Since we collected 16 sailings' log data, this process can be illustrated as in Table 2. In Table 2, Classifiers 1–15 represent 15 different classifiers train with 1–15 training sets (for example, a possible training-set combination for Classifier 3 could be Sailing dataset No. 1, 2 and 3 or any other combinations of three sailing datasets), while test sets 1–16 mean No. 1–16 sailing datasets (single sailing dataset).

### 2.5. Likelihood map and safety level calculation

As log data accumulated along the sailings run times by times, the database for training the SVM classifier is getting larger. Besides the eight featured data items, the geographical information is also recorded. Therefore, another database can be constructed based on the geographical information of those data points which are correctly classified by the classifier. And data points can be drawn on a geographical map reflecting the site of each scenario in the sailing route. Then the map can be converted into a heat map in terms of the density of the geographical distribution of data points. At this step, kernel density estimation method helps to calculate the estimated density at each datum point  $x_j$ :

$$\hat{p}(x_j) = \frac{1}{mh} \sum_{i=1}^m K\left(\frac{x_j - x_i}{h}\right) \quad (6)$$

Table 2. Illustration of the classifier evolution process.

Testset	Classifier			
	1	2	...	15
1	–	–	–	–
2	*	*	–	–
...	*	*	...	–
15	*	*	*	*
16	*	*	*	*
Mean value	*	*	*	*

\*represents a numeric value; – represents no calculation.

where  $h$  ( $h > 0$ ) is a smoothing parameter;  $K$  is the kernel for scaling, and Gaussian kernel is chosen in this paper to estimate the density. Then a 2D heat map illustrating the density distribution can be drawn accordingly. Since the database is updated after new sailing data are appended, the numerical value of the density will become larger and larger, which implies that raw density value itself does not contain standard useful information to help the human to make decision. Therefore, to avoid it from being nothing but fancy, we normalise the density scale into  $[0, 1]$ :

$$\hat{p}_N(x_j) = \frac{\hat{p}(x_j) - \min(\hat{p})}{\max(\hat{p}) - \min(\hat{p})} \quad (7)$$

After the normalisation, the density will always be in a certain scale and in a manner that we explicitly understand: the normalised density 1 refers to the densest site on the sailing route, while 0 refers to the sparsest site. The ferry is believed to be safer when travelling on a site where the normalised density is higher, while the captain should be vigilant when the ferry goes into the low normalised density site. Meanwhile, heat maps can be converted to contours by an interpolation operation based on the normalised density distribution. In this paper, we choose the cubic spline interpolation method to realise this conversion. Then the map is gridded, and the density is calculated by the interpolation. By connecting grid points with the same density value, the contour map is obtained to demonstrate continuous approximation of the density distribution at the vicinity area of the scenario. The distribution function  $SL(y)$  can be obtained by ploy-fitting the statistics of the safety level, where  $y$  represents the position.

### 2.6. Verification of how the safety level benefits in MPC

In this part, the concept of safety level is integrated into the cost function to implement the MPC. The control scheme is illustrated as in Figure 4. The vessel kinematics can be



represented as Equation (8). Since we do not consider environment loads at this stage, the right-hand side of the kinetic equation  $\tau$  is the input force which equals  $[f_u, f_v, t_r]'$ .  $\eta$  is the pose vector as  $[N, E, \psi]'$ .  $R(\psi)$  is the horizontal plane rotation matrix in terms of the yaw angle  $\psi$ .  $M$  is the system inertia matrix.  $C(v)$  is the Coriolis-centripetal matrix.  $D(v)$  is the damping matrix.  $H$  equals  $[1, 0, 0; 0, 1, 0]$ , and  $y$  equals  $[N, E]'$ .

$$\begin{aligned}\dot{\eta} &= R(\psi)v \\ M\dot{v} + C(v)v + D(v)v &= \tau \\ y &= H\eta\end{aligned}\quad (8)$$

The original cost function is defined as follows:

$$\begin{aligned}J(t) &= (y(t+1) - y_{\text{ref}})^T Q (y(t+1) - y_{\text{ref}}) \\ &+ \Delta u(t+1)^T R \Delta u(t+1)\end{aligned}\quad (9)$$

The optimisation goal is to minimise the cost function  $J$ ; we use the positive term  $(1 - \text{SL}(y))$  to conform to the implication of safety level and the optimisation target. The cost function is thus augmented as follows:

$$\begin{aligned}J^*(t) &= (y(t+1) - y_{\text{ref}})^T Q (y(t+1) - y_{\text{ref}}) \\ &+ \Delta u(t+1)^T R \Delta u(t+1) + W(1 - \text{SL}(y(t+1)))\end{aligned}\quad (10)$$

Equations (9) and (10) give the cost function at one time-step prediction, while MPC is predicting over a length of time horizon  $N_p$  to determine the best control candidate, so the overall cost prediction at a certain time step can be represented as Equation (11).

$$J^*(t) = \sum_{k=t+1}^{t+N_p} J^*(k) \quad (11)$$

The sailing with the least MSL, among 16 historical sailings, is selected as the reference to carry out the path following task. Comparison will be made between the simulations with different cost functions to verify the effect of the safety level term.

## 2.7. Assessing the safety level by the contour map

At the last step in the proposed method, we establish a concept of safety levels with respect to the normalised density distribution described by contour maps. Safety levels (SL) are

directly represented by the normalised density of the geographical location. Hereupon, two dimensionless items can be further calculated to reflect different aims of evaluation: receding safety level (RSL) expressed as Equation (12) and mean safety level (MSL) as Equation (13).

$$\text{RSL}(t) = \frac{\sum_{i=N(t)-\Delta T}^{N(t)} p_i}{\Delta T} \quad (12)$$

$$\text{MSL}(t) = \frac{\sum_{i=0}^{N(t)} p_i}{N(t)} \quad (13)$$

$N$  is the number of accumulated log data points until the moment  $t$ .  $\Delta T$  is the number of sampled data points in the receding horizon, while the receding horizon is chosen manually.

RSL calculates the mean safety level in a fixed time scale. The receding horizon for calculation is updated after each sampling. MSL calculates the mean safety level from the start to current moment  $t$ . MSL may reflect the overall safety level; hence, it can be used to evaluate the performance of the human manoeuvring in a sailing.

## 3. Results

The proposed method is implemented to the database built upon collected 16 sailings' log data. In this section, results are presented in three parts: classification results from the SVM classifier; the derived likelihood heat maps and normalised numerical contour maps, and online testing. To make the demonstration of the results and the corresponding visualisation more comprehensible, result figures will be partially demonstrated. While the selection of figures is unbiased, it is believed that they are able to reflect the global performance.

### 3.1. Classification result

According to Section 2.4 and Table 2, the classifier is built once the first sailing's log data is added to the SVM training database. As the database evolves when new log data come into, the classifier will be updated therewith. The demonstration of the evolution result irrespective of scenarios is shown as Table 3 and Figure 5.

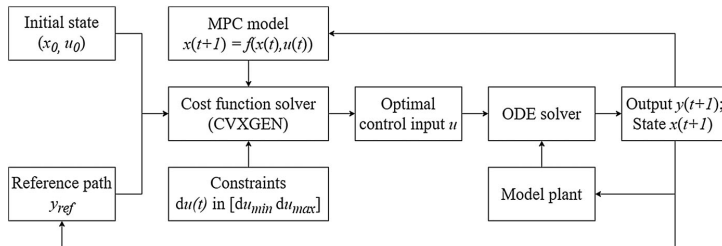


Figure 4. Flowchart of the MPC control scheme. (This figure is available in colour online.)



Table 3 shows that the precision of the classification result is increasing as the classifier evolves. While in Figure 5, the precision plunges at the early stage and then rises back rapidly. The diversity between datasets collected from different sailings may account for it, since it is difficult to make an entirely correct description of another sailing by a classifier only trained by very few sailing datasets (one or two). However, after four sailings' log data are added into the database, the classifier can almost guarantee a precision over 90%. As the database is larger, the precision of the classifier keeps growing. At last, the mean value of the classification precision has been developed over 96% based on whole collected sailings' data.

After illustrating the result in a macro-scope, Figure 6 shows the classification precision with respect to different scenarios, and it comprehensively reveals how different scenarios correlate pairwise. In Figure 6, the labels are abbreviated: DPT for departing; CRS for cruising; TRN for turning; CVG for converging and DCK for docking. From CLF No. 4 to No. 9, the evolution improves its predicting capacity on CVG scenario significantly, but the classifier incorrectly predicts many TRN data points as CVG, which results in the declination of the prediction precision on TRN. Meanwhile, the prediction precision on DCK also grows slightly. Then by comparing the latter two, it shows that the predicting precision is improved remarkably on DPT from 84% to 90%. However, the same problem occurs again that the prediction precision on CVG continues to grow on sacrifice of the declination on TRN, in a moderate manner. In general, the performance of the classifier is improved after several evolutions.

for converging and DCK for docking. From CLF No. 4 to No. 9, the evolution improves its predicting capacity on CVG scenario significantly, but the classifier incorrectly predicts many TRN data points as CVG, which results in the declination of the prediction precision on TRN. Meanwhile, the prediction precision on DCK also grows slightly. Then by comparing the latter two, it shows that the predicting precision is improved remarkably on DPT from 84% to 90%. However, the same problem occurs again that the prediction precision on CVG continues to grow on sacrifice of the declination on TRN, in a moderate manner. In general, the performance of the classifier is improved after several evolutions.

### 3.2. Likelihood heat maps and derived contours

According to the method introduced in Section 2.4, heat maps, based on the accumulated database, can be drawn, as shown in Figure 7. The first five subplots show the heat map of each scenario, while the last subplot at the right bottom shows an overview of the complete route.

The heat maps can help the reader, for example, captains have a direct sense of the most travelled sites. And this feature is prominent especially in scenarios cruising, turning, and converging. However, since both the departing and docking are

Table 3. Illustration of the classifier evolution process.

Testset	Classifier		
	4	9	14
5	0.9031	–	–
10	0.9723	0.9815	–
15	0.9675	0.9578	0.9610
Mean value	0.9370	0.9593	0.9684

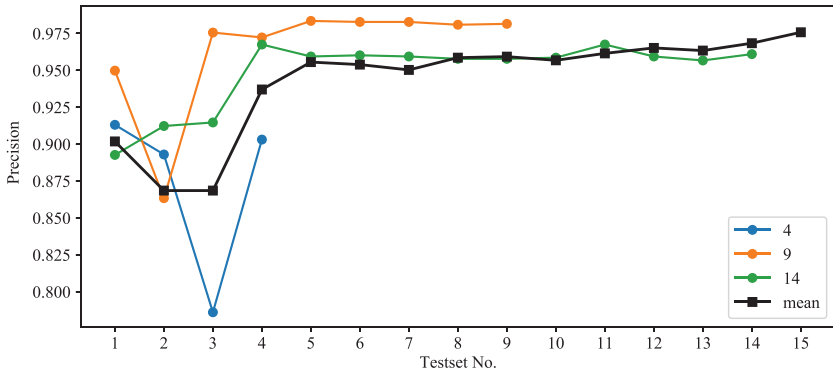


Figure 5. Evolution of the classifier according to Table 2. (This figure is available in colour online.)



Figure 6. Confusion matrix reflecting precision by scenarios (left: CLF No.4; middle: CLF No. 9; right: CLF No. 14). (This figure is available in colour online.)

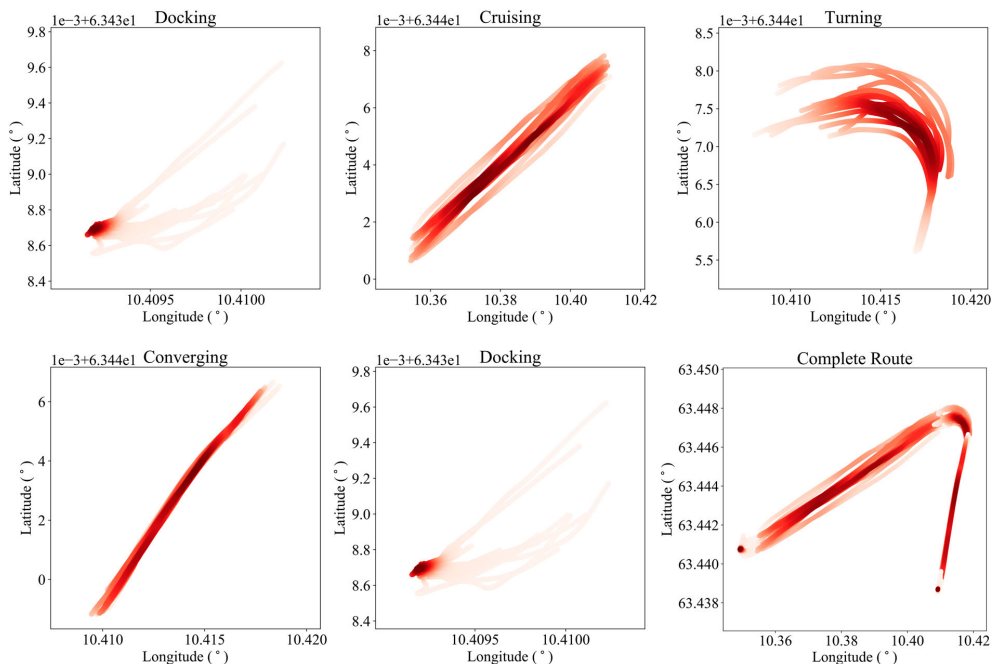


Figure 7. Heat maps of different scenarios. (This figure is available in colour online.)

undergoing in a very concentrated site, the density distribution appears to be somewhat diffusion. However, it is thought to be in a tolerant extent, and can be ameliorated as the database is larger.

Based on heat maps shown in Figure 7, a set of contours with respect to each scenario can be drawn as Figure 8. Different from the heat maps that provide an intuitive illustration and sense of the most travelled area, the set of contours quantitatively demonstrates how the density distributes on a geographical map. Since contours are obtained by an interpolation operation, its fidelity and creditability are dependent on the quantity of data. In general, the overall trend in each scenario has been shown. For example, in the contour of cruising scenario – the closer to the centre of the heat area, the larger the normalised density.

### 3.3. Accumulative manoeuvring knowledge for on-board decision support

As the sailing data are classified by SVM (in Section 2.4) and the results are obtained (in Section 3.1), informative statistics on how captains manoeuvre the ferry during different scenarios are made as in Table 4.

Bow thruster is only turned on during departing and docking when a side force is needed to push the ferry into/out the quay. The behaviours of port- and star-thruster are almost in the same scale, except for the azimuth angle during docking scenario. It depends on which side the ferry docks since solely adjusting the azimuth angle of the outer thruster is able to balance the torque generated at the bow thrust. Since in

this commuting route, the ferry docks at its star-board side (e.g. the coastal to its right), the port-thruster becomes the outer thruster so that its azimuth angle is adjusted as required.

Since the calculated safety levels MSL and RSL are returned to the captain in real time, when the calculated safety levels are falling down to a certain extent, the captain can inspect his manoeuvring commands according to the accumulative manoeuvring knowledge to help him regulate the ferry running in a correct status.

### 3.4. Verification in the MPC loop

In this part, the path following simulation results will be shown and assessed. Figure 9 shows the path of reference (Sailing No. 6), the original MPC and the improved MPC with safety level (MPC-SL). The safety level assessment is given as Table 5. The prediction horizon  $N_p$  in MPC and MPC-SL is set as 10.

It should be emphasised that the way how we evaluate the control performance shown in Figure 9 is slightly different from the traditional approach. Traditionally, we balance the input cost and the error reduction to have an optimal solution. In addition to those two items, we augment the cost function with a safety level  $SL(y)$  factor, as in Equation (10). Then it becomes a balance among these three dimensions. Besides having an acceptable reference path following, it requires to have a better safety level evaluation, which is shown in Table 5 in detail.

From the safety level statistics in Table 5, we can implicitly summarise that the safety level has a strong impact on the

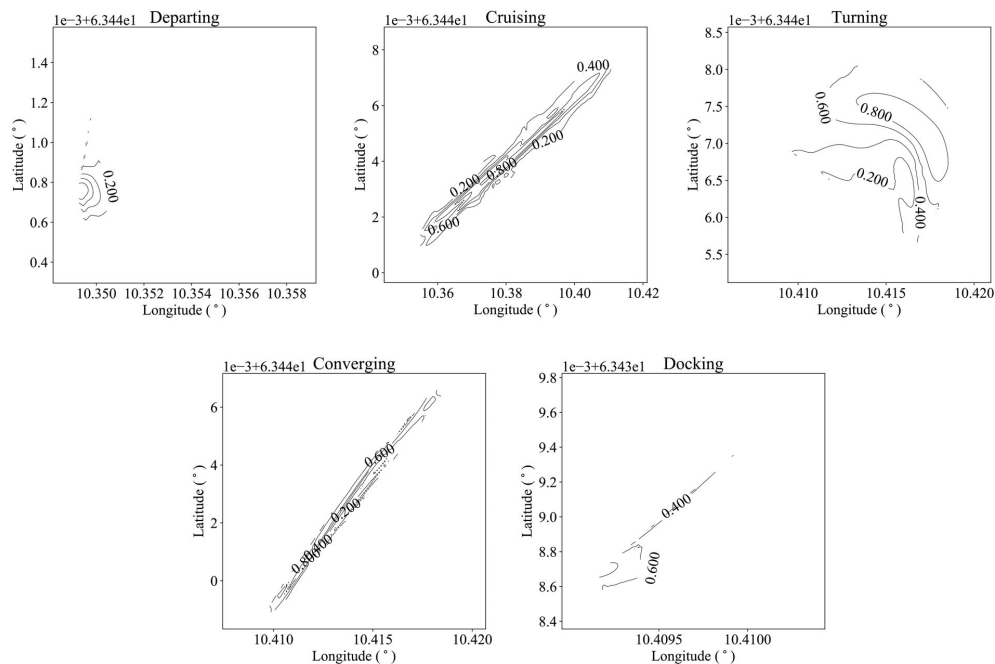


Figure 8. Contour of different scenarios. (This figure is available in colour online.)

Table 4. On-board machinery status in different scenarios.

Actuator	DPT	CRS	TRN	CVG	DCK
Bow-thruster (%)	>0.1	–	–	–	>10
Port-RPM (%)	<60	>75	[40, 60]	[40, 60]	[0, 30]
Star-RPM (%)	<60	>75	[40, 60]	[40, 60]	[0, 30]
Port-azimuth (°)	>0.5	<1	>0.5	<2	>50
Star-azimuth (°)	>0.5	<1	>0.5	<2	<1

control. After the safety level term is added into the cost function, the overall safety level increases significantly, and so as in scenarios DPT, CRS and TRN.

When the vessel travels in a narrow water tunnel in CVG, where the gradient of the safety level can be very sharp, the safety level suffers a decline but in a moderate level. When the vessel is in the final bow thrusting stage, where the safety

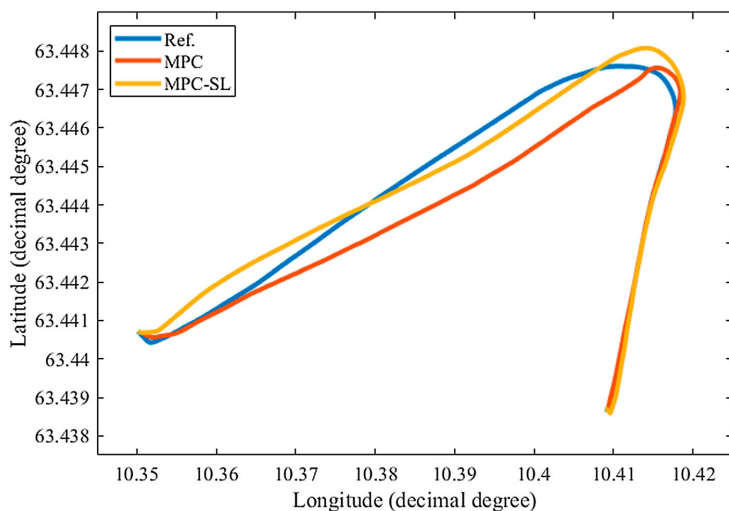


Figure 9. Path following simulation by MPC (the path corresponds to Figure 1). (This figure is available in colour online.)

Table 5. Illustration of the classifier evolution process.

Scenario	Ref.	Safety level	
		MPC	MPC-SL
DPT	0.4203	0.4574	<b>0.5449</b>
CRS	0.4259	0.5135	<b>0.6743</b>
TRN	0.6851	0.6304	<b>0.6999</b>
CVG	0.5065	<b>0.5938</b>	0.5059
DCK	<b>0.6161</b>	0.4157	0.4158
Overall	0.5199	0.4574	0.5681

level heat map almost concentrates on a point, it is difficult for the vessel to be strictly in the circle of high safety so that the safety level in DCK is low. In general, the safety level term improves the control in terms of safety noticeably, which suggests that the proposed methodology attains a good performance and further study can be conducted in practice.

3.5. Safety level assessment

In this part, safety level assessments are conducted from two aspects. One is sailing status recognition for a whole sailing dataset, and another is safety level evaluation.

Figure 10 shows the result of the online sailing status recognition testing. The dashed lines divide the timeline into segments remarking real periods of each scenario, while the mark ‘+’ represents the recognised status at each sampling step. There are two wild points in the DPT stage, where the sampled data are incorrectly recognised as DCK and TRN. The problem occurs mainly at the TRN stage, where the classifier improperly recognises the ferry to enter the next stage ahead of the real situation, which may be resulted from the similarity between the manoeuvring operations during the late phase in TRN and the early phase in CVG. The classifier has a good performance in judging CRS and DCK during the online testing.

According to the defined terms in Section 2.7 and the obtained contour maps, safety level evaluation is implemented accordingly. The real-time safety level at each sampling step is represented by diluted lines in Figure 11. Firstly, it should be mentioned that since contour maps are derived for each scenario separately and are not merged into one ensemble, the safety level evaluation experiences a gap when the ferry transits between two scenarios. Secondly, it is notable that, excluding

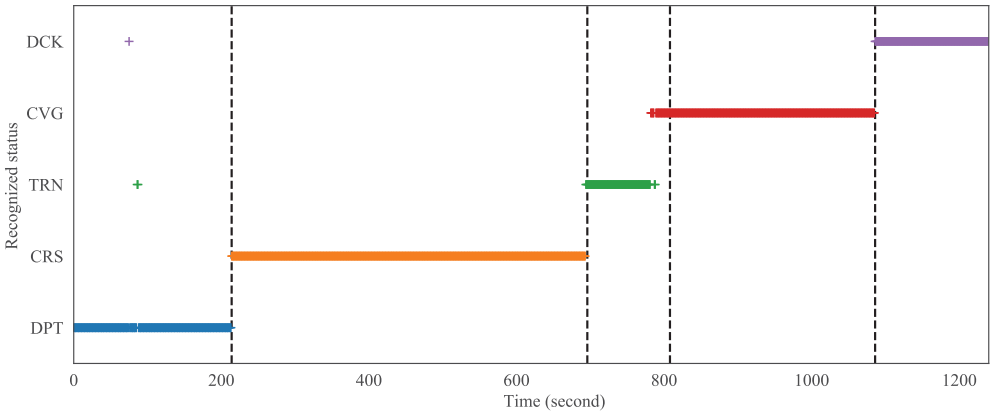


Figure 10. Online testing of the sailing status recognition. (This figure is available in colour online.)

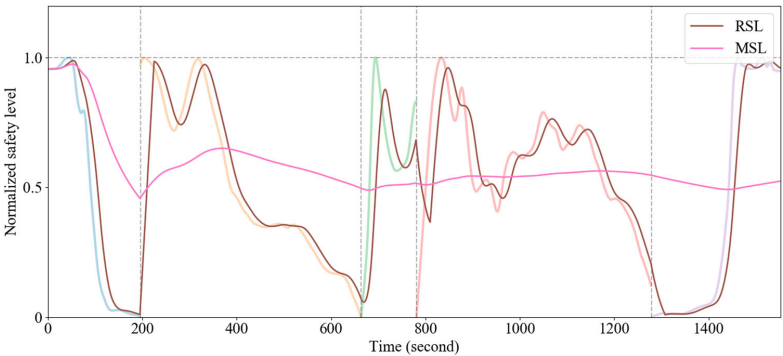


Figure 11. Calculated MSL and RSL (diluted lines are the real-time safe level). (This figure is available in colour online.)

the start and the end stage of the whole sailing, the safety level is usually low at the start and end of each single scenario. It may be explained according to the distribution shown in Figure 7. In those heat maps, there is a conspicuous high-density area in each scenario, while at the start and the end, the distribution inclines to disperse, which consequently results in the decline of the safety level at the marginal area.

According to Section 2.7, the two items MSL and RSL, reflecting the safety level from different aspects, are calculated, and shown as in Figure 11. Since RSL calculates the average safety level at a fixed length of the past period, there is a delay to reflect the change of the safety level. This delay provides RSL the ability to reduce the effect at the start and the end during the transition time between different scenarios, which makes RSL to describe the sailing safety in a moderate way. Since critical operations are expected to be taken at the transition period between two scenarios, RSL drastically decreases to a low level to reflect the high possibility of committing a mistake during the transition. MSL demonstrate the safety level with a global insight. It is noticed that because of the long-term steady sailing of the ferry, there is a swell of the safety level during both CRS and CVG scenarios. At last, MSL can provide an overall evaluation of the sailing safety.

RSL and MSL reflect the safety level from two aspects based on the constructed safety level contour maps by a numerical judgement explicitly. It provides an intuitive and quantitative approach for the captain to take the advantage of the knowledge accumulated on this commuting route.

## 4. Conclusion

This paper introduces a method to utilise log data from a ferry to establish an on-board safety awareness system in order to help humans to make decisions. Successful sailings are still thought to be a good paradigm for both designing autonomous ferries and evaluating the manoeuvre quality of every sailing. Hence, we split a customised sailing route and define different scenarios in favour of the human expertise. Collected data are classified by an SVM algorithm and its results are presented as figures of heat maps and contours by the statistical method. Both sets of figures together may assist to evaluate the sailing safety level. Since the ferry may deviate from the designated path no matter under human operations or under autonomous manoeuvring, the figures give a set of metrics to qualitatively and quantitatively know whether the current situation is safe or not, based on the past experience which is reflected by historical log data. By defining new items reflecting safety levels with respect to geographical locations, the result can be used to optimise the control. MPC is designed with the safety level term integrated to verify its significance. From the simulation results, the safety level has a great impact on and ameliorates the control loop. From this research work, we suggest a framework how log data can be comprehensively used to provide on-board support and enhance the sailing route safety. The main idea in this paper is to synthetically use both human expertise and objective log data to make rudiment work for autonomous navigation. It is also under a grand framework that we aim to achieve reliable on-board decision support and ship autonomy by finding, interpreting, learning,

and imitating the captains' operating behaviours. For the future work, first, since the log data collected in this paper are from only one commuting route in moderate environment conditions, log data from other commuting routes and types of weather windows should be collected and analysed to examine the universality of the proposed method; second, further study can be focused on the sensitivity of the safety level to the gradient in terms of geographic distance to optimise the control performance.

## Acknowledgements

The research is supported, in part, by the MAROFF KPN project 'Digital Twins for Vessel Life Cycle Service' (Project no.: 280703), and, in part, by the IKTPLUSS Project 'Remote Control Centre for Autonomous Ship Support' (Project no.: 309323) in Norway.

## Disclosure statement

No potential conflict of interest was reported by the author(s).

## Funding

This work was supported by Norges Forskningsråd [grant numbers 309323, 280703].

## ORCID

Baiheng Wu  <http://orcid.org/0000-0002-1824-6784>

Guoyuan Li  <http://orcid.org/0000-0001-7553-0899>

Hans Petter Hildre  <http://orcid.org/0000-0003-1444-7818>

Houxiang Zhang  <http://orcid.org/0000-0003-0122-0964>

## References

- Ally M. 2005. Survey on multiclass classification methods. *Neural Netw.* 19:1–9.
- Berrar D. 2019. Cross-validation. *Encycl Bioinform Comput Biol.* 1:542–545.
- Borkowski P. 2012. Data fusion in a navigational decision support system on a sea-going vessel. *Pol Marit Res.* 19(4):78–85.
- Calabrese F, Corallo A, Margherita A, Zizzari AA. 2012. A knowledge-based decision support system for shipboard damage control. *Expert Syst Appl.* 39(9):8204–8211.
- Chauvin C, Clostermann JP, Hoc J-M. 2008. Situation awareness and the decision-making process in a dynamic situation: avoiding collisions at sea. *J Cogn Eng Decis Mak.* 2(1):1–23.
- Elkins L, Sellers D, Monach WR. 2010. The autonomous maritime navigation (AMN) project: field tests, autonomous and cooperative behaviors, data fusion, sensors, and vehicles. *J Field Robot.* 27(6):790–818.
- Fossdal M. 2018. Online consequence analysis of situational awareness for autonomous vehicles [master's thesis]. NTNU.
- Hagen IB, Kufoalor DKM, Brekke EF, Johansen TA. 2018. MPC-based collision avoidance strategy for existing marine vessel guidance systems. 2018 IEEE International Conference on Robotics and Automation (ICRA). IEEE; p. 7618–7623.
- Islam R, Yu H, Abbassi R, Garaniya V, Khan F. 2017. Development of a monograph for human error likelihood assessment in marine operations. *Saf Sci.* 91:33–39.
- Lazarowska A. 2012. Decision support system for collision avoidance at sea. *Pol Marit Res.* 19(Special):19–24.
- Li G, Lai W, Sui X, Li X, Qu X, Zhang T, Li Y. 2020. Influence of traffic congestion on driver behavior in post-congestion driving. *Accid Anal Prev.* 141:105508.

- Li G, Li SE, Cheng B, Green P. 2017. Estimation of driving style in naturalistic highway traffic using maneuver transition probabilities. *Transp Res C Emerg Technol.* 74:113–125.
- Li G, Mao R, Hildre HP, Zhang H. 2019. Visual attention assessment for expert-in-the-loop training in a maritime operation simulator. *IEEE Trans Ind Inf.* 16(1):522–531.
- Li G, Wang Y, Zhu F, Sui X, Wang N, Qu X, Green P. 2019b. Drivers' visual scanning behavior at signalized and unsignalized intersections: a naturalistic driving study in China. *J Saf Res.* 71:219–229.
- Li G, Zhu F, Qu X, Cheng B, Li S, Green P. 2019a. Driving style classification based on driving operational pictures. *IEEE Access.* 7:90180–90189.
- Maaten LVD, Hinton G. 2008. Visualizing data using t-SNE. *J Mach Learn Res.* 9(Nov):2579–2605.
- Nielsen UD, Jensen JJ. 2011. A novel approach for navigational guidance of ships using onboard monitoring systems. *Ocean Eng.* 38(2-3):444–455.
- Nilsson M, Van Laere J, Ziemke T, Edlund J. 2008. Extracting rules from expert operators to support situation awareness in maritime surveillance. 2008 11th International Conference on Information Fusion; Jun. IEEE; p. 1–8.
- Nisizaki C. 2019. Onboard measurements of navigator's situation awareness in congested sea area. 2019 IEEE International Conference on Systems, Man and Cybernetics (SMC); Oct. IEEE; p. 4296–4301.
- Perera LPH, Rodrigues JMJD, Pascoal R, Soares CG. 2012. Development of an onboard decision support system for ship navigation under rough weather conditions. In: E. Rizzuto, C. Guedes Soares, editors. *Sustainable maritime transportation and exploitation of sea resources*. London, UK: Taylor & Francis Group; p. 837–844.
- Pietrzykowski Z, Magaj J, Wolejsza P, Chomski J. 2010. Fuzzy logic in the navigational decision support process onboard a sea-going vessel. *International Conference on Artificial Intelligence and Soft Computing*; Jun. Berlin: Springer; p. 185–193.
- Pietrzykowski Z, Wolejsza P, Borkowski P. 2017. Decision support in collision situations at sea. *J Navig.* 70(3):447–464.
- Ren Z, Han X, Verma AS, Dirdal JA, Skjetne R. 2021. Sea state estimation based on vessel motion responses: Improved smoothness and robustness using Bézier surface and L1 optimization. *Marine Structures.* 76: 102904.
- Simsir U, Amasyalı MF, Bal M, Çelebi UB, Ertugrul S. 2014. Decision support system for collision avoidance of vessels. *Appl Soft Comput.* 25:369–378.
- Tengesdal T, Brekke EF, Johansen TA. On collision risk assessment for autonomous ships using scenario-based MPC.
- Tøndel P, Johansen TA, Bemporad A. 2003. An algorithm for multi-parametric quadratic programming and explicit MPC solutions. *Automatica (Oxf).* 39(3):489–497.
- Vettor R, Soares CG. 2015. Multi-objective route optimization for onboard decision support system. In: Weintritz A, Neumann T, editors. *Information, communication and environment: marine navigation and safety of sea transportation*. Leiden: CRC Press, Taylor & Francis; p. 99–106.
- Wiegmann DA, Shappell SA. 2017. *A human error approach to aviation accident analysis: the human factors analysis and classification system*. London, UK: Routledge.
- Wu B, Li G, Zhao L, Hildre HP, Zhang H. 2020. A human-expertise based statistical method for analysis of log data from a commuter ferry. 2020 15th IEEE Conference on Industrial Electronics and Applications (ICIEA); Nov. IEEE; p. 1471–1477.
- Xu H, Rong H, Soares CG. 2019. Use of AIS data for guidance and control of path-following autonomous vessels. *Ocean Eng.* 194: 106635.
- Zhang L, Meng Q, Xiao Z, Fu X. 2018. A novel ship trajectory reconstruction approach using AIS data. *Ocean Eng.* 159:165–174.





## Paper III

This paper is not included due to copyright







## Paper IV

This paper is awaiting publication and is not included in NTNU Open



This paper is awaiting publication and is not included in NTNU Open





This paper is awaiting publication and is not included in NTNU Open

This paper is awaiting publication and is not included in NTNU Open

ISBN 978-82-326-5455-0 (printed ver.)  
ISBN 978-82-326-5796-4 (electronic ver.)  
ISSN 1503-8181 (printed ver.)  
ISSN 2703-8084 (online ver.)



**NTNU**

Norwegian University of  
Science and Technology